UNCLASSIFIED

AD 286 928

Reproduced
by the

ARMED SERVICES TECHNICAL INFORMATION AGENCY
ARLINGTON HALL STATION
ARLINGTON 12, VIRGINIA

UNCLASSIFIED

NOTICE: When government or other drawings, specifications or other data are used for any purpose other than in connection with a definitely related government procurement operation, the U. S. Government thereby incurs no responsibility, nor any obligation whatsoever; and the fact that the Government may have formulated, furnished, or in any way supplied the said drawings, specifications, or other data is not to be regarded by implication or otherwise as in any manner licensing the holder or any other person or corporation, or conveying any rights or permission to manufacture, use or sell any patented invention that may in any way be related thereto.

63-1-3

CATALOGED BY ASTIA
AS AD No. 286928

AIR FORCE INSTITUTE OF TECHNOLOGY

AIR UNIVERSITY
UNITED STATES AIR FORCE

286 928

ASTIA
RECEIVED
OCT 30 1962
TISIA

SCHOOL OF ENGINEERING

WRIGHT-PATTERSON AIR FORCE BASE, OHIO

AF-WP-O-MAY 62 3,500

DESIGN AND CONSTRUCTION OF A FAST NEUTRON SPECTROMETER USING SOLID STATE DETECTORS

Captain Phillip D. Weinert, U.S. Army

GNE/Phys/62-17

DESIGN AND CONSTRUCTION
OF A FAST NEUTRON SPECTROMETER
USING SOLID STATE DETECTORS

THESIS

Presented to the Faculty of the School of Engineering of

the Air Force Institute of Technology

Air University

In Partial Fulfillment of the

Requirements for the Degree of

Master of Science

By

Phillip Darden Weinert, B.S. C.E.

Captain U.S. Army

Graduate Nuclear Engineering

May 1962

AF-WP-O-SEP 62 30

Preface

The work performed in connection with this thesis was done under the direction of the Aeronautical Research Laboratories at Wright-Patterson Air Force Base, Ohio. The 2 mev Van de Graaff facility and the major part of the equipment belongs to that organization. The thesis advisor at the Aeronautical Research Laboratories is Dr. William Price and the faculty advisor at the Air Force Institute is Major Edward Zawalick.

Assistance was received from many quarters and appreciation is extended to the Air Force Institute shops, ARL shops, various ARL personnel and personnel of the Electron Technology Laboratory at WPAFB. Special thanks are given to Dr. Geoff Dearnaley for his cooperation and assistance. Much help in solving problems of assembling the hardware was received from the Propulsion Division of the Directorate of Engineering Test, Aeronautical Systems Division, WPAFB, and especially Mr. Dick Miller of that organization. The assistance with the electronics given generously by Mr. John Dooley of the Nuclear Engineering Test Facility, WPAFB, is appreciated. Help on many facets of the work was provided by Mr. Ken Kissel of ARL. Incorportation of the plotting option into the computer program was made

possible by Mr. Edward Van Schaik of the IBM Dayton office whom I thank for his help. To Mr. Bill Weiss of Oak Ridge Technical Enterprises Corporation, I extend my thanks for the loan of detectors for this work. Help on many phases of the work was given by Dr. Wm. C. Eppers of the Advanced Techniques Branch, Electron Technology Laboratory, WPAFB.

This thesis was typed by Miss Joan Allen, an employee of The National Cash Register Company, Dayton, Ohio, to whom I extend my deep appreciation for not only the fine typing job but also the encouragement in persevering with my work.

List of Figures

Figure		Page
1	Proton Recoil Geometry	15
2	Target - Detector Geometry	19
3	Comparison of Reaction Rate and Energy Loss	22
4	Section of Target Chamber	37
5	Volume Relationships for Computing Pressure	41
6	Elevation of Spectrometer	47
7	Equipment Layout	48
8	Schematic of Alarm Circuit	51
9	Input Circuit Parameters for Charge Sensitive and Voltage Sensitive Amplifiers	60
10	Importance of Pulse Shape in Summing	62
11	Schematic of Coincidence Circuit	64
12	Schematic of Summing Circuit	65
13	Schematic of Sputtering Apparatus	79
14	Apparatus for Reduction of $Zr(TFA)_4$	86
15	Condition for Double Value Energies for E3 and E4	91
16	Flow Chart of Main Program	96
17	Flow Chart for Plotting Program	97
18	Proposed Gas Pressurizing Device	100

Contents

	Page
Preface	ii
List of Figures	iv
Abstract	x
I Introduction	1
General	1
Choice of Reacting Medium	2
Pressure System	3
Computer Program	4
Neutron Production	5
II Preliminary Investigation	6
Solid State Detectors	6
Characteristics	6
Energy Range	8
Resolution	8
Applications	9
Experimental Results	10

Page

II Preliminary Investigation (Cont'd)

Comparison of Reacting Media 11

Spectrometer Types 11

Choice of Media 12

Properties. 12

He^3 13

Target-Detector Geometry 14

Proton Recoil 14

Reactions with Light Nuclei 18

Resolution-Efficiency Comparison 20

Reaction Rate 20

Resolution Loss 24

Efficiency 26

Final Comparison 27

III Design and Construction of Spectrometer 29

Design. 29

Choice of He^3 29

He^3 Pressure 30

Page

III Design and Construction of Spectrometer (Cont'd)

Equipment Capabilities 33

Target Chamber 35

Pressure System 39

Construction and Operation 43

General 43

Protective Control Devices 46

Leak Detecting 52

Target Chamber 53

Pressure Control 54

Operation 55

IV Electronic Circuitry 58

General 58

Special Requirements 58

Detector Output 58

Pulse Shaping 61

Circuit and Equipment 63

Calibration of Circuit 66

Circuit Modification 69

Page

V Neutron Sources 71

General 71

Types 71

Homogeneous Sources 73

Van de Graaff (d,D) Sources 75

Target Preparation 78

General 78

Ion Sputtering 80

Results of Sputtering 82

$Zr(TFA)_4$ Compound 83

VI Computer Program 87

Introduction 87

Basic Theory 87

Program 93

Results 98

VII Discussion and Conclusions 99

Page

Bibliography 102

Appendix A: Plot - Sub-Routine of IBM 1620 FORTRAN with Format 108

Appendix B: Sample Output of Computer Program . 117

Appendix C: Calculation of Solid Angle 136

Appendix D: Photographs of Equipment 138

Vita. 143

Abstract

A fast neutron spectrometer is designed and constructed. The spectrometer uses He^3 gas at pressures up to 1500 psi as the reacting medium for fast neutrons and solid state detectors as the means of detecting the product particles of the reaction. An investigation is made into the best geometry and materials to use in order to obtain optimum use of the solid state detectors. A digital computer program is presented to calculate and plot the energy and angular distribution of the products of the reaction. To prepare targets for neutrons production with a Van de Graaff generator, two means of obtaining a thin metallic coating on a target disc are investigated. These are ion sputtering and reduction of a metal from a new metallic compound, $Zr(TFA)_4$. The design and construction of the spectrometer are completed but no spectroscopic data taken. Use of the computer program provides data with good correlation to that found in the literature. Some experimental data is obtained concerning the ion sputtering process.

I. Introduction

General

A spectroscopic analysis of a source of neutrons requires the determination of the number of neutrons emitted at various energies. For both thermal and fast neutrons this is usually done by having the neutrons interact with some reacting medium from which one or more secondary charged particles are produced and subsequently detected. These secondary particles are detected to indicate the number of neutrons in a region of space and to provide a means of determining the neutron energies. The primary requirements are a target material with the proper cross section, product charged particles with energies at the time of detection accurately representing the neutron energies over a given range, and a detection and display system which does not introduce undue distortion to the neutron count for each energy.

The $He^3(n,p)T$ reaction may be used to study the energy distribution of fast neutrons by employing a geometry which provides for introducing the helium gas in a small volume between two solid state detectors and by using coincidence circuitry which admits to the pulse analyzer only those pulses representing one neutron interacting with the target gas. Solid state detectors are used to take

advantage of the excellent resolution and linearity, small size and low bias voltage requirements inherent with their use. To increase the efficiency of the spectrometer, and study the effect of varying gas pressure on count rate and resolution, provisions are made to introduce the gas between the detectors and regulate the pressure over the range of 0 to 1500 psi. Due to requirements peculiar to controlling helium pressures over this range while maintaining the ability to monitor the pulses from the detectors and the ability to vary the spacing and aperature between them; the design and construction of the equipment occupies the major portion of the effort.

Choice of Reacting Medium

This work was initiated by an interest in continuing that done by Major Rucker (Ref 29) in investigation of the use of solid state detectors in conjunction with fast neutron spectroscopy. The equipment used by Major Rucker employed a Li^6 target sandwiched between two solid state detectors. Use of the Li^6 target was compared to use of He^3 and proton recoil from a hydrogenous target. Using efficiency and resolution as a basis of comparison, the Li^6 target was ruled out leaving the proton recoil and He^3 systems under consideration. Because of the interest in the use of He^3 for fast neutron spectroscopy,

the relatively small amount of He^3 data available, and other considerations discussed in detail in following chapters, it was decided to pursue the use of He^3 as a target gas. At the time of this decision, the only known work done using He^3 for fast neutron spectroscopy was that performed by Dr. Geoff Dearnaley of the Atomic Energy Research Establishment, Harwell, England. It was hoped that additional data could be obtained using the gas at near atmospheric pressure and, in addition, data with the gas at much higher pressures.

Pressure System

The design of the gas pressuring equipment is based on use of 1000 cm^3 of gas at one-half atmosphere which was left over from another earlier project. This gas is to be compressed by reducing its volume to the point that the pressure is the value desired. Initially, this was to be accomplished by the use of solid metal pistons; but after working with these for some time, it was decided to switch to the use of a liquid mercury piston. Although much time was spent in constructing a device from which no spectroscopic data was obtained, it is felt that a great deal of valuable experience was obtained and some interesting and valuable design characteristics explored.

A different approach to compressing the gas is discussed in Chapter VII of this report and it is believed that a device of this type can be built to pressurize helium gas to 2000 psi simply and reliably.

Computer Program

The computer program that forms a part of this thesis is a result of the investigation of the energy and angular distribution of the products of the nuclear reactions used in neutron spectroscopy. Equations governing these reactions are available in various forms and some hand calculations were made using equations found in Evans (Ref 12:408-417). Due to the tedious nature of the mathematics involved for more than a few angles and energies, it was decided to develop a digital computer program which would perform these calculations for numerous reactions. At the beginning, the program was written to handle only a few reactions of special interest but later was modified to be of more general use. The program was written for the IBM 1620 computer located at the Air Force Institute, WPAFB. The computer program was developed more as an available tool than as a means of obtaining data for this project, although data of value to this work was obtained. Sufficient results of the executed program are enclosed to show its capabilities. Those interested in using this program more

extensively are provided with the program statements and write-up.

Neutron Production

Although two means of preparing neutron targets are discussed relative to the production of neutrons using a Van de Graaff particle accelerator, no detailed data was obtained to indicate what advantage there might be in using these procedures. The two methods are discussed as a possible improvement over the more commonly used methods of obtaining a thin coating of absorbing metal on a target disc. The ion sputtering process was tried by attempting to coat a glass slide with zirconium. Some rough data is presented concerning this experiment, and the results are favorable enough to warrant some additional experimentation. The other process, reduction of a metal from a volatile compound onto the target disc, is the most interesting from the standpoint that the compound to be used is entirely new and the process relatively simple. Experimentation with this compound may be a fruitful area of study. Characteristics of neutron sources are discussed because of their importance in development of a spectrometer of this type.

II. Preliminary Investigation

Solid State Detectors

Time was devoted to the study of solid state detector characteristics to insure understanding of their operation and proper integration into the spectrometer. Prior to any work on the spectrometer, some preliminary experiments were performed with ORTEC (Oak Ridge Technical Enterprises Corporation) detectors and detectors manufactured by RCA Victor Co. Ltd. of Canada. A brief discussion of solid state radiation detectors is presented for those not familiar with their characteristics. More detailed information is available in the references.

Characteristics. The solid state detector is similar to the common gas-filled ionization chamber and the principle of operation is identical. There exists a charge-free region across which a field is applied. Ionization in the charge-free region results in migration of electric charges to the anode and cathode of the chamber and the charge collected is amplified as a voltage pulse to provide a usable output. Gases require about ten times the ionization energy as do the semiconductor solids used in solid-state detectors. Here, then, is the first big difference in the gas-filled chamber and

solid. The same energy particle reacting in both media will provide ten times the usable charge in the solid. As is the case in the ionization chamber, there is no internal amplification of charge so the signal is still small compared to a gas tube operated in the GM region.

The dimensions of a solid state chamber are much smaller than the common gas-filled tube. The volume of the charge-free region of the solid is on the order of 100 mm^3 and the distance between the collection terminals for the positive and negative charges is usually less than 1 mm. The reduced cathode to anode distance results in a much larger field for the same bias voltage. Presence of a larger field provides more efficient and rapid collection of charge. Normally the maximum bias of a solid detector is governed by the material. A nominal value of bias voltage for a solid detector is 60 volts. Larger values up to several hundred volts are used for special applications. The products of ionization by an incident particle do not travel as far and have less opportunity for recombination. The faster collection time results in a faster rise time ($\approx 10^{-9}$ sec) of the voltage pulse produced which, in turn, makes possible faster counting rates.

Energy Range. Since the energy deposition per unit length (i.e., dE/dX) of a charged particle in a solid is much greater than in a gas, complete ionization (i.e., complete deposition of energy) is easily obtained in a solid detector. This leads to a wider range of linearity for pulse height versus energy. This "dynamic range" of the detector is important for a spectrometer where it is desired to look at a spread of energies and to be able to detect each energy particle equally well.

Resolution. Energy loss per ion pair produced by charged particles is independent of particle type and also energy over a wide energy range. Since complete energy deposition can be assured for a wide energy range of particles and fast and complete charge collection are inherent, the energy spread of a peak of a monoenergetic source can be limited largely to other factors. One of these would be varying amounts of energy lost in reaching the sensitive volume of the detector. This turns out to be insignificant as the "window" thickness of most solid state detectors is quite small. Another contribution to a spread of energy in a counts as a function of energy plot is the noise level of the detector which would broaden the peak from a monoenergetic source. The noise of a semiconductor

detector is a function of leakage current and voltage drop through the detector. Both of these generally can be maintained at an acceptable level. The leakage current is usually less than 1 μa and is partially a function of applied bias.

Adding all contributions which would increase the energy width of a monoenergetic peak (i.e., hurt resolution), the resolving power obtainable is much better than for any other available detection device with experimental results showing the resolution of 0.1% possible. It is primarily this excellent resolution which makes the use of solid state detectors look promising for a spectrometer where the ability to separate energy peaks is very important. An added advantage is relative insensitivity to the γ's which are usually present in a region of neutron flux.

Applications. The charge-free region of a solid state detector is called the depletion region and is usually produced by the application of a bias. The thickness of the region can be controlled by the amount of bias and the resistivity of the semiconductor material. Increasing the bias on a detector increases the depletion region depth and the range of linear response of pulse height to particle energy. These detectors have been constructed to provide linear detection for all but high energy

protons, betas, and γ rays. Presently most commercially available detectors are most suitable for α's, protons, deuterons or other heavy charged particles. Through processes which extend the depth of the depletion region, detectors for radiation of lower ionization potential have been developed. There is no problem in obtaining detectors which are suitable for detecting product particles for the neutron energy range considered for this spectrometer (.01 to 10 mev). At higher energies, detectors of greater depletion region depth must be used.

Experimental Results. The experiments performed with the ORTEC and RCA detectors investigated and confirmed the effects of bias on the depletion region and leakage current. Resolutions of less than 3% (width at half-maximum) were obtained for both the ORTEC and RCA detectors using a U-233 source of 4.8 mev α's. The effect of bias on leakage current was checked and the results confirmed the figures found in the literature. The leakage currents observed while varying bias of a type "A" RCA detector from 10 to 50 volts were on the order of .3 μa. For later reference, it should be mentioned that the capacitance of the semiconductor detector is a function of the detector area and inversely proportional to the square root of the bias.

Comparison of Reacting Media

Spectrometer Types. To detect neutrons, they must first interact in some way to produce one or more charged particles which can then be detected. For a spectrometer, the energy of the neutron must be conserved in the process so that there will be true energy representation when the product particles are detected and their energy converted to pulses. Basically, there are three types of interaction which may be used for a spectrometer.

1. Method of associated particle in creating a neutron: the neutron energy is determined knowing the nature of the reaction from which the neutron and its associated particle are produced.
2. Recoil method: the neutron transfers its energy to a second mass. The neutron energy is a known function of the recoil mass energy.
3. Reaction with light nuclides: such reactions as $B^{10}(n, \alpha)Li^{7}$ and $He^{3}(n,p)T$ are representative.

In addition, a fission reaction may also be used in which two heavy mass particles are emitted with a large "Q" energy.

Choice of Media. A comparison of the reacting media was preceded by a choice of which of the three basic procedures would be used. The first is of limited use and was not considered. The second and third were limited for this comparison to proton recoil for the second type reaction and $Li^6(n,\alpha)T$ (Q = 4.78 mev) and $He^3(n,p)T$ (Q = .764 mev) for the third. It should be noted at this point that comparison between proton recoil and nuclear reactions is based on more than just the reacting media. The proton recoil method involves one detector instead of two and different circuitry. At the present time, only the reacting media is considered.

Properties. Properties of interest are the cross section for interaction, the energy range of usefulness of the reaction, and the effect on the resolving power of the spectrometer. The cross section must be both large enough and free of resonant peaks in the energy range under consideration. Also there should be no alternative reactions producing additional charged particles. The "Q" of the reaction should be positive for proper detection of low energy neutrons. A comparison of the cross sections was made for a 5.24 mev neutron which is approximately the maximum energy neutron available from a 2 mev Van de Graaff accelerator using a (D,d)

reaction. The "D" is deuterium gas. The cross sections are as follows (Ref. 4):

$$\sigma|_{H} = 1.55 \times 10^{-24} \text{ cm}^2$$

$$\sigma|_{Li^6} = 0.082 \times 10^{-24} \text{ cm}^2$$

$$\sigma|_{He^3} = 0.28 \times 10^{-24} \text{ cm}^2$$

Of course these cross sections don't tell the whole story, as the number of target nuclei must be considered. This is done in the resolution-efficiency comparison. The cross section for all three of these reactions is smoothly varying in the range from .01 to 10 mev except for the Li^6 reaction which has a resonance at about .25 mev and there is only one possible reaction. In each case at low neutron energies, the higher Q of the Li^6 reaction results in poorer resolution than the He^3 reaction in that the resolution is proportional to Δ (E + Q)/E (Ref. 18:33). A change in E for a Q of 0.764 mev represents a smaller fractional change than for a Q of 4.78 mev.

He^3. The lower Q of the He^3 reaction causes more of the pulses for low neutron energies to fall within the noise level of the circuit and in this regard, is a disadvantage. The triton from the He^3

reaction will penetrate further than the $Li^6 \alpha$ into the depletion region of the solid state detector before giving up all of its energy. This results in a slower rise time and higher probability of spurious coincidences due to various background radiation. Another disadvantage of the use of He^3 is that the elastic scatter cross section is greater than the (n,p) cross section up to 2.5 mev. Contributions from the He^3 recoil spectrum must be accounted for in this range.

Target-Detector Geometry

Proton Recoil. The relationship between the recoil proton and neutron energies is given by (Ref. 25:5-42):

$$E_p = E_n \cos^2 \phi$$

where ϕ is the angle of scatter of the proton measured from the path of the neutron. The following sketch shows the relation of the target and detector. E_p is defined as the proton energy and E_n the neutron energy.

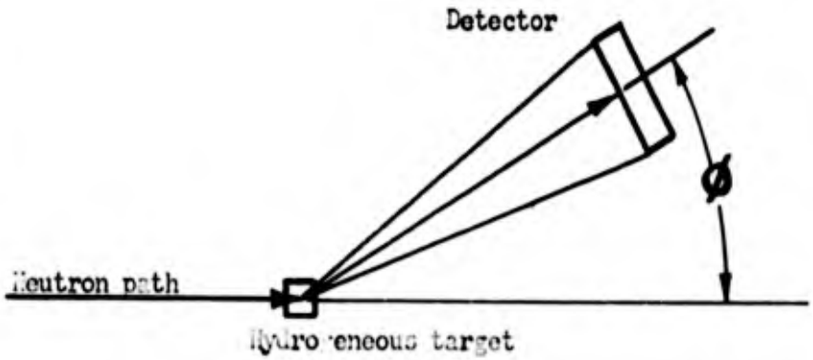

Figure 1 Proton Recoil Geometry

The probability for scatter per unit solid angle is expressed by (Ref 25:5-42):

$$\frac{1}{\pi} \cos \phi$$

The unit solid angle is defined as a number equal in magnitude to the area subtended on a sphere equal to the radius of the sphere squared. The units are steradians with one steradian equal to $1/4\pi$ of the solid angle around a point. Protons scattered from hydrogenous material by neutrons are emitted within 90^{o} of the neutron path or in the forward 2π steradians. The probability for scatter can be expressed as:

$$dp = \frac{\cos\phi}{\pi} d\omega \; ; \; d\omega = \frac{dA}{R^2}$$

$$p = \frac{1}{\pi}\int \cos\phi \, d\omega$$

$$dA = 2\pi R^2 \sin\phi \, d\phi$$

Changing to ϕ as the variable of integration where ϕ is the intercept angle of the zone of the sphere with radius R gives:

$$P = \frac{2\pi}{\pi}\int_{\phi} \frac{R^2 \sin\phi \cos\phi \, d\phi}{R^2}$$

so that the final probability function is

$$P = 2 \int_{\phi} \sin\phi \cos\phi \, d\phi$$

In these calculations, the neutron source is assumed to be collimated.

It can be seen then that in order to establish a relationship between the proton and neutron energies, the angle of proton recoil must be accurately determined. The same thing is true for calculating the efficiency of the system since the probability of scatter is also a function of recoil angle.

The maximum recoil proton energy occurs at an angle ϕ of 0^{o}. By plotting $\cos^{2}\phi$ as a function of ϕ, it is seen that the function varies most slowly in the vicinity of 0^{o} and fastest at 45^{o}. It is desirable to measure the energy of a proton at an angle where $dE_{p}/d\phi$ is maximum so that the separate energies can be better resolved. It is best, therefore, to work at ϕ close to 0^{o} in detecting the recoil protons to obtain the highest energy and efficiency and at 45^{o} for the best energy resolution.

The distance of the detector from the source of protons will be a compromise between detection efficiency and energy resolution. The further the detector is from the source of protons, the smaller will be

the angle subtended and, consequently, a smaller range of energies will be covered. At the same time, a greater separation distance will permit fewer protons to be detected.

Reactions With Light Nuclei. For this case, there are two particles which must be detected. These particles generally are emitted isotropically; however, contrary to a common misconception, the two particles are not scattered very closely to 180^{o} of one another in the lab system except for low neutron energies. The energies are greatest in the direction of the neutron with the forward shift in product particle energies becoming more pronounced as neutron energy is increased. See Appendix B for examples of the larger energies of those particles emitted in the forward direction. For the two reactions considered, no angles of emission are prohibited so that the detectors cannot be preferentially located. The ideal target-detector geometry would be one in which a solid angle of 4π steradians is subtended by the detectors. This can be most closely approximated by placing two detectors close together with the target material between. The following sketch shows the geometry used. The angle notation is that used in Chapter VI.

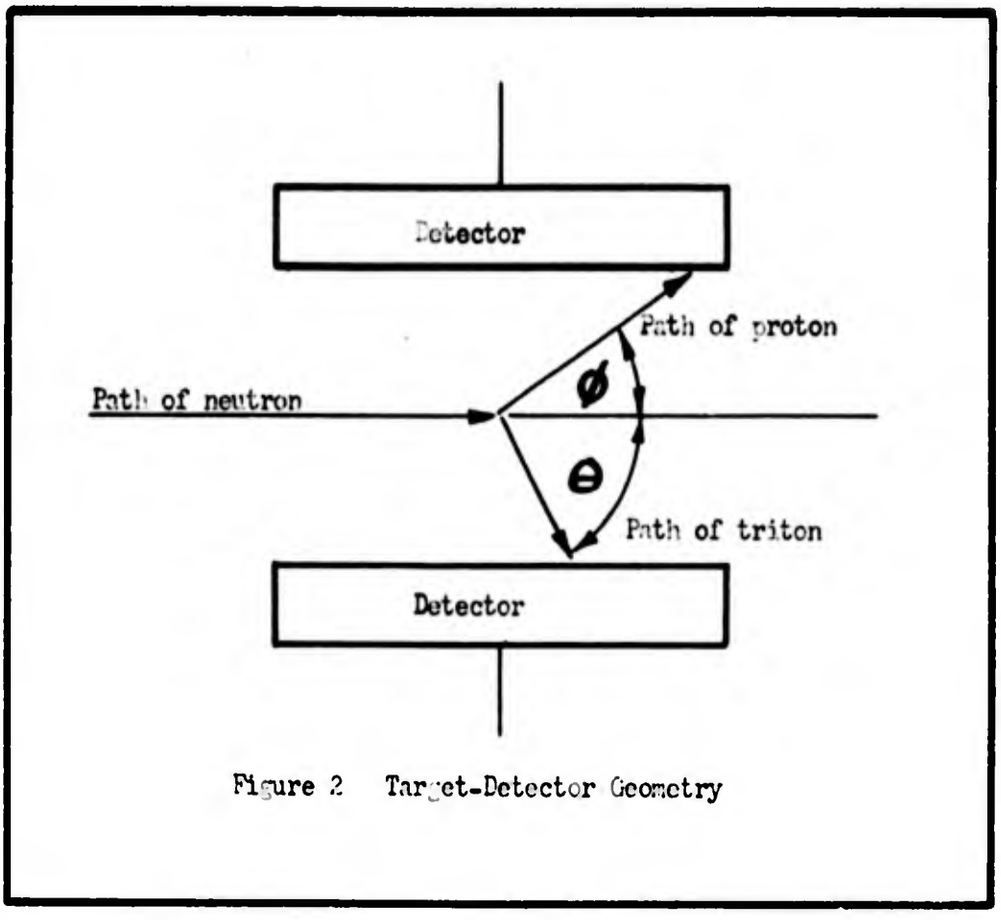

Figure 2 Target-Detector Geometry

A measure of the efficiency of detection of the two product particles is the fraction of 4π steradians subtended or $\Omega/4\pi$. Ω is defined as the solid angle subtended at a point by the detector. Calculations for determining Ω for circular detectors is contained Appendix C.

Resolution-Efficiency Comparison

In a comparison of this type, one must be careful not to weigh calculations in favor of one particular reaction. The same neutron energy must be used in the calculations for each reaction, and energies of the secondary charged particles must be realistic. For this comparison, a neutron energy of 5.24 mev was used. Again, this is the approximate maximum neutron energy produced by the (D,d) reaction using a 2 mev deuteron.

Reaction Rate. A 5% loss in energy of the heaviest charged particle in the reacting medium was chosen as a standard of comparison. Using this figure, the thickness of target material was calculated for Li^6, He^3 and H_2. Next, the effective reaction cross sections were calculated for each of the three volumes considering a cross sectional area of 1 cm^2. The number of atoms/cm^3 for each material is:

$$N|_{He^3} = 2.69 \times 10^{19} \text{ atoms/cm}^3 \text{ (STP)}$$

$$N|_{H_2} = 2.69 \times 10^{19} \text{ molecules (STP)}$$

$$N|_{Li^6} = 0.536 \times 10^{25} \text{ atoms/cm}^3$$

The dE/dX figures were taken from Whaling (Ref. 33) and are as follows:

0.0153 mev/cm for a 5 mev proton in H_2 gas

0.065 mev/cm for a 2 mev triton in He^3 gas

473 mev/cm for a 3.5 mev in Li^6

The different energies chosen for each particle are based on essentially complete energy transfer to the recoil proton and rough averages of the triton and alpha particles emitted by the nuclear reactions. Subsequent work with the computer program (Chapter VI) made possible exact average energy computation over any range of angle of emission. Results of this program are tabulated in Appendix B for a 5.24 mev neutron on Li^6 and He^3. It can be seen that the values chosen here are not accurate averages but are close enough for this comparison.

Figure 3 shows how the volume of Li^6 is limited by the much larger dE/dX of Li^6 as compared to H_2. Using the 5% energy decrement, the thickness of each material was calculated for a 5.24 mev neutron to be:

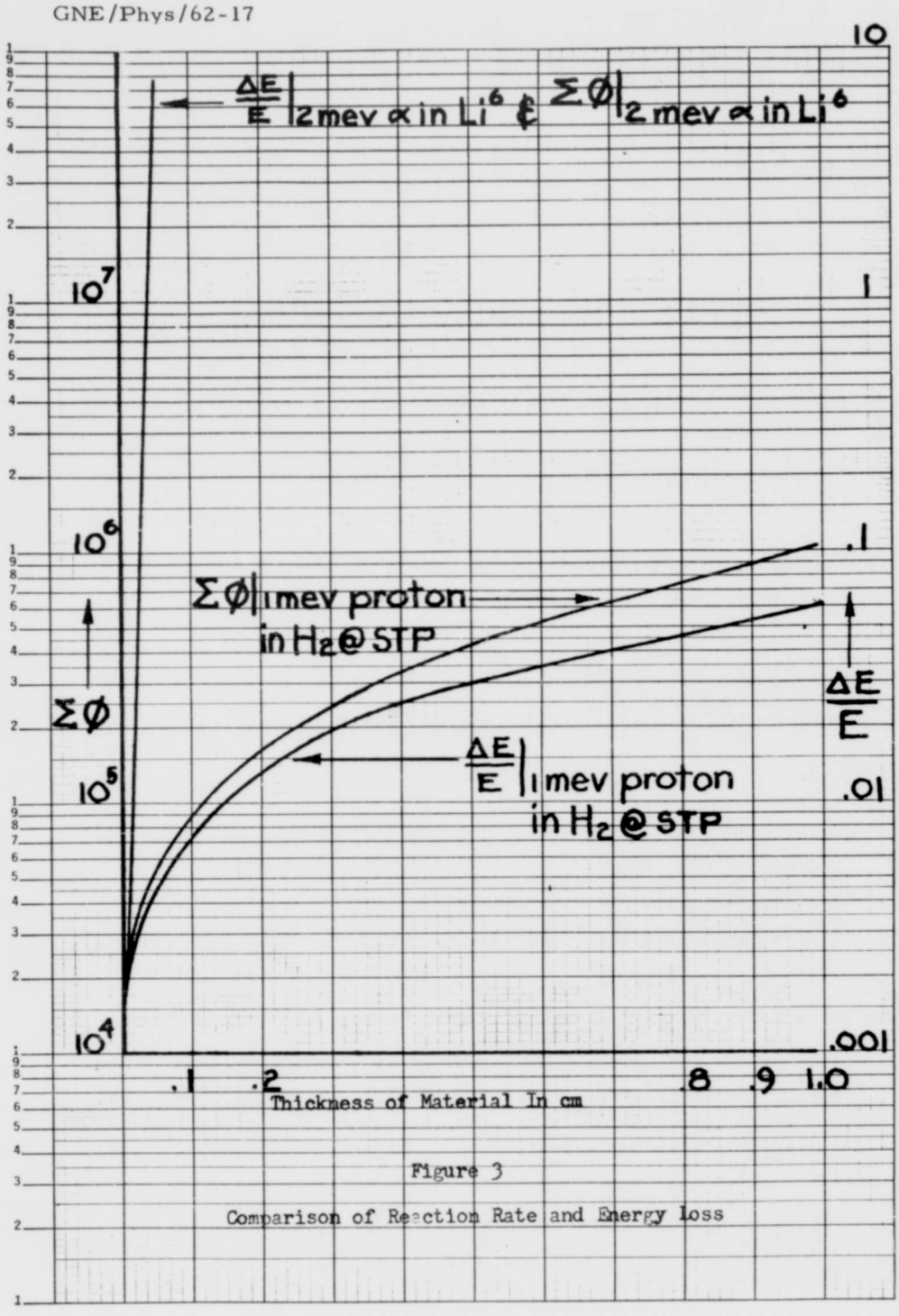

Figure 3

Comparison of Reaction Rate and Energy Loss

$\Delta X|_{H_2}$ = 16.3 cm (To maintain a point source, 1 cm was used and the pressure considered to be 16.3 times atmospheric.)

$\Delta X|_{He^3}$ = 1.54 cm

$\Delta X|_{Li^6}$ = 3.7×10^{-4} cm

With these figures as the thickness of 1 cm^2 sections of the materials, the number of atoms was calculated and multiplied by the microscopic cross sections given earlier. The resulting effective macroscopic cross sections for the three volumes are given below.

$$\Sigma|_{He} = 13.6 \times 10^{-4} cm^{-1}$$

$$\Sigma|_{He^3} = 1.16 \times 10^{-5} cm^{-1}$$

$$\Sigma|_{Li^6} = 0.163 \times 10^{-5} cm^{-1}$$

For an arbitrary flux of 10^{10} neutrons/cm^2-sec, the reaction rates are merely the above cross section values increased by a factor of 10^{10}.

$$\Sigma\phi|_{H_2} = 1.36 \times 10^7$$

$$\Sigma\phi|_{He^3} = 1.16 \times 10^5$$

$$\Sigma\phi|_{Li^6} = 1.63 \times 10^4$$

Resolution Loss. The loss in resolution by the charged particles traveling from the target to the detector is now considered. An arbitrary separation distance of 10 cm was used for the proton. At this distance, a 1 cm^2 circular detector subtends an angle that will give an energy spread of 0.063 mev. This figure was calculated as follows.

$$\measuredangle \text{ subtended} = 6^\circ 28'$$

$$E_p = E_n \cos^2 \phi$$

$$\Delta E_p = E_n \cos^2 \phi_1 - E_n \cos^2 \phi_2$$

$$\phi_1 = 0^\circ$$

$$\Delta E_p = (1 - .988) 5.24 \text{ mev} = 0.063 \text{ mev}$$

This represents 1.2% loss of resolution of a 5.24 mev neutron. The calculations for proton recoil up to now have been based on use of H_2 gas as the radiator of protons; however, for the present discussion, it will be assumed that the radiator is some hydrogenous material with the same cross section and energy decrement as H_2 gas. The proton is assumed to pass through a vacuum in reaching the detector so that no further energy is lost. This modification is made to permit ignoring energy loss of the proton in passing through a container for the H_2 gas.

For the case of He^3 sandwiched between two detectors, there is no additional energy lost from the triton in reaching the detector. On the other hand, the Li^6 must be supported by a thin foil and the energy loss through the foil must be considered. If the foil is nickel and is 2.03×10^{-5} cm thick (8×10^{-8} in.), the energy loss of a 3.5 mev α passing through the foil is 0.0906 mev, which amounts to 2.6% of the neutron energy.

Efficiency. Up to this point, the efficiency of the various systems has not been considered except to compare the macroscopic cross sections. The next step is to compare the efficiency of the proton-recoil arrangement to that of the detector sandwich geometry. At a distance of 10 cm from a point radiator, a 1 cm^2 circular detector subtends an angle of about 0.01 steradians. This figure was calculated using the expression given in Appendix C. With Ω equal to 0.01, the ratio of Ω to the total solid angle is $0.01/2\pi$ or 1/628. It should be remembered that the proton recoil is restricted to a solid angle of 2π in the forward direction. Therefore, on this basis alone, only 1/628 of the total recoil protons will be detected; however, the probability of scatter at different angles ($dP/d\omega = \cos\phi / \pi$) must also be considered. Plotting the differential

probability as a function of angle yield an average $dP/d\phi$ of 0.16. Since detection is made at an angle of recoil near 0°, the probability is greatest ($\cos \phi = 1$) and the fraction detected must be modified accordingly as follows:

Probability of scatter at $0^{\circ} = 0.318$

Corrected fraction detected = $1/628 \times 0.318 = 0.318/628$

The separation distance between detectors in the case of the He^3 and Li^6 reactions can be made quite small. It is only limited by the requirement to provide an adequate volume of target material. Again, using the expression for the angle subtended by a circular detector 1 cm^2 in area and assuming the reaction to take place on the center line of the detectors and half-way between them, the solid angle subtended 0.01 cm away from one detector is 6.15 steradians and $\Omega/2\pi = 0.98$. The total loss in detection efficiency is 2%, or considerably less than for the proton-recoil geometry.

Final Comparison. It is now possible to compare the total detection efficiency of each of the three systems.

TARGET	REACTION RATE	LOSS IN RESOLUTION	NUMBER DETECTED
H_2	1.36×10^7	6.2%	$(1.38 \times 10^7) \times .318/628 = 7.0 \times 10^3$
He^3	1.16×10^5	5.0%	$.98 \times (1.16 \times 10^5) = 1.14 \times 10^5$
Li^6	1.63×10^4	7.6%	$.98 \times (1.63 \times 10^4) = 1.6 \times 10^4$

It should be apparent that low angles of incidence to the detectors can result in partial energy deposition as can a particle which passes through the depletion region of the detector without giving up all its energy. Both of these factors contributing to loss of resolution were not considered for this comparison but are discussed in the next chapter. In addition, the α particle is considered to be emitted at right angles to the nickel foil. If this is not the case, which is true for many α's, the energy loss in the foil is greater.

III. Design and Construction of Spectrometer

Design

Choice of He^3. From the preceding chapter, He^3 is seen to offer some advantages over the use of a Li^6 reaction or proton recoil from a hydrogenous target. Not mentioned before is the(n, p) background caused by fast neutrons interacting with the silicon of the detectors. This presents a problem in using proton recoil in that pulses are only being received from one detector and there is no way to discriminate against the contribution of pulses from the (n, p) protons. In the case of the He^3 and Li^6 reactions, two detectors are necessary to detect the two particles simultaneously; and by the use of proper coincidence circuitry, background from the(n, p) reaction can be virtually eliminated. The(n, p) reaction in silicon has a Q of 5.598 mev (Ref. 13) and the cross section becomes significant at neutron energies above 4 mev. At 8 mev, the cross section is 0.4 barns (Ref. 4). It would be possible to circumvent the problem of the(n, p) background in proton recoil for neutron energies above 4 mev by setting the detector at an angle that would prevent neutron interaction with the silicon. This could only be done, of course, with the collimated beam of neutrons on which

previous calculations were based. Because of the problem of (n,p) background in silicon and the lower efficiency, proton recoil was not chosen for use in the spectrometer. He^3 was chosen over Li^6 because of the better resolution possible and the higher efficiency. In addition, little data was available concerning use of He^3 in a fast neutron spectrometer, whereas a number of commercial spectrometers are constructed using Li^6 as the target medium.

<u>He^3 Pressure</u>. From Chapter II, the thickness of He^3 to give a maximum loss of 5% of a 5.24 mev neutron energy is 1.54 cm. With this detector separation, the counting efficiency is reduced due to the smaller solid angle subtended. An arbitrary detector separation distance of 0.02 cm was chosen and a pressure calculated to give the same number of target atoms in 0.02 cm^2 as are in 1.54 cm^2. The cross-sectional area of the target chamber is assumed to be 1 cm^2. The basic gas law equation for confined gases is:

$$\frac{PV_1}{T_1} = \frac{P_2V_2}{T_2}$$

Assuming an adiabatic process for compression, the expression becomes:

$$P_1V_1 = P_2V_2$$

from which

$$P_2 = \frac{(1.54)(1)}{(.02)} = 77 \text{ atmospheres}$$

At this point, the source of He^3 was checked to determine its purity. A qualitative and quantitative analysis of the gas was performed. This analysis was performed by Dr. J. H. Futrell of the Chemistry Laboratory, Aeronautical Research Laboratories, WPAFB, using a mass spectrometer Model 21-103C manufactured by Consolidated Electrodynamics Corporation, Pasadena, California. Since He^3 gas contains a small percentage of tritium, it was first necessary to eliminate the possibility of a health hazard in performing the test. Tritium is a beta emitter giving off betas of 0.018 mev. Because the mass spectrometer is not vented to the building exterior, it was necessary to insure that the amount of He^3 released in the room would receive

adequate dilution to keep the tritium concentration below the maximum allowable of 2×10^{-4} microcuries per cubic centimeter of air. By checking with Mound Laboratories, Miamisburg, Ohio, it was found that the nominal percentage of tritium in the He^3 they produce is about 10^{-4}. From the tritium half-life of 12.26 years and the above percentage figure, one cubic centimeter of He^3 is found to have an activity of 1.19×10^{-6} curies due to tritium. Therefore, there must be approximately a 10^4 dilution of the gas. The spectrometer uses less than 1 cm^3 of the gas to perform the analysis and it was deemed safe to run the experiment without special precautions. The He^3 is below atmospheric pressure and can only leave the container when connected to a vacuum line or if the container is ruptured.

The first step is to analyze a standard sample of air used for calibration purposes. In this manner, it is possible to establish the sensitivity of the spectrometer to different mass particles. Using this calibration, the unknown sample is then introduced and analyzed. By subtracting out those components for which sensitivity factors had been found, the amount of He^3 could be established. This procedure is predicated on all the contaminants in the unknown gas sample being present in the standard air sample so that their sensitivity factors could be established. Since the most logical

thing to happen would be an intrusion of air, this was a safe assumption. There is a contamination of 15.95% air and 2.3% of other unknown contaminants leaving a He^3 content in the volume of gas of 81.8%.

The pressure of 77 atmospheres was modified to account for the impurities in the He^3. The new pressure is simply 1.18 X 77, or 91 atmospheres. The psi equivalent is 1340.

Equipment Capabilities. To permit operation of the spectrometer with adequate safety factors, a maximum design pressure of 3000 psi was chosen, using a maximum operating pressure of 1500 psi. The 1500 psi figure was chosen to provide a wider operating range for resolution and efficiency studies. The He^3 gas must be introduced and compressed into the target chamber with a minimum of contamination. There can be virtually no leakage out of the chamber and a very small fractional loss of the gas in recovery to the source container.

Besides increasing the target volume, larger detector separation distances will provide better system resolution. The product particles are incident to the detectors at larger angles from the detector surface. This means that there is less opportunity for

charged particles to lose only part of their energy by passing through part of the depletion region. The design makes it possible to vary the detector separation distance from virtually zero to approximately two centimeters.

The betas from the tritium in the He^3 will increase random coincidence counts as will the (n,p) reaction of neutrons in the silicon detectors. Although the fast neutrons are collimated, the spread of the beam at the target chamber is considered to include the detectors. There are no provisions for minimizing either of these contributions to random counts except by discrimination of the 0.018 mev beta pulse using a fixed discriminator in the circuit.

The limiting factor of linear response of pulse height to energy is the range in silicon of the least ionizing particle which, in this case, is the proton. The ORTEC detectors for which the equipment was designed have a maximum depletion depth of 300 μ. This limits the energy range of the spectrometer to 6 mev neutrons assuming that the protons' share of the neutron energy and Q of the reaction will be 6 mev.

Exposure of the solid state detectors to integrated dosage of radiation effects the operation of the detectors. No detailed investigation was made of the amount of radiation that can be

tolerated before the detector characteristics begin to change; however, a brief check of the literature indicates that there are no significant detrimental effects up to an integrated dose of 10^{10} fast neutrons/cm^2. One of the effects of an integrated flux of fast neutrons is to decrease the signal-to-noise ratio.

Target Chamber. The aperature as well as separation distance between the two detectors can be varied by inserting different size washers with different openings. Additional resolution studies may be made by drilling a washer with a series of small diameter holes rather than one larger hole. This will restrict the angle of incidence to the detectors to large values. Varying the aperature makes possible masking the edges of detectors as another means of eliminating partial energy deposition and consequent loss of resolution. The inside diameter of the target chamber is large enough, approximately one and one-eighth inches, to handle a variety of detector sizes. The two detector holders can be bored for detectors with outside diameters up to approximately seven-eighths of one inch and whose overall depth is approximately one-half inch. The simplicity of design makes it possible to easily change detectors by having available a number of detector holders bored for different outside dimensions. The detector holders can be easily removed

and replaced with a wrench with no detrimental effect on the vacuum and pressure seal. The detector holders were designed for ORTEC Series SA surface barrier detectors with an outside case diameter of 0.875 inch and would have to be modified for other types. The sensitive area of the detectors used is 64 mm^2. See Figure 4 for a section view of the target chamber. The chamber is approximately four inches long with an outside diameter of 1.25 inches and inside diameter of 1.125 inches. The left side is identical to the right side shown except for the absence of the pressure fitting and turned-down section of the front of the detector holder. These two items are required to provide a means of pumping a vacuum in the chamber and introducing the gas. The gas fills the chamber up to the "O" rings which seal for the vacuum and pressure. The space behind the detector is evacuated and filled with pressurized gas also so that the detectors experience equal pressure on all surfaces. The reduced diameter of the right hand holder provides a passage through which the chamber is evacuated. The spacing washers are also grooved to create a channel for evacuating the volume between the detectors and to the left of the washer.

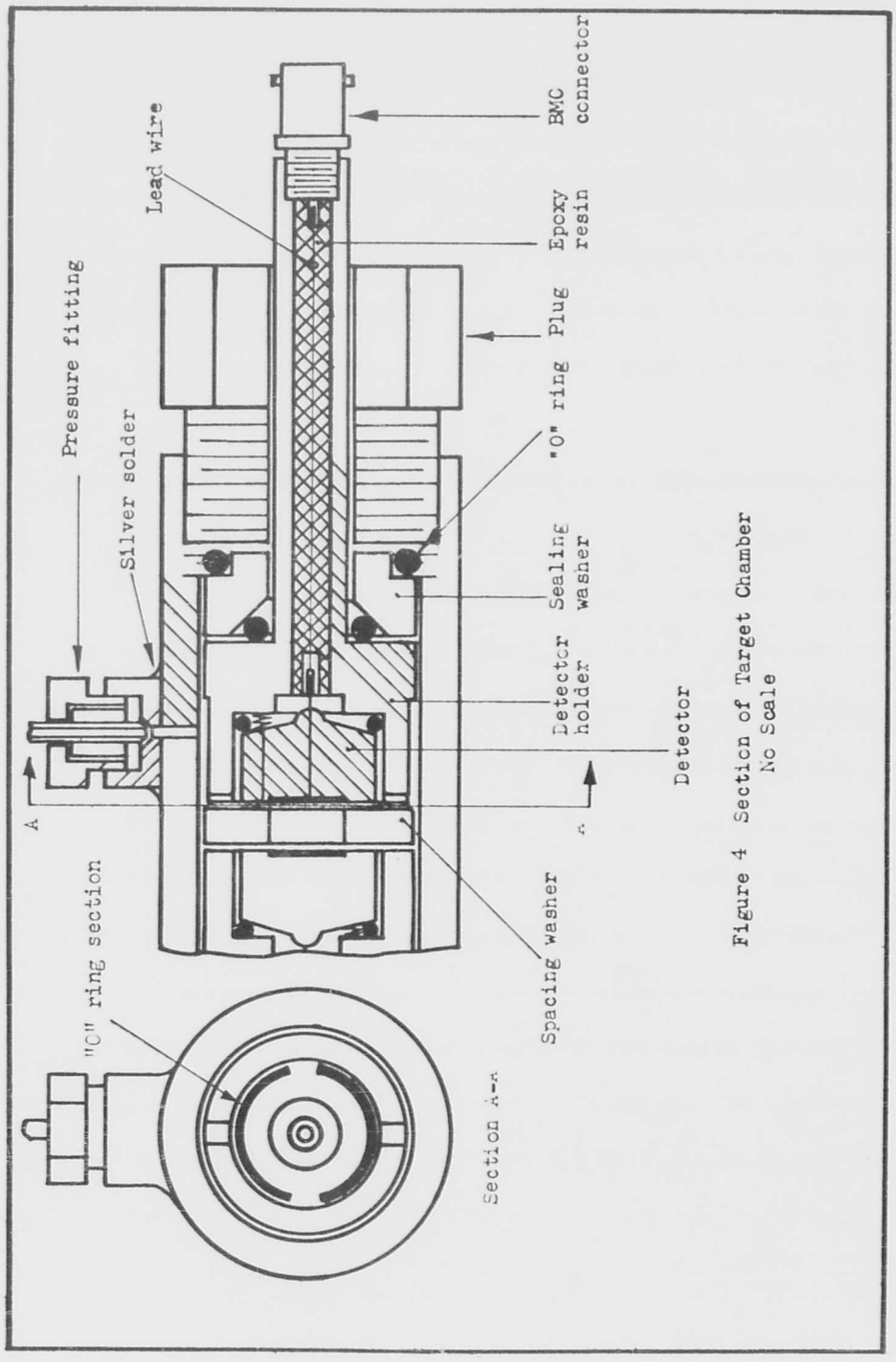

Figure 4 Section of Target Chamber
No Scale

The "O" ring sections behind the detectors serve as a means of insuring that the detectors are always flush with the face of the holders and also make removal easy. When in place, the detectors compress the rubber sections. The center lead of the detectors fits into a female receptacle taken out of a BMC connector. The receptacle was drilled out to provide an exact fit for the lead wire from the detector. The ground conductor is a thin metal strip seen on the drawing as an accordian-shaped piece behind the detector and below the "O" ring section. This strip is folded in spring fashion to make contact with the detector holder.

An uninsulated wire is soldered to the receptacle for the detector and is soldered to the BMC connector. The space between the receptacle and the BMC fitting is filled with an epoxy resin cement which acts as a seal and insulator. The detector receptacle is also set in the epoxy. The BMC fitting is threaded into the end of the holder to provide an additional seal.

The detector holders are held in place against the washer by threaded plugs. The "O" rings seal between the sealing washer and detector plug shank and between the washer and inner wall of the chamber. The chamber is threaded far enough to

permit sealing for pressure with no washer in place and to provide enough threads to hold when the largest washer is used. The threads are coarse to provide maximum holding power.

The pressure fitting is made by the High Pressure Equipment Company of Erie, Pennsylvania. The fittings and stainless steel tubing are rated at greater than the 3000 psi design pressure. The inside diameter of the tubing is 0.04 inch.

The thickness of the walls of the chamber is approximately one-eighth inch which provides for a factor of safety of greater than 100% based on the calculated stress in the walls due to the internal pressure and tabulated yield strength of brass.

Pressure System. The first design considered for compressing the gas was a solid mechanically-driven piston. This had the disadvantage of not being able to accurately monitor the pressure. In addition, achieving a good piston seal was felt to be too much of a problem with the stringent leakage prevention requirements. From a solid "O" ring piston, the design went to use of a mercury piston driven by a gas. This eliminated both of the problems of the solid piston but introduced others.

To prevent contamination of the gas, the target chamber and valves and lines from the He^3 source must be pumped to a vacuum.

After the target chamber is filled with the gas, the source container is closed off and the gas compressed. To compress the gas to the desired pressures in a finite volume, a much larger initial volume than the target chamber must be used as can be seen by the pressure and volume relationship of the basic gas law equation. Since the He^3 source is at one-half atmosphere, to provide for compression to 1500 psi requires a greater reduction of volume than if the gas were at higher pressure initially.

Figure 5 provides a means of understanding how the pressure system works to meet the design requirements. Valves "A" and "C" are closed and v_a and v_b are evacuated as is the mercury reservoir above the mercury level. Valve "B" is then closed and valve "A" opened to admit the He^3 gas. After the pressure stabilizes, valve "A" is closed and valve "C" is opened and pressure is applied to the top of the mercury column in the reservoir. The vacuum line to the reservoir is for out-gassing the mercury to help remove trapped air.

As the pressure is applied, the mercury level changes from level 1 to level 2 and can be regulated by controlling the pressure applied to the top of the mercury in the reservoir. The pressure in v_a and v_b will be essentially that of the gas forcing the mercury up in v_b with a difference equal to the height of mercury

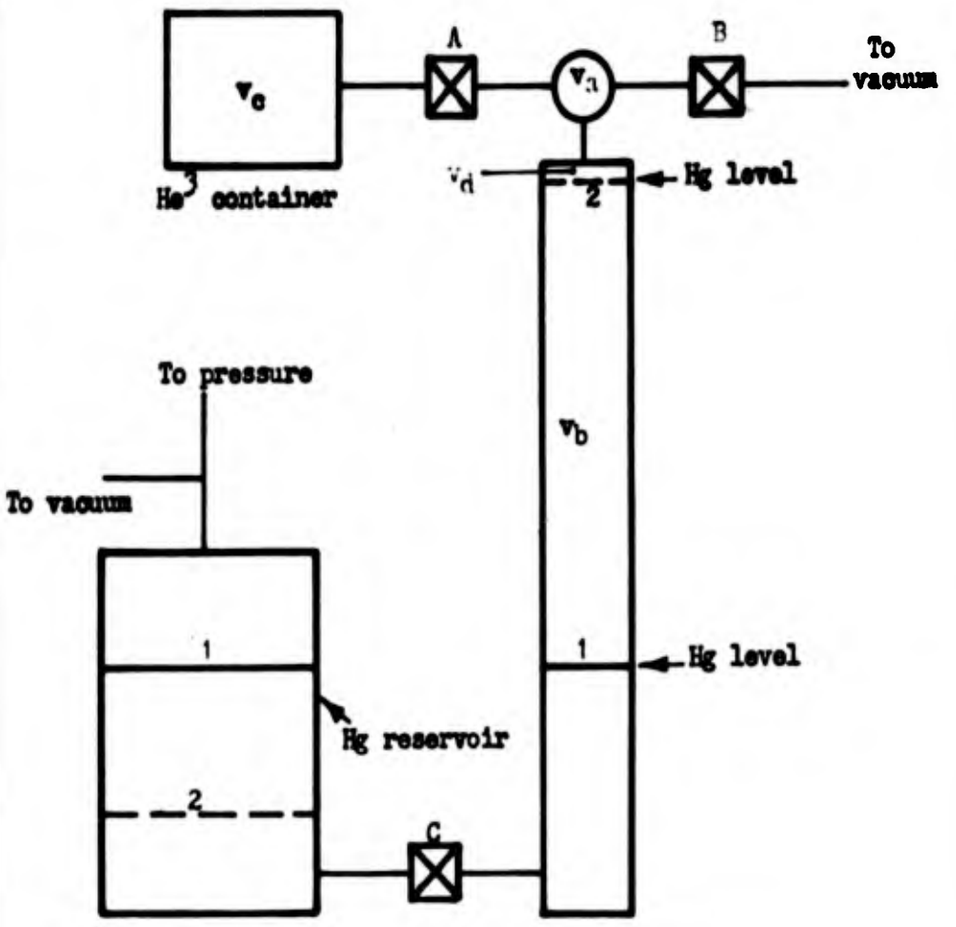

A, B&C are valves.
v_a represents volume of target chamber and valves and lines that contain He^3.

$V1 = v_a + v_b + v_c$

$V2 = v_a + v_d$

Hg level #1 represents conditions before pressure is applied.
Hg level #2 represents conditions after pressure is applied.

Figure 5

Volume Relationships for Computing Pressure

supported in v_b. v_b must be large enough so that after pressurizing, there will be a buffer volume, v_d, which will insure that no mercury enters the detector chamber. The valve "C" serves the purpose of holding v_b constant while that volume is being evacuated and while the target gas is being introduced.

Once again, reference is made to the basic gas law equation and to Figure 5 to demonstrate the relation between the starting pressure in V1 and the final pressure in V2. First of all, the drop in pressure is calculated after He^3 is let into v_a and v_b. Pressures are in atmospheres.

$$v_c \times P_c = P1 \times V1$$

$$v_c = 1000 \text{ cm}^3$$

$$P_c = 1/2$$

$$V1 = 2000 \text{ cm}^3$$

$$P1 = 1/4$$

and for compression into V2

$$V1' \times P1 = V2 \times P2$$

$$V1' = V1 - v_c = 1000 \text{ cm}^3$$

$$V2 = 1 \text{ cm}^3$$

$$P2 = 250$$

This is a hypothetical example. The final volume, V2, is controlled by the fixed volume of the valves and the lines. The initial volume above the mercury in the target chamber, v_b, was calculated to be 930 cm^3. For a final pressure of 1500 psi (102 atmospheres), the volume, V2 would be 2.3 cm^3. This is considered to be the volume of the target chamber, lines and valves (v_a).

Several factors must be carefully controlled for this system. The level of the mercury column is the most critical since mercury, or its vapors, will damage the detectors. The valves "A" and "B" must be tightly closed to prevent leakage when the gas is being compressed. Loss of the gas constitutes a health hazard as well as considerable expense. In addition, leakage of either of these valves will permit the mercury to rise into the target chamber.

Construction and Operation

General. The most difficult facet of this equipment is the gas pressurizing system. This is largely true due to inexperience on the part of the writer. It is also true, however, that the design requirements pose problems which are not easily solved.

All valves which are exposed to He^3 are miniature valves made by the High Pressure Equipment Company and are rated in excess of the 3000 psi design pressure. All tubing leading to the target chamber is small inside diameter high pressure tubing.

All tube fittings between v_a and v_b and between valves "A" and "B" are the same type as shown on the target chamber. Standard 1/4 inch stainless steel tubing and flared tube fittings were used to make connections such as between the mercury reservoir and He^3 pressure chamber. The pressure chamber is 1 inch stainless steel tubing made up in the form of a "U" to permit having the required volume, v_b, without excessive height. The use of standard tube fittings for the lines and pressure chamber where there are no small volume requirements was planned to permit flexibility in modifying the equipment. After initial efforts to achieve a leak-proof system it became apparent that the only sure way to prevent leaks is to weld or silver solder all connections in addition to using the standard fittings or special high pressure fittings. Accordingly, all connections where absolute leak prevention is required are arc welded, heli-arc welded or silver soldered. Silver solder is not used where the fitting is exposed to mercury due to the rapid amalgamation of the solder. For the same reason, only steel is used for the chambers containing mercury.

Before the equipment was constructed to use mercury, solid "O" ring pistons were tried as a means of forcing the gas into the target chamber under pressure. The pistons were gas driven in the same way the mercury piston is driven. The experiment with solid pistons was not a matter of academic interest since the

large volume of mercury required promised some difficult problems. If the solid pistons could be used, they would eliminate controling the large mercury volume required. The pistons are made from brass and are sealed with two "O" rings. They are approximately two inches long and made to fit each leg of the stainless steel "U" tube. For more positive sealing and to lubricate the pistons, octoil for vacuum pumps was placed in a thin layer on top of the pistons. Two steel rods were welded in place at the bottom of the straight sections of the "U" tube to prevent the pistons from sticking when they reach the bottom of their stroke.

It was hoped that it would be possible to move the pistons without undue additional pressure to overcome friction. The stainless steel tubing used for the cylinder is not perfectly symmetrical which is one problem in obtaining a perfect seal without too much friction. In addition, the pistons build up considerable static friction which required as much as 100 psi to overcome. This converted the two legs of the "U" tube into a lethal two-barrel pneumatic cannon instead of the desired device to pressurize the gas. Work with the solid pistons was abandoned when it looked so unpromising as to require excessive time to give the desired results.

Once the decision to use mercury was established, a reservoir for the mercury had to be obtained. A container for the filter of a 3000 psi oxygen system was available and modified for this purpose. This reservoir has sufficient volume to permit filling the pressure chamber without the mercury falling below the outlet level of the reservoir.

The relationship of all the components of the spectrometer is shown on Figure 7, and the relationship of the spectrometer to the auxiliary equipment is shown on Figure 6. The pressure equipment and target chamber are mounted on a 2 X 4 wood frame on coasters to permit moving around easily. The height of the frame is governed by the height of the beam tube of the Van de Graaff accelerator. The target chamber is positioned exactly by blocking under the frame. The frame also serves the purpose of providing a support for the preamplifiers and other equipment which must be close to the target chamber.

Protective Control Devices. The height of the mercury is monitored in two ways. A tungsten probe is inserted in the top of the reservoir through a pressure fitting manufactured by Conax Corporation, Buffalo, New York. The probe in contact with the

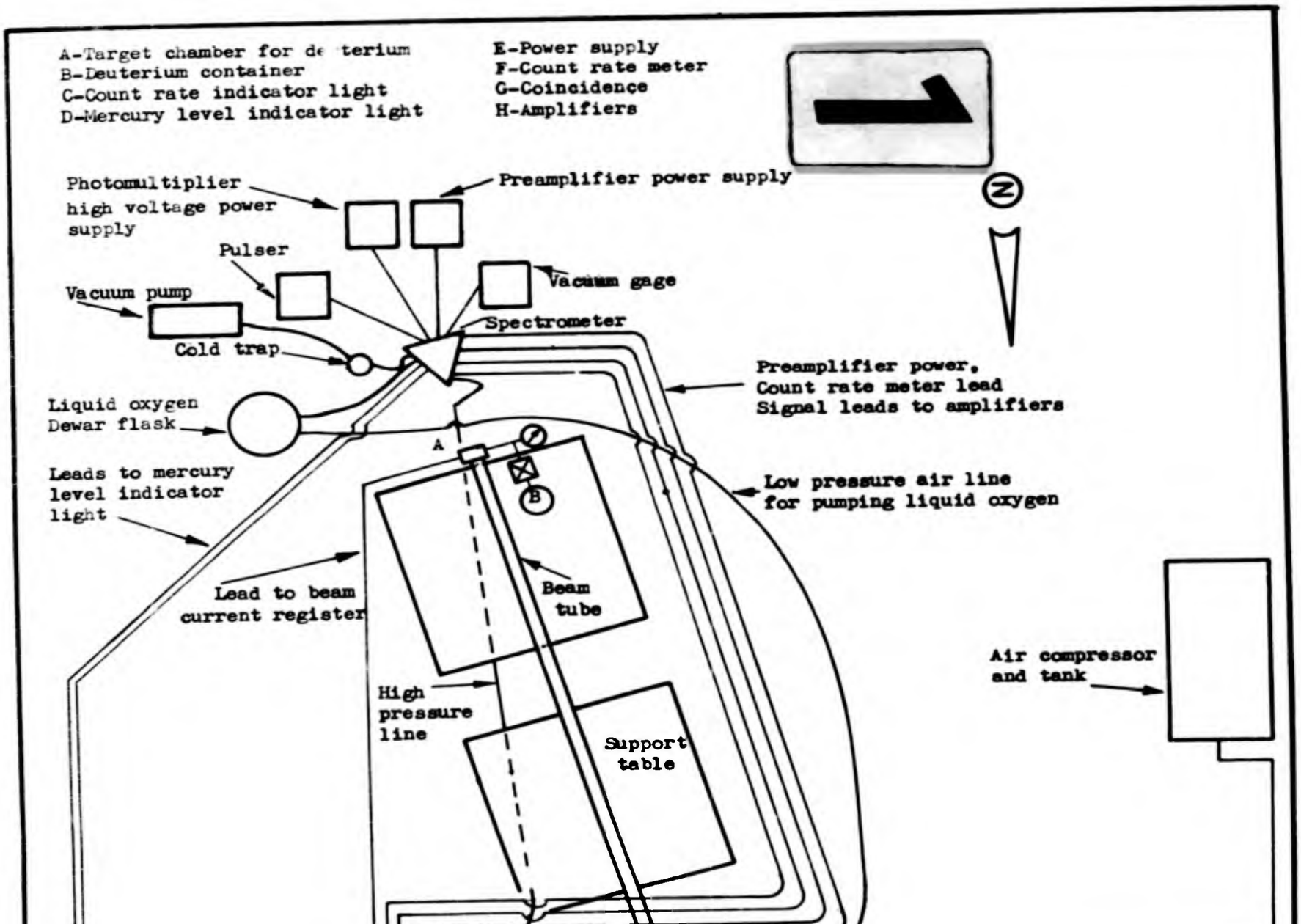
A-Target chamber for deuterium
B-Deuterium container
C-Count rate indicator light
D-Mercury level indicator light
E-Power supply
F-Count rate meter
G-Coincidence
H-Amplifiers
N
Photomultiplier high voltage power supply
Preamplifier power supply
Pulser
Vacuum gage
Vacuum pump
Spectrometer
Cold trap
Preamplifier power, Count rate meter lead Signal leads to amplifiers
Liquid oxygen Dewar flask
A
B
Leads to mercury level indicator light
Low pressure air line for pumping liquid oxygen
Lead to beam current register
Beam tube
Air compressor and tank
High pressure line
Support table

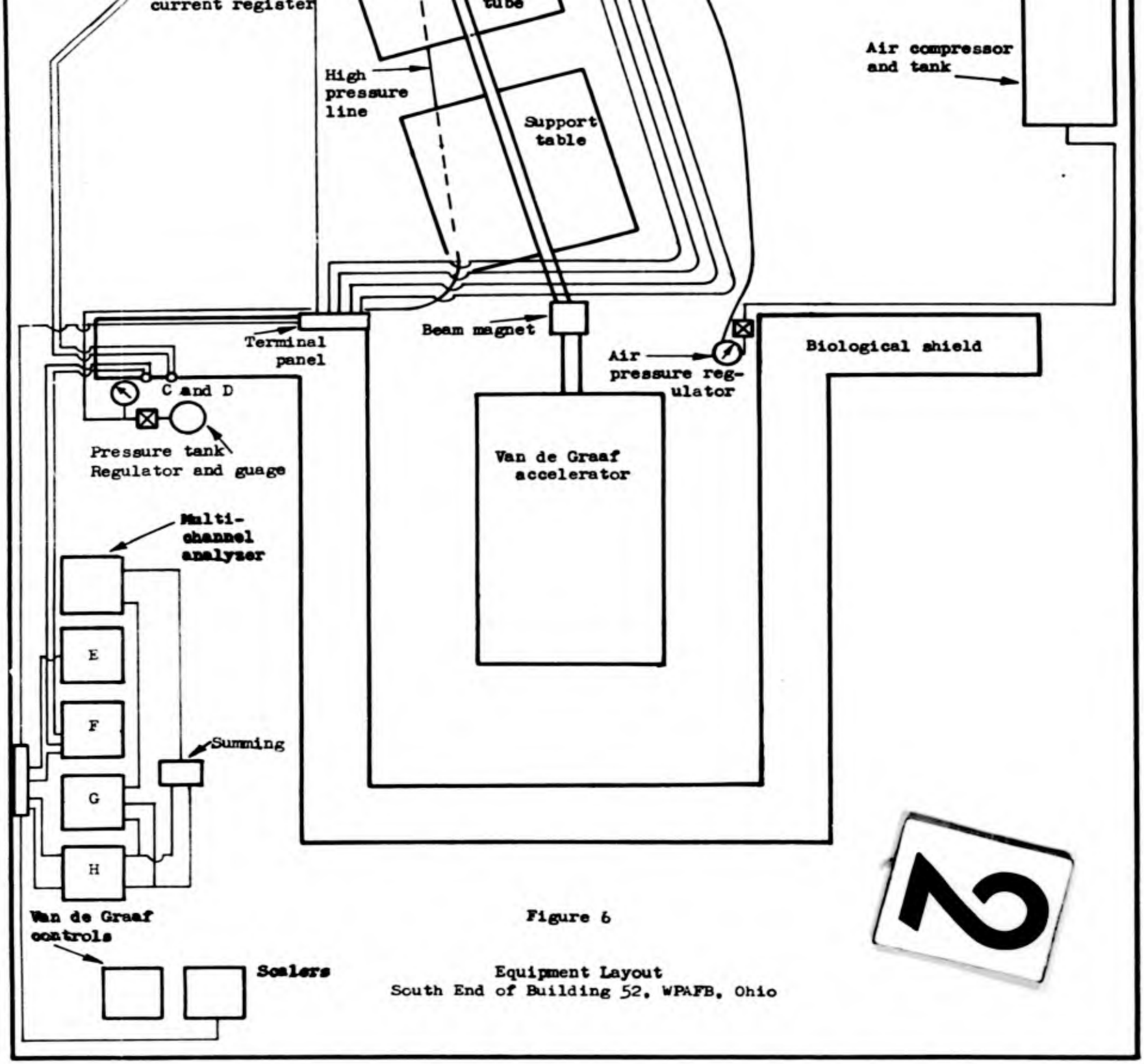

Figure 6

Equipment Layout
South End of Building 52, WPAFB, Ohio

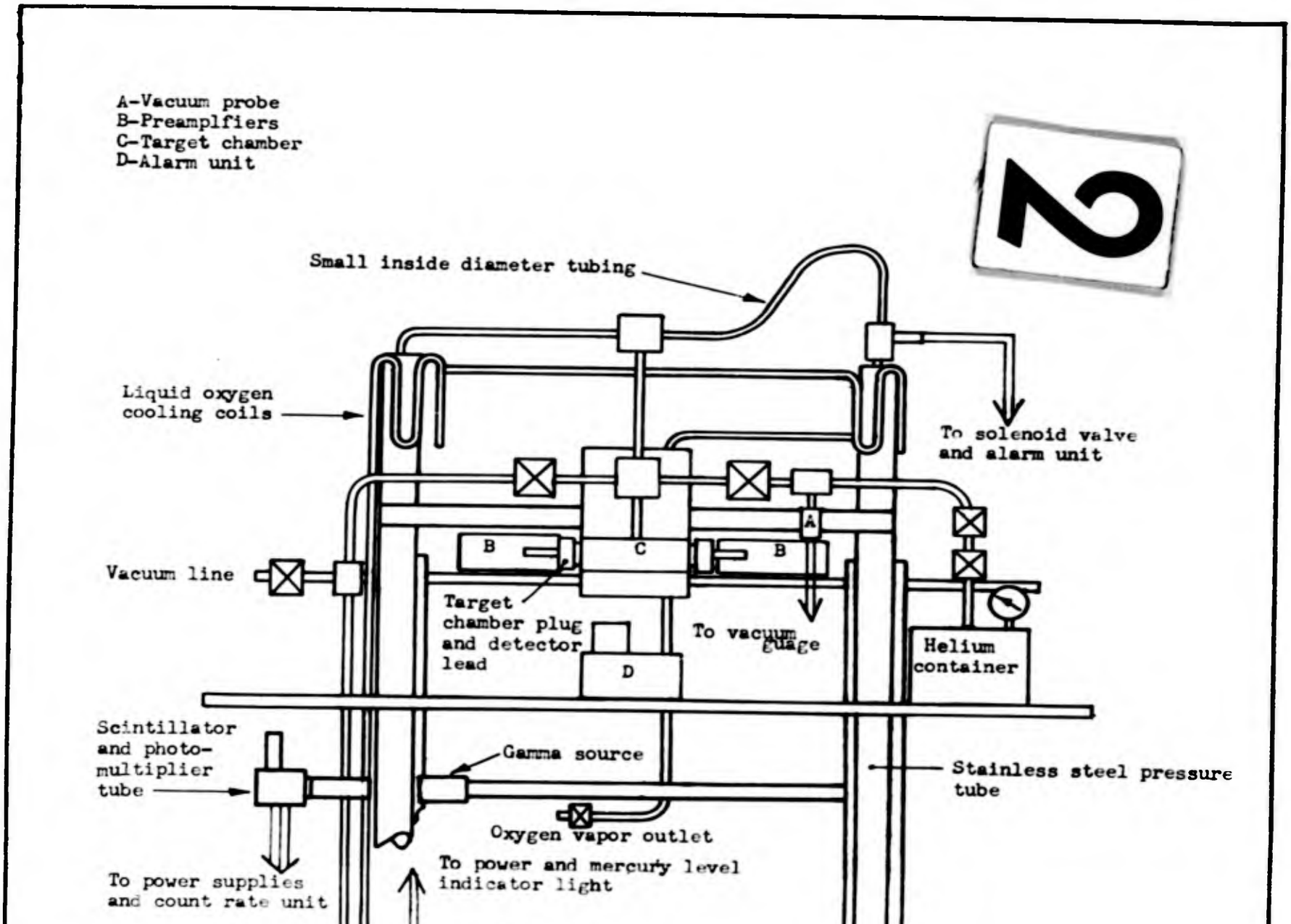
A-Vacuum probe
B-Preamplfiers
C-Target chamber
D-Alarm unit
Small inside diameter tubing
Liquid oxygen cooling coils
To solenoid valve and alarm unit
A
B
C
B
Vacuum line
Target chamber plug and detector lead
To vacuum gauge
Helium container
D
Scintillator and photo-multiplier tube
Gamma source
Stainless steel pressure tube
Oxygen vapor outlet
To power and mercury level indicator light
To power supplies and count rate unit

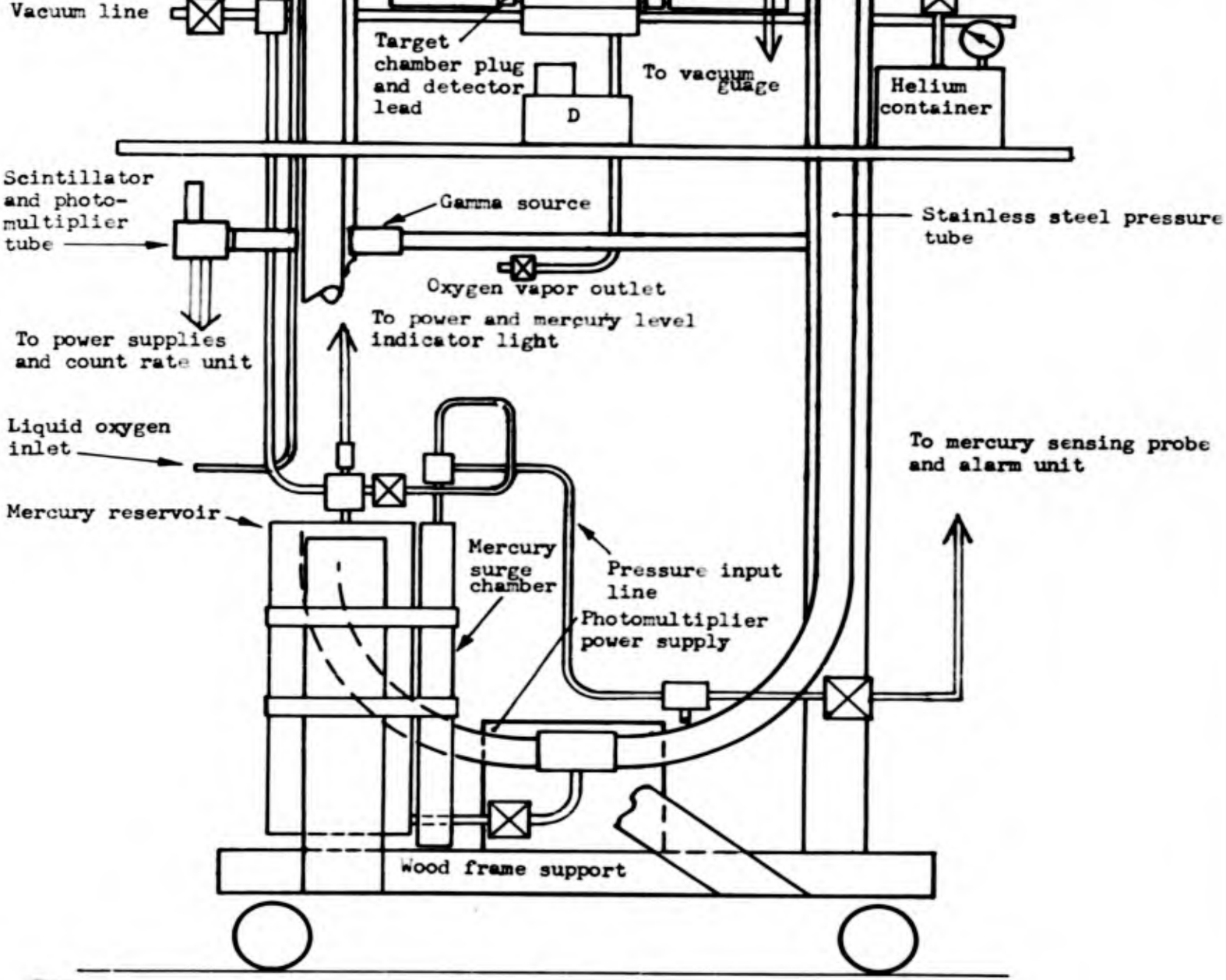

Figure 7

Elevation of Spectrometer

mercury keeps a light on at the pressure regulator. When the light goes out, the level of the mercury has dropped to within a few inches of the outlet. There is enough mercury above the point where the light goes out to fill the pressure chamber almost to the top. This is a positive indicator of the mercury level in the pressure chamber. In addition, a gamma source is placed on the opposite side of the pressure tube from a scintillation crystal and photomultiplier tube about half-way up the pressure chamber. The gamma source is Cs 137 with a strength of 1 microcurie and is placed in a lead block with a small hole facing the pressure tube to collimate the gammas. The output of the photomultiplier tube is fed back to a count rate meter from which the output is taken to the pressure regulator where the count rate is displayed visually by a flashing light. The count rate is much greater before the mercury has reached that level than after the pressure has forced it to that point. The difference in count rate is very pronounced and can be readily detected by the flashing light. At first, the gamma source was too far from the tube and did not supply a high enough count rate to detect the mercury level. The present position can be seen in Figure 6 and in the photographs.

The mercury should never leave the pressure chamber and

enter the lines leading to the target chamber. To insure that this never happens, another probe is inserted through a pressure fitting into the top of the pressure chamber on one leg of the "U". This probe maintains a break in an alarm circuit which is not actuated until the mercury reaches the probe. Once the mercury reaches the two wires of the probe, the circuit is closed and a solenoid valve on the pressure line is opened. At the same time, a doorbell rings. The valve stays open and the bell rings until the circuit is opened once more by the mercury dropping down and the reset switch being pushed. See Figure 8 for a schematic of the alarm circuit. The alarm circuit was tested numerous times and worked perfectly.

Since any mercury reaching the detectors would cause considerable damage, protection against mercury vapors is provided also. The gas is pressurized slowly enough to prevent any significant increase in temperature, but it is felt that the added safety device is warranted in view of the high cost of the detectors. The top of both legs of the pressure tube is cooled by coils wrapped around the outside. Liquid nitrogen or oxygen is pumped through the coils by low air pressure which forces the coolant out of the Dewar flask and through the coils. The pressure is regulated

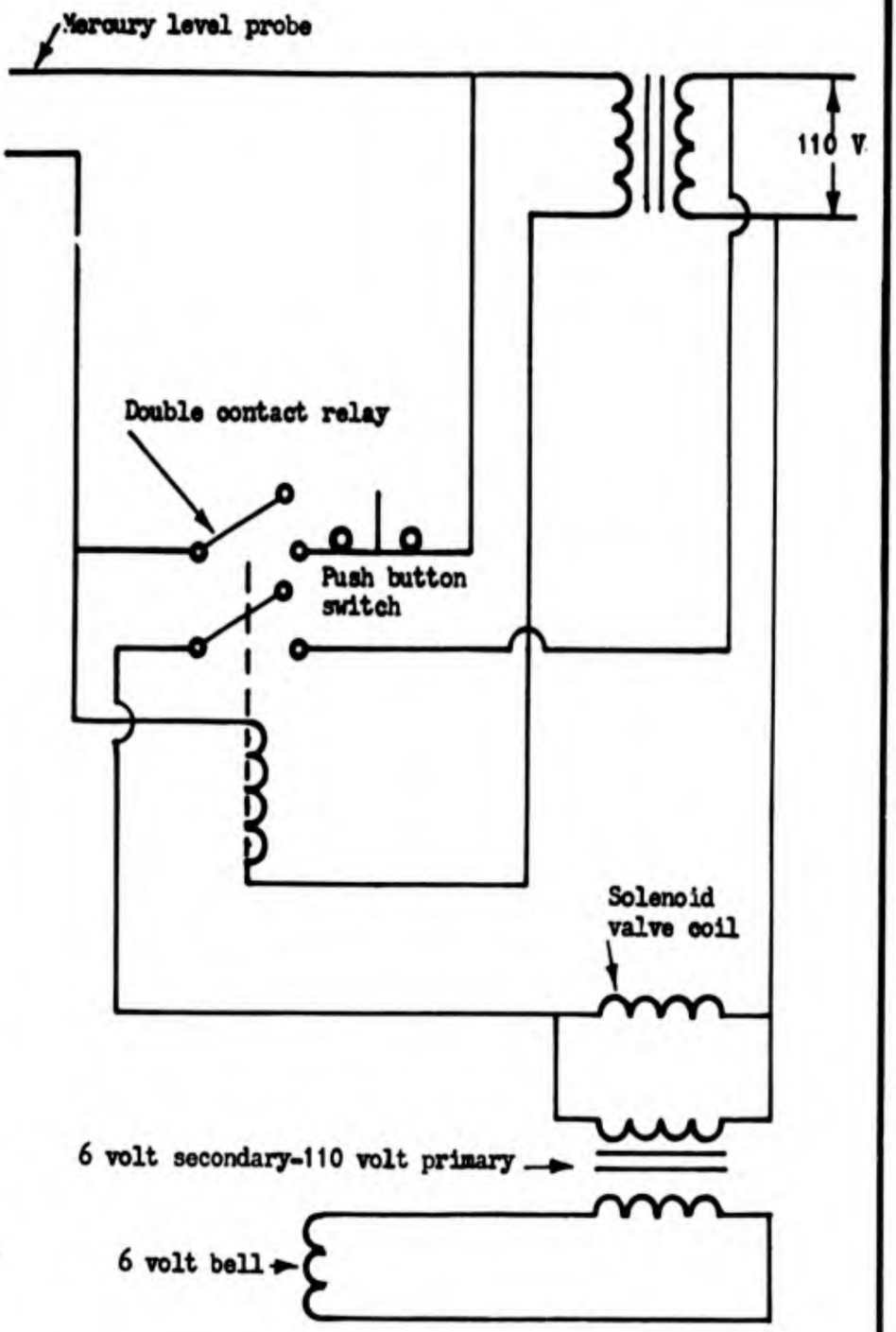

Figure 8

Schematic of Alarm Unit

to keep the liquid gas flowing at such a rate that it is vaporized by the time it reaches the outlet. The amount of cooling is controlled by the air pressure.

A cold trap is used on the vacuum line to prevent oil vapors from reaching the detectors which are very sensitive to surface contamination.

Leak Detecting. All lines and fittings were checked for leaks first by using a leak detector to check for vacuum leaks. The leak detector used is Model 24-101A manufactured by the Consolidated Engineering Corporation, Pasadena, California. Once all leaks were located and stopped, 1500 psi pressure was applied to the inside of the system and leaks searched for by using a soap solution brushed on the outside of the joints where leaks might be found. Once leaks detectable in this manner had been found and fixed, a leak detector was used again, only this time in reverse by filling the system with helium at high pressure and "sniffing" around the fittings with a probe with a very small opening. The leak detector used in this manner is a Vecco Leak Detector, Model MS-9, manufactured by the Vecco Vacuum Corporation, New Hyde Park, Long Island, N.Y. The pump used for evacuating the system is a Duo Seal manufactured by the W. M.

Welch Company of Chicago. Chasing down leaks was a time consuming proposition since attempts were made to correct them by soft solder and epoxy cement, neither of which is satisfactory when the system must be able to hold pressures up to 3000 psi. As was mentioned earlier, almost all fittings ended up either welded or silver soldered.

Target Chamber. The target chamber was initially to be sealed by letting the threaded plugs bear against some rubber and teflon washers. It was hoped that these would extrude against the chamber walls and detector holder to seal against pressure and vacuum. The final design shown in Figure 4 was arrived at only after much trial and error. The sealing washer shown in the photographs differs from that in the drawing in that the "O" ring around the middle is not shown on the drawing. This is because it was found that the "O" ring around the outside of the sealing washer made it too difficult to install and take out. Lack of time prevented modifying the washers accordingly.

The target chamber could be improved by making the diameter of the plugs slightly larger than the bore of the chamber. This would keep the washer and detector holders from having to pass over the threads when installed and removed. In its present

form, the target chamber holds both the vacuum and pressures required and with some refinements should be a very workable design.

Pressure Control. The pressure to drive the mercury piston is supplied by bottled gas at 3000 psi and is regulated by a pressure regulator which regulates the pressure from zero to 3000 psi. The pressure is monitored by the regulator gauge and by a larger zero to 2000 psi gauge manufactured by the Astra Corporation, Hatboro, Pennsylvania. This gauge was adjusted and checked using a large accurate gauge manufactured by Heise of Newton, Connecticut. The Astra gauge showed no hysterisis effect up to 600 psi and a maximum of 10 psi above this pressure. The pressure can be released by a bleed valve located just below the gauge. The bottled gas, regulator, and gauge are located behind the concrete block biological shield wall for the Van de Graaff. A heavy-wall copper tube runs from the pressure gauge to the end of the beam tube where it is attached to the spectrometer by a 3000 psi flexible line. With this arrangement, it is possible to change the pressure without shutting off the Van de Graaff beam. In addition, the wall affords protection should any part of the pressure system rupture.

Operation. Once leaks had been stopped and the system seemed to be operating properly, the mercury was put into the reservoir. Approximately one hundred pounds of mercury is required. It was found that once the mercury is put in, it is difficult to obtain a good vacuum. Apparently, this is due to air that gets trapped and escapes as the vacuum is improved. This seems to be substantiated by the fact that mercury is carried up from the surface by air escaping. If the valve to the vacuum pump is opened too fast, the mercury "bubbles" violently so that the reservoir and pressure tube actually vibrate. On one occasion, mercury was carried 35 inches above the surface. If the vacuum is applied slowly, this phenomenum is minimized and eventually the valve can be opened all the way with no further evidence of escaping air. However, once pressure is applied to move the mercury, the escaping air once again becomes a problem. It is not known how long the escaping air will be a problem, although recycling several times seemed to have little effect in reducing the amount of "bubbling". Once the target chamber is evacuated, the He^3 gas is let in and compressed. A vacuum of 100 microns was considered suitable and, in fact, is about the best that can be obtained after several hours pumping with the Duo Seal pump.

Even though this is not a very good vacuum, it does not cause significant contamination of the He^3 gas. The vacuum was monitored by a gauge manufactured by National Research Corporation, Cambridge, Massachusetts.

Because of problems involving the circuitry, the He^3 gas was never let into the target and pressure chambers. Air was compressed to 1100 psi several times using the mercury piston as would be done in actual operation and the system worked satisfactorily. A higher pressure was not used because the volume of the tubing, valves and target chamber above the pressure chamber is probably greater than the 2.3 cm^3 calculated as the final volume of gas at 1500 psi starting with 930 cm^3 at 7 psi. A larger fixed volume requires a lower pressure. The problems with the circuitry are discussed in the next chapter.

Since the pressure doesn't begin to reach the 1500 psi figure until the mercury is almost to the top, care must be exercised to be sure that the solenoid valve is not opened by mercury rising too far. A small leak in a valve would let the mercury keep rising. A surge chamber is shown on the drawing and is installed to absorb any overflow that may occur if the solenoid valve opens with the mercury under high pressure. No problems were experienced with

the mercury overflowing the reservoir. With the pressure removed, the mercury dropped down in the pressure chamber and filled the reservoir back to the original level.

IV Electronic Circuitry

General

Special Requirements. Use of solid state detectors requires circuitry to obtain maximum advantage of the improved detector resolution. This implies low noise components which will contribute a negligible amount to loss of resolving power of the spectrometer. The very fast pulse rise time of the detectors requires fast circuit response to take advantage of this characteristic. The effect of bias on the capacitance of the detectors and thereby on the voltage output requires that a non-voltage sensitive amplifier be used to prevent fluctuations with changes in the bias voltage.

Detector Output. The voltage output of a semiconductor detector is essentially that of a charged capacitor. As was mentioned earlier, the capacitance of these detectors is a function of the bias and area. The well known relationship of the voltage across a capacitor is

$$V = \frac{Q}{C}$$

The charge liberated in the detector by an ionizing particle will appear as a voltage which obeys this relationship. If the capacitance of the detector changes, the voltage response for the same energy particle will vary. Since the capacitance of a detector of area A is given by:

$$C = \frac{A}{\sqrt{V}}$$

where V is the bias voltage, it can be seen that a fluctuation of the bias will have a corresponding effect on the voltage output of the detector. Use of charge sensitive amplifiers eliminates this problem by making the amplifier sensitive to the charge collected and not the voltage. There are applications, however, when faster response time of the voltage sensitive amplifier will dictate its use. Figure 9 taken from Reference 7 shows the difference between the charge sensitive and voltage sensitive amplifiers. The voltage gain of the charge sensitive amplifier is about unity; however, it acts as a charge integrator to provide a charge gain of about 1000. At high count rates, it is important for the amplifier to collect the charge rapidly to prevent "pile-up" of pulses. This is especially true when working at low energies.

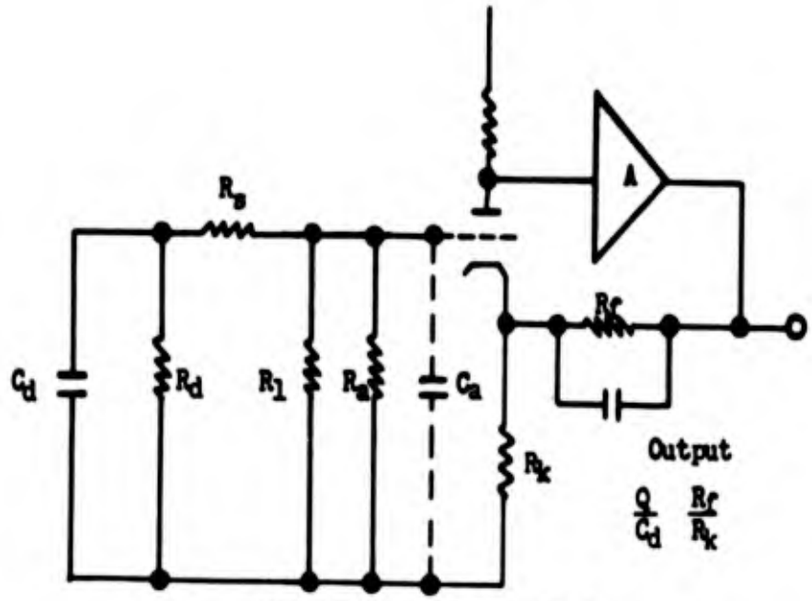

Voltage-Sensitive Amplifier

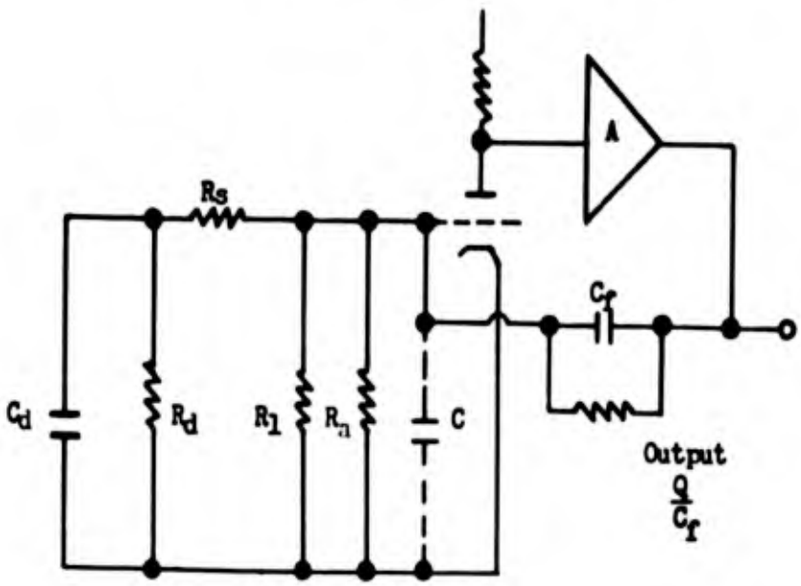

Figure 9

Input Circuit Parameters for Charge Sensitive and Voltage Sensitive Amplifiers (From Reference 7)

Pulse Shaping. The shape of the pulses fed through the circuit is important because of the relationship to noise. Considering three components of noise to be high, intermediate and low frequency, the relationship between pulse shape and noise will be briefly considered. Integration of the pulse eliminates most of the high frequency noise, and differentiating takes out most of the low frequency component. This leaves the intermediate frequencies as the main contributor to circuit noise. The best signal to noise ratio is obtained when the integrating and differentiating time constants are equal (Ref. 7). Also, the resolution is best for this shape pulse.

The two detectors should be matched as closely as possible to facilitate adjusting the pulses. Since the pulses are being added, the peak values should arrive at the summing unit at the same time so that correct summation will take place. Use of a summing amplifier obviates this requirement. Figure 10 represents the effect of summing two pulses that have different rise times. The same problem exists if there is a slight time delay of one of the pulses. Shaping of the pulses can be accomplished in the preamplifiers where RC integrating takes place and in the amplifiers where RC differentiating is

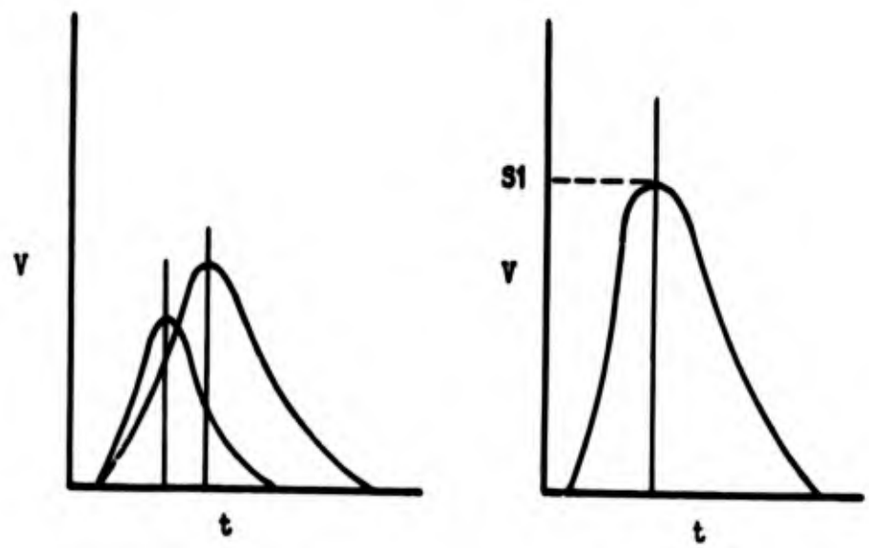

Individual Pulses Summed Pulse

Incorrect Pulse Summing

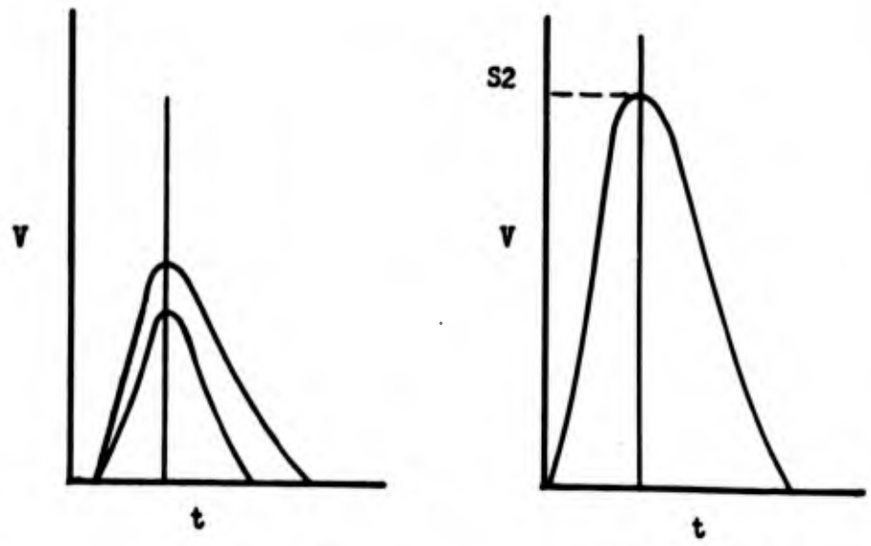

Individual Pulses Summed Pulse

Correct Pulse Summing-S1< S2

Figure 10

Importance of Pulse Shape in Summing

done. An added reason for matching the two pulses from the detectors is to insure correct operation of the coincidence unit.

Circuit and Equipment

A block diagram of the circuit is shown in Figure 11. The preamplifiers are a Tennelec Low Noise Preamplifier, Model 100 A, and one built on a Miller design from Brookhaven National Laboratory. The preamplifiers supply the bias to the detectors and are both of the charge sensitive type. The pulser is a Radiation Instruments Development Laboratory Mercury Pulser, Model M-60. The two amplifiers are Cosmic Radiation Laboratories, Inc., Linear Amplifiers, Model 101. The coincidence unit is Model 801 manufactured by Cosmic. The 256 multi-channel analyzer is Radiation Instruments Development Laboratory Model A-261.

The summing circuit was made in the laboratory and consists of a voltage dividing resistor circuit shown in the following schematic.

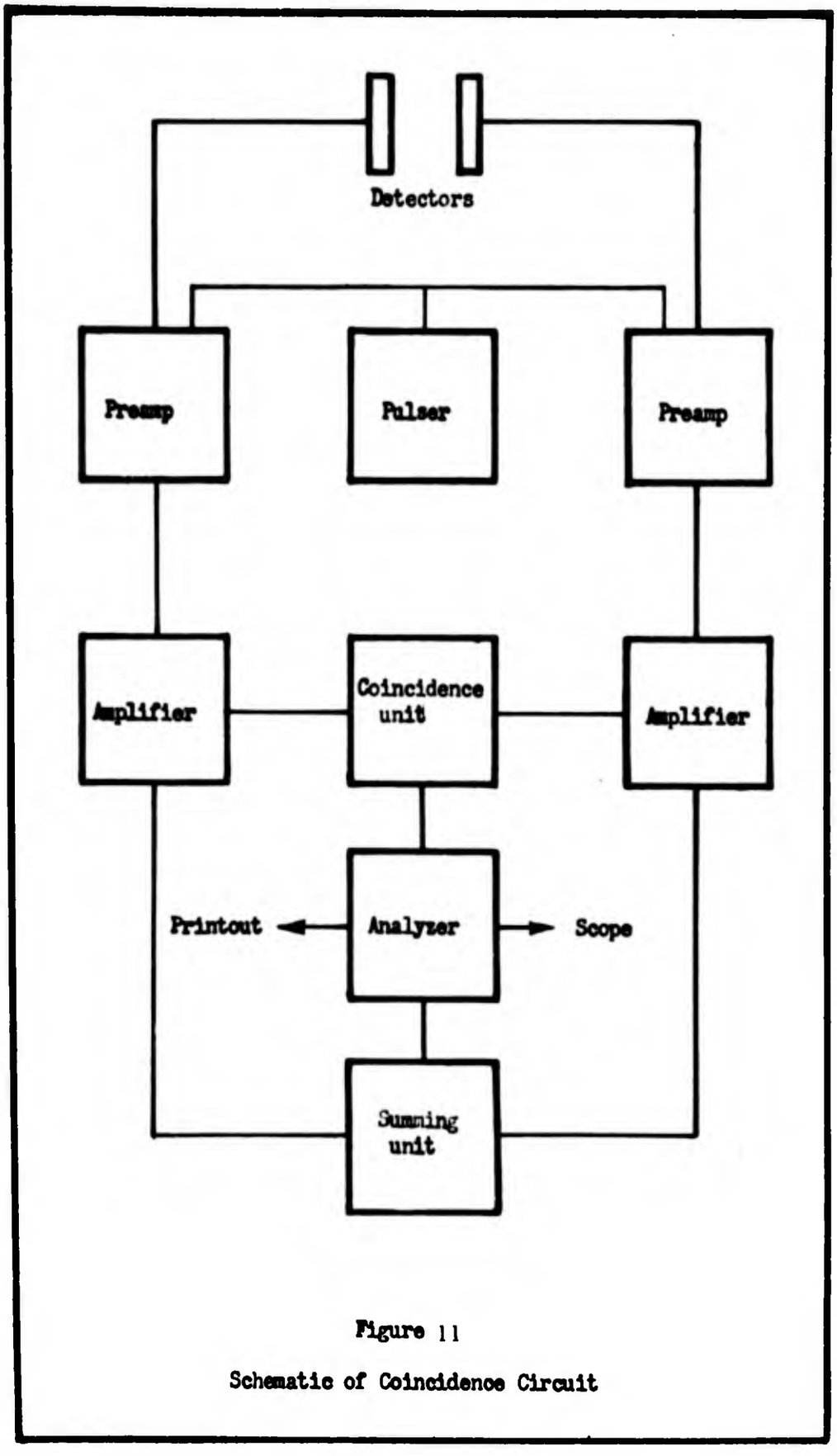

Figure 11

Schematic of Coincidence Circuit

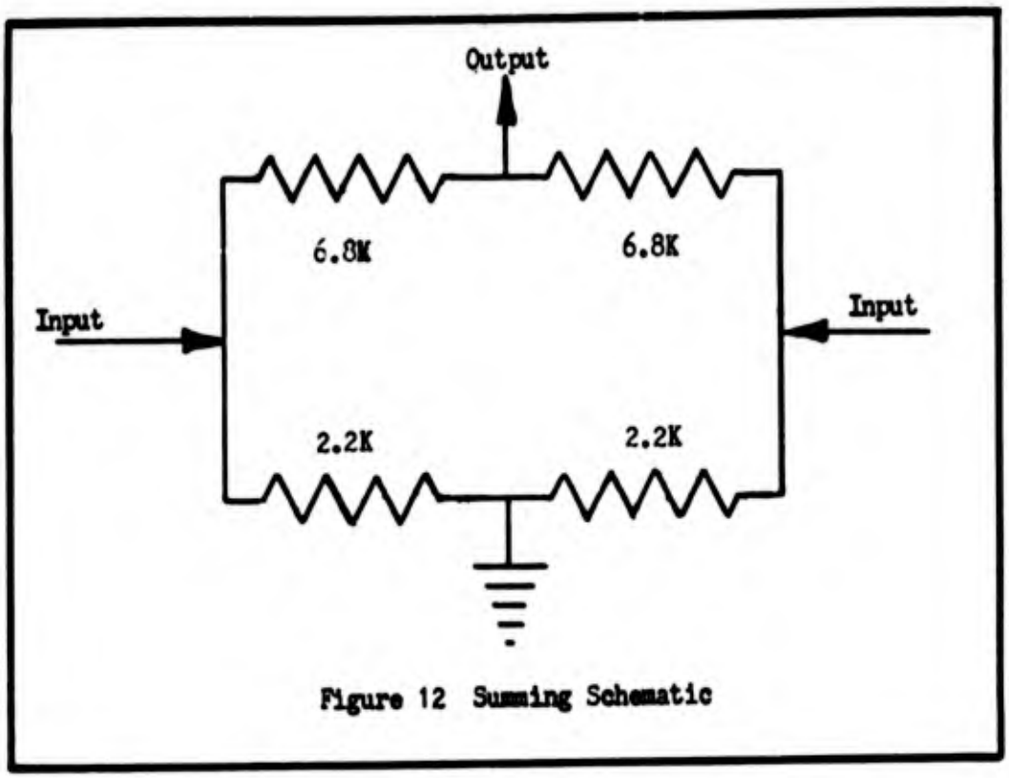

Figure 12 Summing Schematic

The two input pulses do not effect one another and the output voltage is one-half the sum of the two inputs. If the input inpedance begins to match the summing circuit inpedance, a drop in pulse height will result. The summing circuit acts as a fixed potentiometer and the two 2.2 K resistors are line matching resistors to keep the circuit ringing to a minimum.

The pulser input inpedance of the two preamplifiers should be the same so that the pulser output is equally divided. In addition, the pulser input of the preamplifiers should be the

same as the detector input. This is necessary so that the pulser can be used to check the circuit by duplicating the signals from the detectors.

The two preamplifiers are close to the target chamber to keep the lead wire length to a minimum. Any line capacitance added to that of the detectors has an adverse effect on the circuit by increasing the effective capacitance of the detector which, in turn, effects the resolution and charge sensitivity. The problem of line ringing due to mismatch of line impedence and input impedence of the various components can be partially corrected by use of resistors of the correct value such as are used in the summing circuit. Some attenuation results in use of resistors for this purpose.

Calibration of Circuit

There are a number of calibrations and checks that must be performed prior to operating the spectrometer. First, the zero channel of the analyzer must be determined. This is done by feeding in two known value pulses and noting their respective channels. Extrapolation with the straight line connecting these two points will give the channel corresponding to

zero energy.

The next calibration to be made is the pulser ratio which is used to set the gain of each leg of the coincidence circuit during operation. This ratio is obtained as follows. An alpha source is placed in the target chamber and the gains of the two amplifiers independently set to feed the pulse produced by the alpha particle into the same channels. The gain of each leg of the circuit is set independently of the other by disconnecting the preamplifier and amplifier of one leg while the gain of the other is adjusted. Once the gains are set, the pulser output is independently fed into the same channel as the alpha source. The ratio of the pulser settings for each leg of the circuit is used to adjust the gain during operation to compensate for drift. In this manner, it is possible to insure that the same size pulse from either detector will fall in the same channel of the analyzer.

In using the pulser for calibration purposes, the pulses in the range of those expected from neutron interaction with the target gas should be used to give realistic results. The pulse from a detector for a given partical energy deposition can be calculated knowing that it takes 3.5 ev to free an electron in silicon

and knowing the capacitance of the detector.

The following is a sample calculation. The capacitance of the detector includes the line capacitance and preamplifier input capacitance.

$$\text{Energy deposited} = 5 \text{ mev}$$

$$\text{Number of charges released} = \frac{5 \times 10^6}{3.5} = 1.43 \times 10^6$$

$$\text{Total charge} = 1.43 \times 10^3 \times 1.6 \times 10^{-19} = 2.28 \times 10^{-15} \text{ (coulombs)}$$

$$\text{Capacitance of detector} = 30 \times 10^{-12} \text{ farads}$$

$$\text{Voltage output} = \frac{Q}{C} = \frac{2.28 \times 10^{-15}}{30 \times 10^{-11}}$$

$$= 7.6 \times 10^{-3} \text{ volts}$$

Another check that should be made is determining if the adding circuit sums pulses of different values equally well. This check must be made with the summing unit in the circuit as the characteristics are not the same when the amplifiers and analyzer are disconnected. The summing of pulses of different magnitudes can be observed by using fixed settings of

the pulser and varying the gains of the two amplifiers. The pulse from each branch is fed into the analyzer one at a time and then together. With a fixed pulser output, the gain of the two amplifiers can be varied to provide different combinations of pulses to be summed.

To establish a correlation between the analyzer channel numbers and energies they represent, an emitter of known energy alphas is placed in the target chamber to find the channel that corresponds to this energy. This is done after the gains have been set at their final value. This operation assumes that the relationship of energy deposited to pulse fed to the analyzer will hold for the proton and triton and ignores the loss of product particle energy in the target gas. This procedure makes it possible to set the amplifier gains so that the spectrum studied is not in the noise region of the analyzer.

Circuit Modification

The problem with this circuit that makes alteration necessary is the lack of adequate gain to make possible looking at the desired range of neutron energies. With a pulse produced by a 5.3 mev α feeding into the analyzer and with maximum gain, the

pulse fell into channel 16. The maximum energy that can be deposited from a reaction with a 5.24 mev neutron (the maximum available) is 5.24 + 0.764 or 5.904 mev. This means that the energy peak from the most energetic neutron available would fall slightly above the α peak or in the noise region of the analyzer. It is easy to see that the gain is insufficient for the neutron energies available. One of the main reasons for this is that the summing circuit attenuates the signals by much greater than the factor of two expected. Due to lack of further time, no investigation was made into ways of correcting this problem. It appears that another summing circuit would greatly alleviate the situation and certainly there are various suitable circuits that would work. Much added gain should be provided to keep from working the amplifiers at maximum output and to permit looking at lower energy neutron spectra. The noise region referred to above can be considered to be roughly the first thirty channels of the analyzer.

V Neutron Sources

General

An essentially monoenergetic or homogeneous source of neutrons of an appropriate energy and production rate is required to first test the operation of a spectrometer of this type. A homogeneous source is desired so that the resolution can be measured with respect to one particular energy. The importance of the proper neutron source could be expressed simply by asking the following question. If the neutron source characteristics are not known, how can the effectiveness of the spectrometer be determined? Keeping this in mind, a survey was made of various neutron sources suitable for use in testing a fast neutron spectrometer. The discussion of the two means of target preparation is a result of an effort to devise a better way of making thin gas targets for a Van de Graaff accelerator.

Types

There are a number of reactions producing neutrons such as the (p,n), (d,n), (α,n) and (γ,n) reactions. Regardless of the manner in which the neutrons are produced,

there are two main categories of sources. One is the essentially monoenergetic source mentioned above and the other is the heterogeneous source made up of a spectrum of neutron energies. A purely homogeneous source of neutrons is rarely available. In this discussion, the homogeneous sources are of prime concern for making resolution tests with the spectrometer. Besides the nature of the target being bombarded, factors which effect the homogeneity of a neutron source are spread in the bombarding particle energy and finite angle subtended by the target. In addition, the neutron source will be complex if there are a number of secondary reactions possible for one incident particle energy. Examples of this are the complex spectrums from the deuteron reaction with Li^6 and Li^7. There are times when a spectrum of neutrons is desired to further test the operation of the spectrometer. In this case, it is as important to work with a known spectrum as it is important to use a known monoenergetic source.

For the above mentioned reactions, the source of the incident particle is usually a Van de Graaff accelerator except for the (γ ,n) reaction which can be induced by a neutron

photoeffect such as:

$$h\nu + D^2 \longrightarrow H^1 + n^1 \quad (Q = -2.227 \text{ mev})$$

$$h\nu + Be^9 \longrightarrow Be^8 + n^1 \quad (Q = -1.666 \text{ mev})$$

Both of these reactions produce fairly monoenergetic neutrons below 1 mev if radium gammas are used to induce the reaction (Ref. 14).

Homogeneous Sources

The Van de Graaff accelerator provides an essentially monoenergetic source of deuterons, alphas and protons. By using a thin target to minimize the loss of charged particle energy and by a sufficient separation distance between the neutron producing material and spectrometer, a minimum spread in neutron energy can be obtained. The target for the Van de Graaff subtends a finite area, so the source of neutrons is not a point source which increases the spread of neutron energies at the spectrometer. The thickness of the target material is minimized to reduce the energy loss of the charged particles in the target.

Examples of reactions using deuterons from a Van de Graaff are:

$$d^2 + D^2 \longrightarrow He^3 + n^1 + 3.27 \text{ mev}$$

$$d^2 + Be^9 \longrightarrow B^{10} + n^1 + 4.36 \text{ mev}$$

$$d^2 + H^3 \longrightarrow He^4 + n^1 + 17.59 \text{ mev}$$

$$d^2 + F^{19} \longrightarrow Ne^{20} + n^1 + 10.619 \text{ mev}$$

These reactions produce only one energy neutron up to deuteron energies of 2 mev.

Alpha from a Van de Graaff can be used to induce the following reactions:

$$He^4 + Be^9 \longrightarrow C^{12} + n^1 + 5.704 \text{ mev}$$

$$He^4 + B^{10} \longrightarrow N^{13} + n^1 + 1.06 \text{ mev}$$

The B^{10} reaction also produces neutrons from the reaction

$$He^4 + B^{10} \longrightarrow H^1 + n^1 + C^{12} - 0.883 \text{ mev}$$

so use of this reaction for a monoenergetic source is limited. In addition to using a Van deGraaff to supply the alpha particles, a Po^{210} isotope could be used. The source of neutrons would be

limited and a pure Po^{210} sample would be necessary. A comprehensive study of neutron sources is contained in Reference 14.

Van de Graaff (d,D) Source

Because of the availability of a target chamber and source of deuterium gas, the (d,D) reaction was contemplated for the initial source of neutrons to check this spectrometer. The target chamber is merely a small volume with an opening to the deuterium source and separated from the vacuum of the Van de Graaff by a thin nickel foil. The Van de Graaff accelerator shown in Figure 7 is manufactured by the High Voltage Engineering Corporation, Burlington, Massachusetts, and can accelerate deuterons up to 2 mev. The rate of production of neutrons and the energy can be controlled by varying the beam current and accelerated particle energy respectively.

The following sketch shows the relationship of the beam tube, target chamber and spectrometer. The photographs also show the deuterium source and target chamber in place at the end of the beam tube.

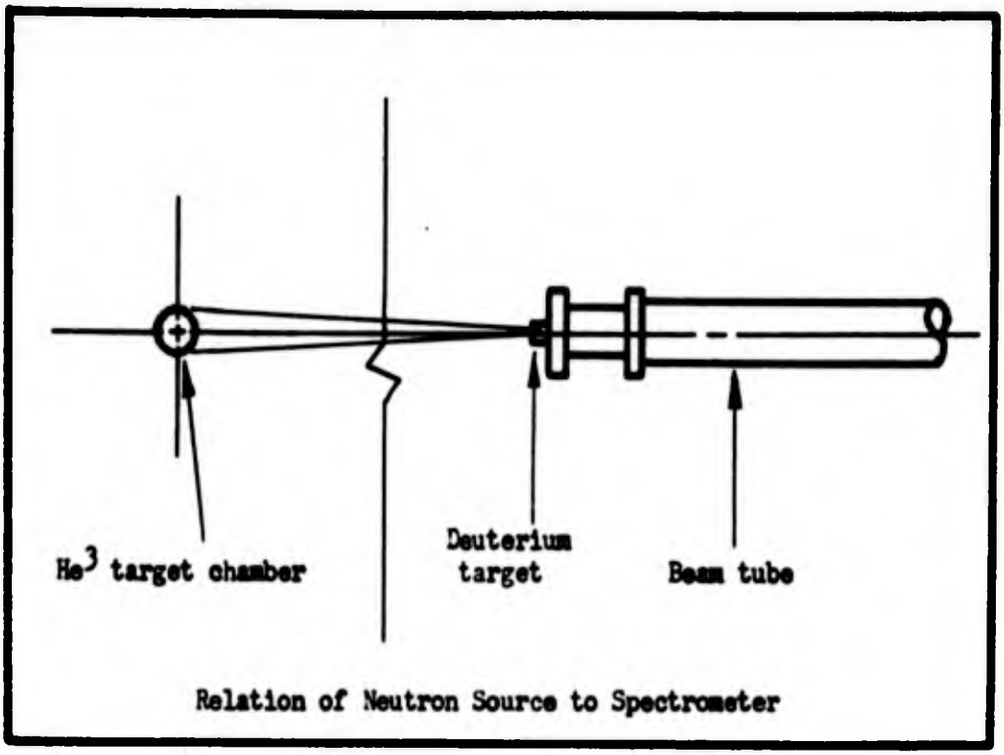

Relation of Neutron Source to Spectrometer

Due to the small size of the target chamber (0.63 cm dia. by 1.6 cm long) a point source is considered. With a distance to the spectrometer target chamber of 100 cm, and a detector separation distance of 1 cm, the He^3 target subtends an angle of about 0.6^o. The energy spread over this angle is not significant as can be seen from the results of the computer program for the (d,D) reaction shown in Appendix B. The loss of the deuteron energy in the nickel foil will be almost a constant value and can be computed. Rucker (Ref. 29) computed this

energy loss to be 0.045 mev for a 2 mev deuteron. The loss of deuteron energy in the deuterium gas at STP is 0.1 mev as calculated by Rucker. This target chamber is the same used by Rucker. Damage of the thin nickel foil by the deuteron beam and the resultant leakage of the deuterium is a disadvantage of this target chamber.

By insulating the target chamber from the beam tube and measuring the charge collected, it is possible to compute the number of deuterons striking the target gas. This information with the cross section of the (d,D) reaction and density of the deuterium gas permits calculation of the intensity of the neutron source. This is important to calculate the efficiency of the spectrometer. The number of neutrons striking the target gas can be calculated by taking the ratio of the solid angle subtended by the He^3 chamber to the total solid angle (4π). Using the dimensions given in the preceding paragraph, it is easy to see that the number of neutrons striking the He^3 target would be a small percentage of those produced. Some compromise between count rate and resolution will be necessary.

Target Preparation

General. As pointed out above, the thickness of the target which is bombarded to produce neutrons is of importance in keeping the neutron energy spread to a minimum. Besides using a gaseous target, thin targets can be made by coating a supporting disc with the desired target material. Obtaining a thin uniform coating is a problem of this method. A different type of target can be made by using materials such as Zr or Ti to act as absorbers for gaseous target material such as deuterium or tritium. Without going into detail, the targets are prepared by first obtaining a thin coating of the absorbing metal on a support disc. The metal is then heated in presence of the deuterium or tritium gas which is absorbed upon cooling. Gas to metal atom ratios of 1:1 are easily obtained. If the absorbing metal is a uniform, thin layer, then a good target is produced. These targets must be cooled to prevent release of the absorbed gas. McCormick (Ref. 22) and Evans (Ref. 11) describe target preparation of this type. Some of the ways in which the absorbing metal is placed on the support are by evaporating and melting. It is difficult to

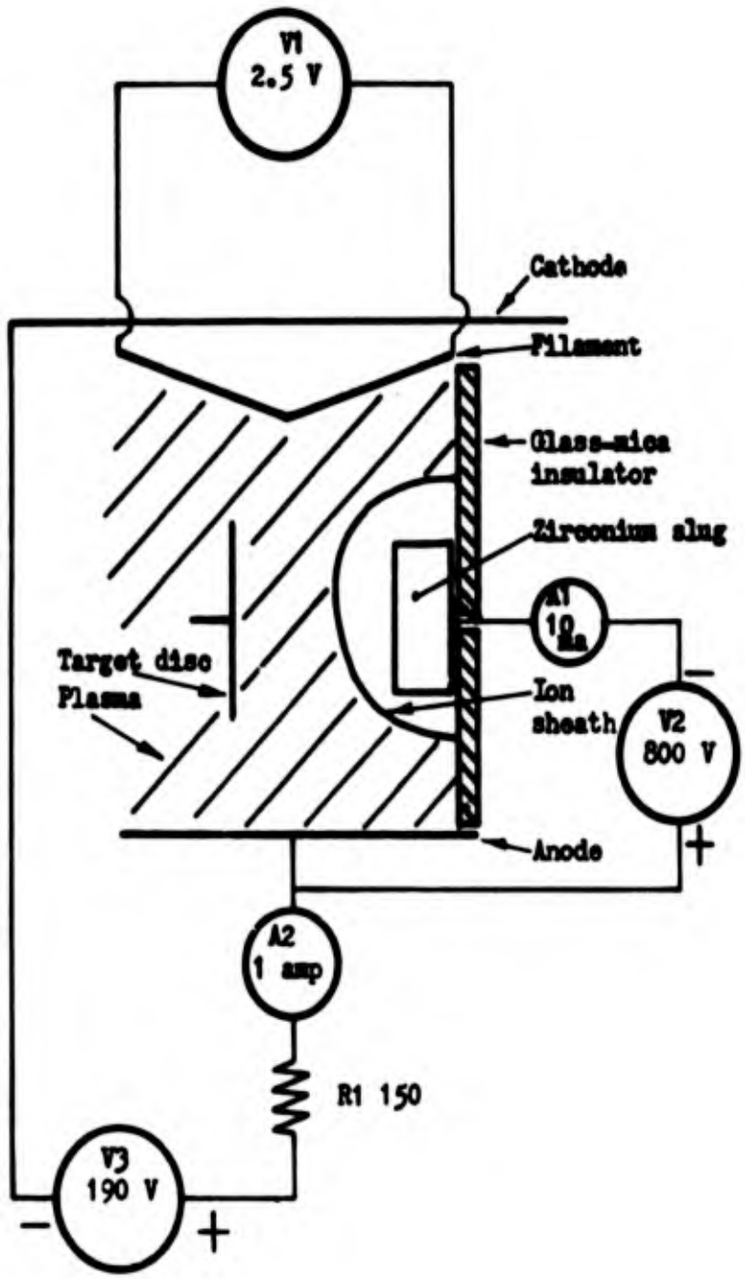

Figure 13

Schematic of Sputtering Apparatus

insure good bonds between the support disc and metal coating. In an effort to find a better method, two different procedures were investigated.

Ion Sputtering. The apparatus used in the sputtering experiment is shown in Figure 13. The assembly shown is contained under a bell jar to permit maintaining the low pressures necessary. Essentially the method is as follows. Absorbing metal atoms are freed by bombarding with ions. These ions are accelerated by a negative potential on the bar of absorbing metal. The freed atoms are dislodged with enough energy to coat the target disc. The region adjacent to the bar is free of ions since the electrons which produce the ionized argon plasma are repelled by the negative potential and do not interact with the argon atoms. The remaining space between the cathode and anode contains argon ions which are attracted by the negative potential on the Zr bar. The energy of these ions is sufficient to dislodge Zr atoms which are accelerated from the metal slug and impinge on the supporting disc. Some ions are attracted by the cathode which must be kept at as low a potential as possible to keep ion attraction to a minimum. Excessive secondary

sputtering of the cathode impairs its effectiveness and, in turn, the ability to maintain a suitable plasma.

The first step in this process was to clean the metal bar by sputtering until the oxide coating is removed. This required two hours of sputtering during which time the test slide was removed from the bell jar. When the metal appeared clean, a small glass slide was placed a few inches from the Zr bar. The sputtering process was resumed for an additional one and one-half hours after which it was felt an adequate coating was obtained.

The main difficulty in this sputtering experiment was maintaining a suitable plasma with a low enough pressure to give the ions a long enough free path to reach the metal bar. The equipment had not been used for several weeks, and even though the bell jar was kept over the filament and low current maintained through it, the filament had to be "brought back to life" by use at higher currents. While this is taking place, it is very difficult to maintain the plasma. Pressure during sputtering was about 10 μ .

Results of Sputtering. After achieving a thin coating on the glass slide, it was decided to analyze the coating to determine its nature. The film had a fair degree of reflectivity and appeared metallic and was assumed to be zirconium or some zirconium compound. The glass slide was taken to the Chemical Research Laboratory, Aeronautical Research Labotories where Dr. F. L. Chan performed a series of tests to determine the nature of the metallic coating. Two tests were performed to accomplish a qualitative analysis of the material. The first test was the use of x-ray fluorescence which revealed presence of Zr. Next, x-ray diffraction revealed that the metal coating had not crystallized and was in an amorphous state as evidenced by a broad band diffraction pattern rather than the sharp lines characteristic of the crystalline structure. X-ray diffraction through the material after it had been annealed at 500^{o}C in the presence of air generated diffraction lines characteristic of a Zr oxide.

The coating was reasonably uniform and quite thin although no precise measurements were made of these two characteristics. Greater uniformity could be achieved by better positioning of the piece to be coated. In the course of

performing the diffraction and fluorescence experiments, the coating was observed to have excellent cohesion with the glass slide. It appears that this process holds promise in obtaining extremely thin coatings of an absorbing metal for preparation of targets where there is a requirement for a layer of target atoms of minimum depth. Such a requirement might exist where very precise resolution studies are to be made and a minimum of distortion of the bombarding particle in the target is required.

Zr $(TFA)_4$ Compound. The metallic compound investigated was synthesized by Dr. R. E. Sievers of the Chemistry Research Laboratory, Aeronautical Research Laboratories, and it was partially interest shown by that group that led to the building of a trial device for coating target discs with zirconium by reduction of a volatile compound of the metal. The purpose of the investigation was two fold:

1. To study the characteristics of reduction of a novel volitile compound of zirconium
2. To determine the feasibility of using this gas plating process for coating target discs.

The use of this compound offers the advantage of carrying out the coating process without the high vacuum which is required in the case of vacuum evaporation. Since the proposed process involves chemical deposition rather than simple physical transfer, it is possible that a coating with better adhesion to the supporting disc would result. Since the chemical process of depositing the metal is one of reduction, a hydrogen atmosphere is necessary. This creates the necessity for making provisions in apparatus design for disposing of the excess hydrogen.

The chemical name for the compound is tetrakis (1, 1 1 trifluro-2, 4-pentanedionato) zirconium (IV), which for obvious reasons will be called $Zr(TFA)_4$ for the remainder of this report. The structure of this compound is as follows:

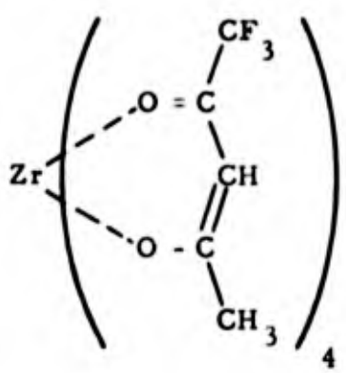

The synthesis of the compound is shown by the following chemical equation:

$$ZrCl_4 + 4H(TFA) \longrightarrow Zr(TFA)_4 + 4HCl$$

and the reduction process can similarly be expressed:

$$Zr(TFA)_4 + 4\,H_2 \xrightarrow{\Delta} Zr + 4H(TFA)$$

This compound is one of a family of metallic compounds with the same basic chemical structure.

The apparatus for studying the reduction of the metal compound was constructed by the glass shop at ARL and represents a preliminary design which should prove the feasibility of using the compound for target preparation and yield some data on the chemical properties of the compound. The apparatus should also be useful for other investigations of volatile metal compounds. A drawing of this device is shown in Figure 14 of this report.

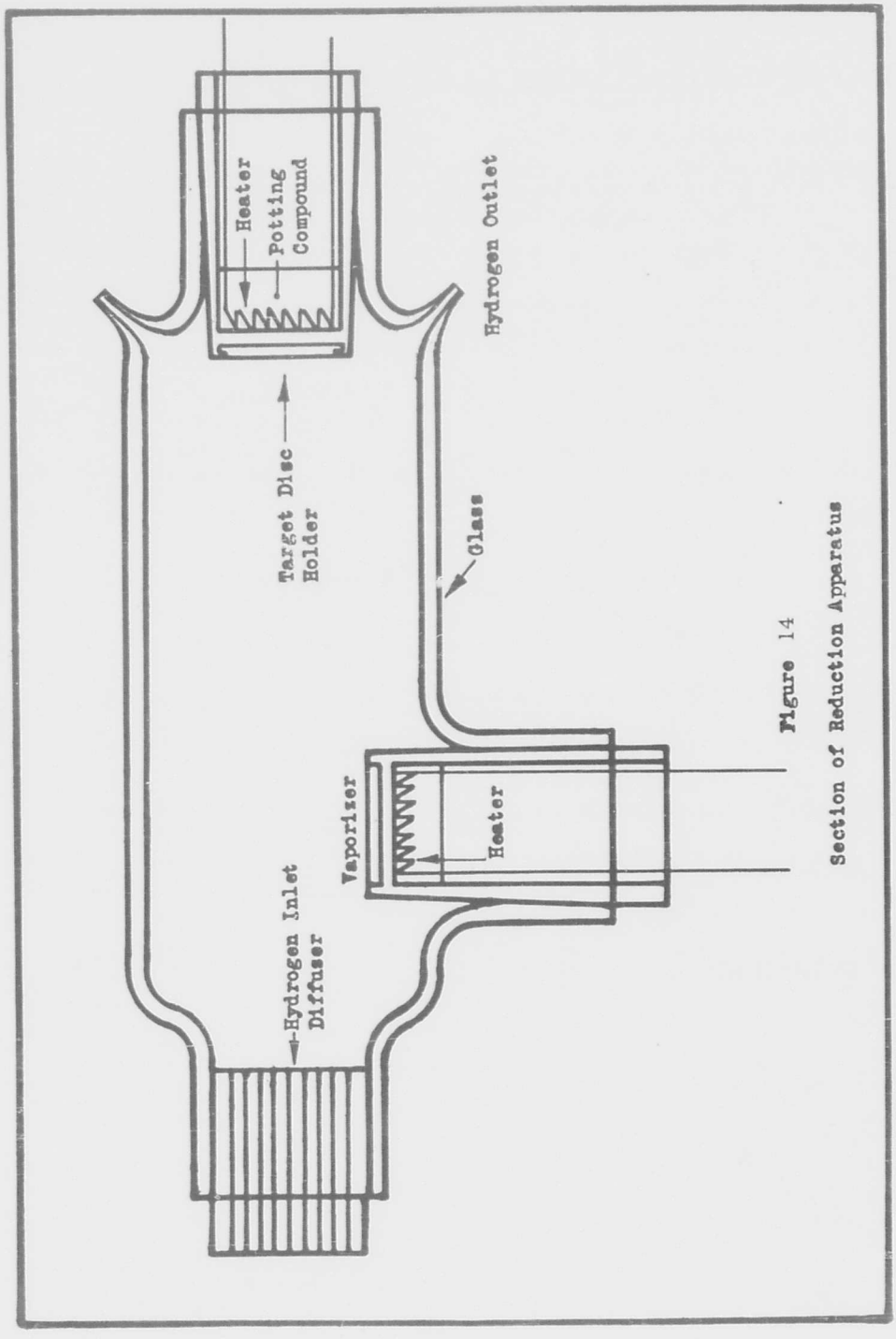

Figure 14

Section of Reduction Apparatus

VI Computer Program

Introduction

As has already been mentioned earlier in this report, the nature of the reaction used to detect and produce neutrons is of importance in constructing and operating a spectrometer of this type. In order to properly detect the product particles of the neutron-induced reaction, their energy, and to a degree, their angular distribution, are of concern. Also, in the case of neutrons produced as secondary particles of a nuclear reaction, the energy and angular distribution are important. To facilitate the study of such nuclear reactions, a digital computer program was written for the IBM 1620 computer located in Building 125, Area B, WPAFB.

Basic Theory

To calculate the distribution in the laboratory system of energy and angular direction of two product particles from a nuclear reaction of the type M2(M1, M3)M4 requires computation of a number of simple relationships involving the masses and velocities of the particles present before and after the reaction takes place. The objection to performing such calculations by hand

is that in order to arrive at enough values of energy as a function of angle of emission to adequately represent the distribution, a great deal of merely tedious and uninstructive work must be performed. In addition, the calculations vary with changes in the energy of the incident particle, angle of scatter, and masses and the "Q" energy of the reaction.

A purely classical mechanics approach was taken in setting up the program. Relativistic corrections are not significant except at very high energies or unless a high degree of accuracy is required. An excellent treatment of the processes involved is given in Evans (Ref 12:408-417) and in Fast Neutron Physics, Part 1 (Ref 14:49-71). The basic theory involves a conservation of energy and momentum of the system. For the purposes of this discussion and the understanding of the program statements, the following symbol definitions are provided.

M1--mass of bombarding particle

M2--mass of target nucleus

M3--mass of lighter of two product particles

M4--mass of heavier of two product particles

Q--energy of reaction--either positive or negative

V1, V3, V4, E1, E3, E4--velocities and energies respectively of the above-defined masses

ϕ --angle from path of M1 to which M3 is emitted (lab system)

θ --angle from path of M1 to which M4 is emitted (lab system)

The equations which the program solves are:

$$\sqrt{E3} = V \pm \sqrt{V^2 + W}$$

$$V = \frac{\sqrt{M1 \cdot M3 \cdot E1 \cdot \cos\phi}}{M3 + M4}$$

$$W = \frac{M4 \cdot Q + E1(M4 - M1)}{M3 + M4}$$

$$E4 = E1 + Q - E3$$

$$E4 = \frac{1}{2} M4(V4)^2 \quad (\text{for } V4)$$

$$E3 = \frac{1}{2} M3(V3)^2 \quad (\text{for } V3)$$

$$M3 \cdot V3 \sin\phi = M4 \cdot V4 \sin\theta \quad (\text{for } \theta)$$

$$EF = \frac{-Q(M3 + M4)}{M3 + M4 - M1 - \dfrac{(M1 \cdot M3)}{M4(\sin^2\phi)}}$$

EF $\equiv$ threshold energy

The expression for $\sqrt{E3}$ arises from solving what is called the "Q" equation by handling it as a quadratic in $\sqrt{E3}$. The "Q" equation is

$$Q = E3\left(1+\frac{M3}{M4}\right) - E1\left(1-\frac{M1}{M4}\right) - \frac{2\sqrt{M1 \cdot E1 \cdot M3 \cdot E3}}{M4}\cos\phi$$

Whether or not the plus or minus sign is to be used, or both signs are to be used, is determined by the requirements that $\sqrt{E3}$ can not be negative or imaginary. If "w" is greater than "v^2" and negative, $\sqrt{E3}$ is imaginary. If "w" is negative and less than v^2, $\sqrt{v^2 + w}$ is less than "v" and both signs are allowed. If "w" is positive, only the plus sign is allowed.

Physically, the double values of E3 and E4 signify low values of momentum of the product masses, M3 and M4, with respect to the momentum of the compound nucleus immediately prior to dissociation into M3 and M4. Figure 15 shows how the two energies are possible at one angle of scatter in the lab system.

When Q is negative, a minimum "threshold" energy, E1, is required for the reaction to take place. This energy is greater than

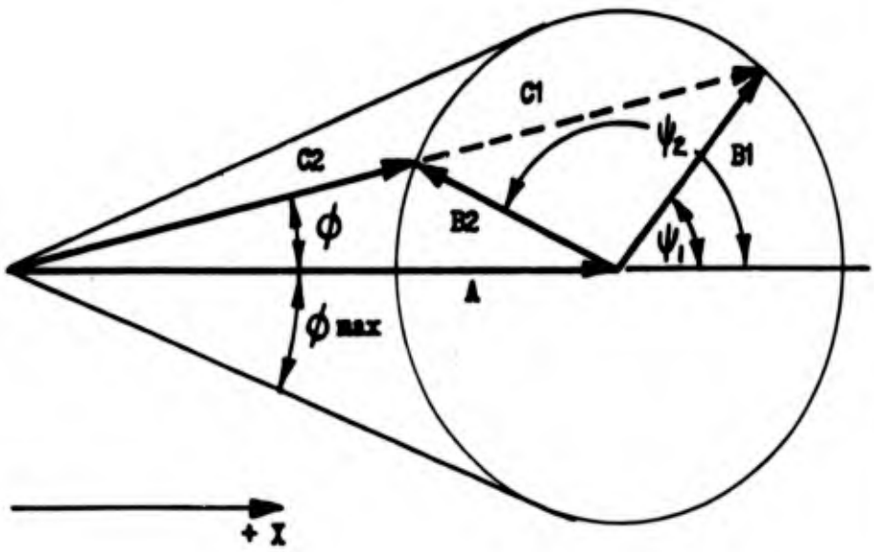

$\vec{A}$ = CM velocity
$\vec{B}$ = velocity of M3 in CM
$\vec{C}$ = velocity of M3 in lab.

ϕ = lab. angle
ψ = CM angle

$\vec{A} + \vec{B1} = \vec{C1}$

$\vec{A} + \vec{B2} = \vec{C2}$

Or the same effect can be expressed in terms of +X momentum vectors where +X is the direction of the bombarding mass, M1.

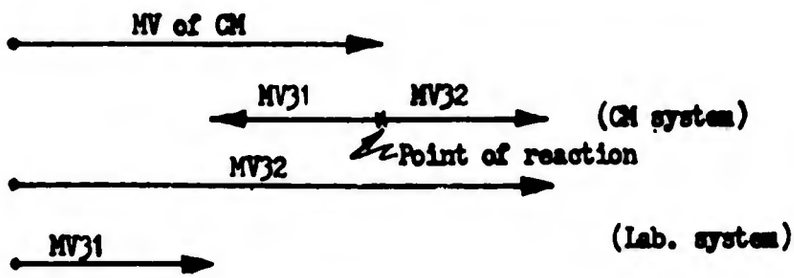

Figure 15 Conditions for Double Value Energies for M3 and M4

the Q value which can be explained by a requirement for energy to give the compound nucleus its forward momentum. The threshold energy varies with the chosen angle of scatter of M3, ϕ, reaching a maximum at 90°.

The program is set up so that the operator can pick any value of ϕ up to 180° as a beginning point and then scan up to 180° at angle increments desired. After the desired number of values of E3, E4, and θ have been calculated for one energy, E1, the program will recalculate values over the same angular range for a new value of E1 and will keep doing this as long as it is desired to increase the energy of the bombarding particle.

By the proper selection of switch settings it is possible to punch out the values of E3, E4, ϕ and θ to use as input for the short plotting program which will plot the values of E3 and E4 for each angle of scatter. This plotting program is made possible by a modification to the IBM Fortran processor and sub-routines developed by Mr. Edward Van Schaik of the Dayton IBM office. A short write-up of this modification is found in Appendix A.

The Fortran language used in the main program is a modification to the IBM Fortran language resulting from changes made to the processor and sub-routines by Lt. Richard Pratt of the Mathematics Department of the Air Force Institute of Technology.

Program

To execute the main program, the values of Q, M1, M3, and M4 peculiar to the reaction to be investigated are entered at the typewriter along with the number of increments to ϕ, M, the initial value of ϕ, PHI(1), the increment to E1, ADD, the increment of ϕ, VINC, and the number of increments to E1, N. The above values must be entered as follows in this sequence.

```
N=+XXX
M=+XXX
ASS1=+X.XX
ASS3=+X.XX
ASS4=+X.XX
E1=+XX.XXXX        (in mev)
Q=±X.XXX           (in mev)
VINC=+XX.XX        (in degrees)
ADD=+XX.XXX        (in mev)
PHI(1)=+XXX.XXX    (in degrees)
```

The number of X's are only representative and do not imply a limit on the size of the numbers.

The X's represent integers. The "+" signs are not required. If a negative Q is to be used, the "-" sign must be present. The identifying abbreviations and the equal signs are not typed; only the corresponding value is typed. The sense switches are used as follows.

Sense Switch 1

ON Continue calculating corresponding values for successive $\phi + \Delta\phi$.

OFF Enter new input.

Sense Switch 2

ON Punch E3, E4, ϕ and θ .

OFF Do not punch.

Sense Switch 3

ON Accept new data from typewriter after operating with first set of data.

OFF Stop.

Sense Switch 4

Used to make corrections to data entered by the typewriter before value typed has been accepted. Turn off and press RELEASE and START, and then turn on to retype entry.

After the object deck has been entered along with the subroutines, the start button is pushed and the program will begin executing by typing instructions to enter the appropriate data. If punched output is desired for plotting, the punch unit must be ready.

If any of the chosen angles scanned do not produce a value of E3, Sense Switch 2 must be off and the plotting option cannot be used.

The plotting is accomplished by first entering the plotting routine object deck and sub-routines after which the previously punched cards are read. The main program punches out the value of "M" for each set of values of E3, E4, ϕ and Θ; and this card must be the first one read. As soon as the cards have been read, the typewriter will begin to plot. After one set of data has been plotted, the machine will plot any number of additional sets as long as Sense Switch 1 is on. Each succeeding set of data cards must begin with the card on which the value of "M" is punched. The scale of energies for E3 and E4 goes to 20 mev limiting the reactions which may be plotted. The values of E3 and E4 are multiplied by a scale factor of three before plotting, and the typewriter plots the integer value of the product truncating decimal fractions.

Flow charts for both the main program and plotting program are found in Figures 16 and 17 respectively. Print outs of the two programs are found in Appendix B. Nominal execution time for the main program to tabulate one set of values is three minutes and nominal plotting time is also three minutes.

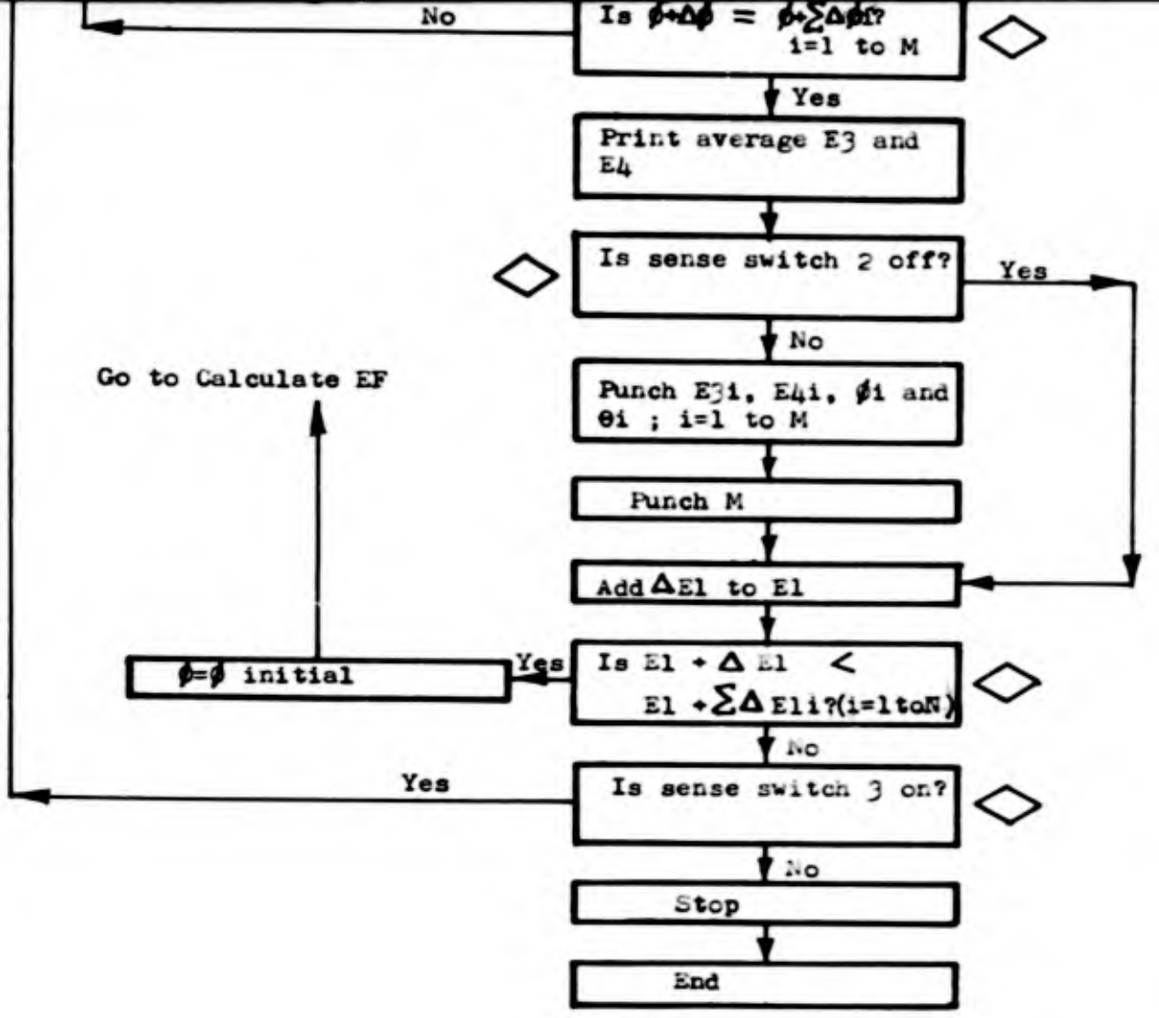

◇ Represents operations involving a choice of options

Figure 16

Flow Chart of Main Program

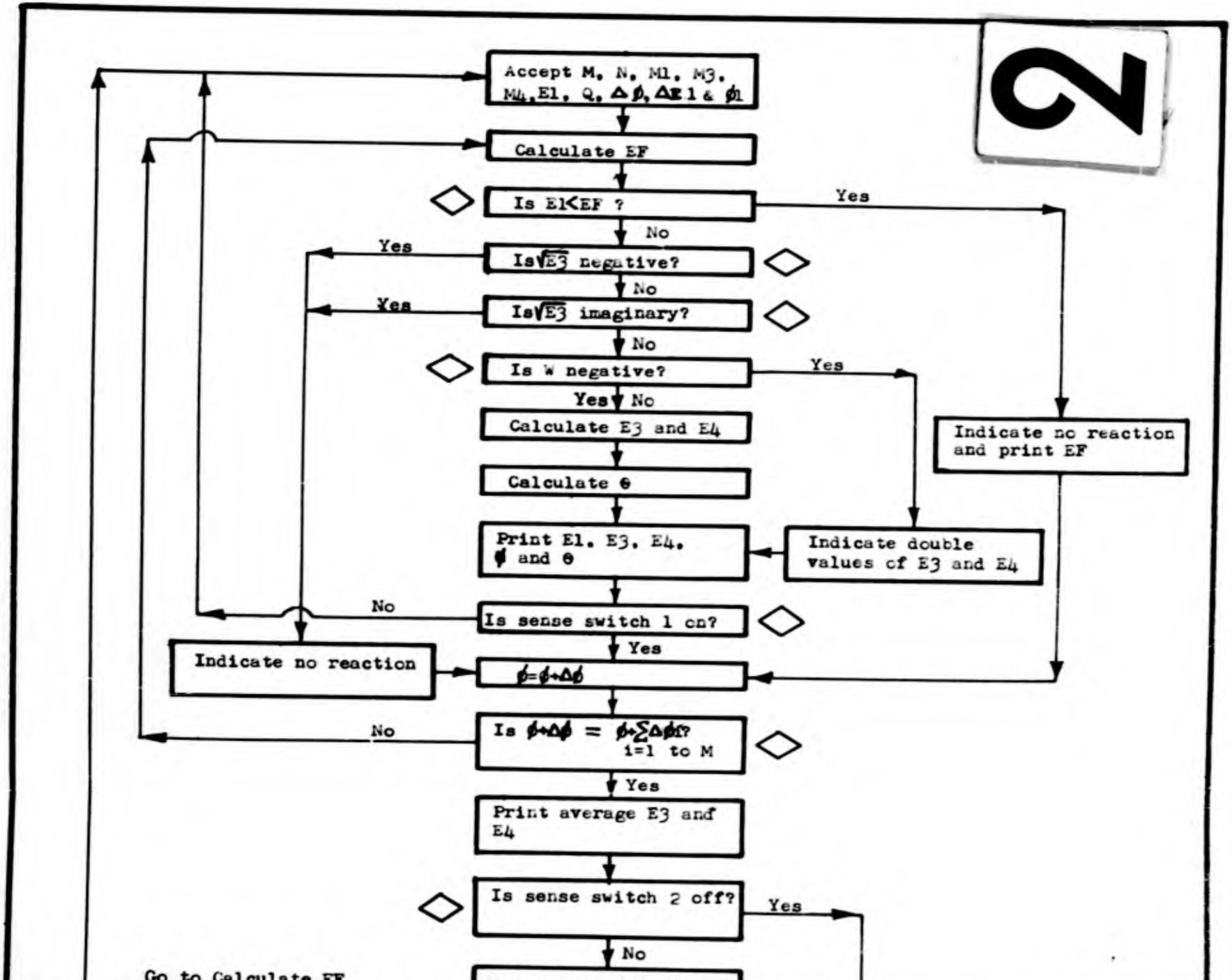
2
Accept M, N, M1, M3, M4, E1, Q, Δφ, ΔE1 & φ1
Calculate EF
Is E1<EF ?
Yes
No
Is √E3 negative?
Yes
No
Is √E3 imaginary?
Yes
No
Is W negative?
Yes
Yes
No
Calculate E3 and E4
Calculate θ
Print E1, E3, E4, φ and θ
Indicate double values of E3 and E4
Indicate no reaction and print EF
No
Is sense switch 1 on?
Yes
Indicate no reaction
φ=φ+Δφ
No
Is φ+Δφ = φ+∑Δφi? i=1 to M
Yes
Print average E3 and E4
Is sense switch 2 off?
Yes
No
Go to Calculate EF

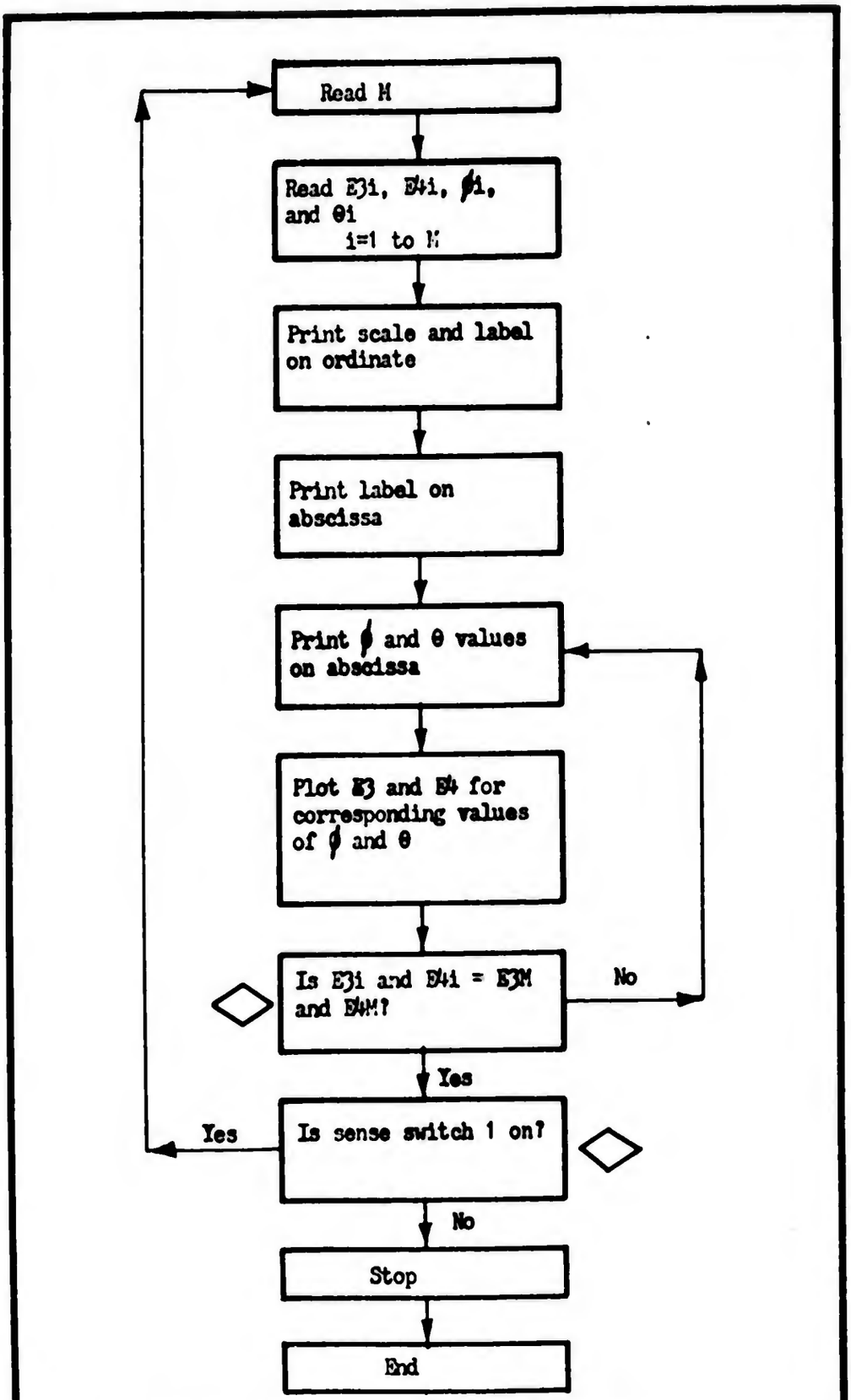

Figure 17 Flow Chart for Plotting Program

Results

Sample printed results of the main and plotting programs are found in Appendix B. The tabulated values of E3 for the Li^7 (p,n) Be^7 reaction show good correlation to those found in Fast Neutron Physics, Part I. There is a slight difference in the values, but no attempt was made to investigate the cause. The results of the program were checked by hand calculations with good correspondence between machine and hand values. The sample printed results include examples of what happens when E1 is below threshold, when E3 and E4 are double valued, and when $\sqrt{E3}$ is negative or imaginary.

VII Discussion and Conclusions

It is interesting to note that this study regarding a fast neutron spectrometer led to the use of He^3 as did the work done by Dearnaley (Ref. 8). The reasons which dictated its use for this thesis are not exactly the same as those in Dr. Dearnaley's report; however, there are differences in the comparison he made with the Li^6 and proton recoil which account for this. The preliminary investigation made in this thesis was made completely independent of the Harwell report which leads to the conclusion that the merits of He^3 as target material for a fast neutron spectrometer are indisputable.

It is felt that the concept of using the gas at high pressure is a sound one and will provide data of value both in terms of spectroscopic data and study of the neutron cross section and energy loss as a function of gas pressure. In addition, some useful data concerning the solid state detectors can be obtained by use of the variable aperature washers used to space between the detectors.

The present equipment design for pressurizing the gas is not considered worthy of further development. A new design is presented in Figure 18 and appears to be sound and relatively easy

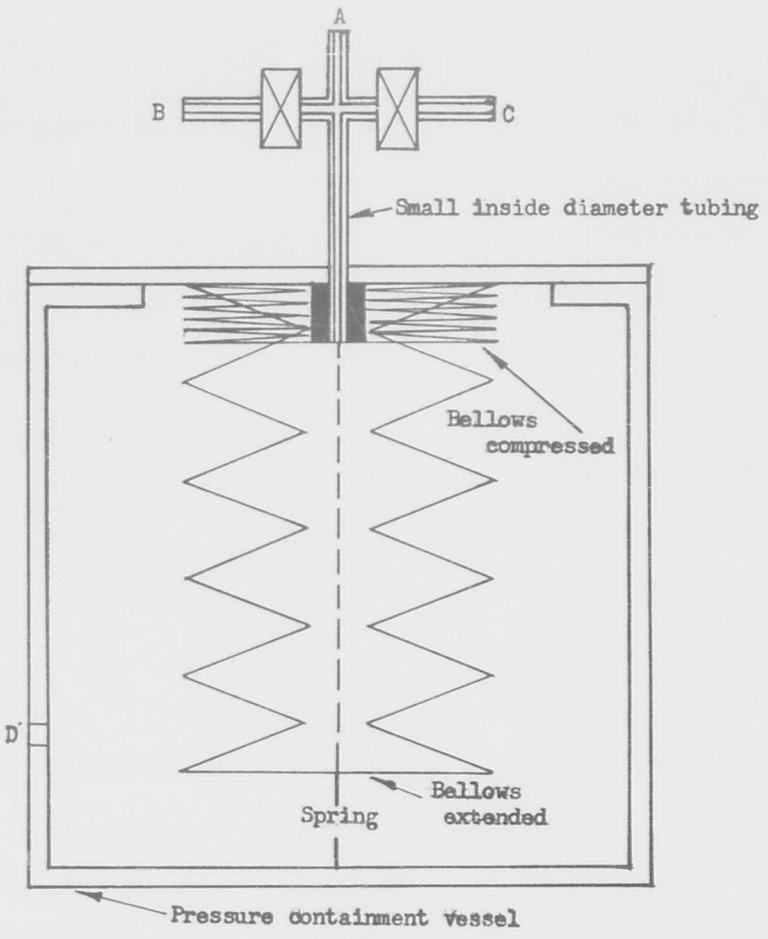

1. Vacuum is pumped in extended bellows through open valve to B.
2. Vacuum line is closed off and low pressure helium is admitted from C through open valve into extended bellows.
3. Pressure is applied to outside of bellows by admitting regulated high pressure air through D. Valve to C is closed.
4. Helium is compressed by reduction of volume into small target chamber at A.
5. As pressure is released, the spring restores the bellows to the extended position.

Figure 18

Proposed Gas Pressuring Device

to construct. The bellows referred to in Figure 18 is commercially available at costs which are not prohibitive. The target chamber design could remain essentially unchanged and the entire apparatus would be small in size and easy to operate.

If a spectrometer is constructed with the good resolution and efficiency possible with He^3, it would be of value in resolving spectra to higher degrees than before possible. If considerable data is to be obtained, consideration should be given to mating the spectrometer with equipment which would automatically correct the spectral output for such parameters as efficiency, background and resolution as a function of neutron energy. By making some assumptions concerning these parameters, it is possible to write a computer program which would use input to the multi-channel analyzer as its input and punch a tape with the corrected counts per analyzer channel. This tape could then become a permanent record that could be displayed in a printed form or on a scope, as desired. Equipment is available today to perform all these functions, and much could be done towards providing more accurate spectroscopic analysis.

Bibliography

1. Amaldi, Edoardo. "The Production and Slowing Down of Neutrons and Related Gamma Ray Problems" in Encyclopedia of Physics, Vol. XXXVIII/2, edited by S. Flügge. Berlin: Springer-Verlag, 1959.

2. Babcock, R.V., et al. "Coated Semiconductor is Tiny Neutron Detector" Nucleonics 4:116, (April 1959).

3. Baum, J.J. The Development of a Fast Neutron Spectrometer Using Silicon Surface Barrier Diodes. Cincinnati 15, Ohio: General Electric Company, August 1961.

4. BNL 325. Neutron Cross Sections. Washington 25, D.C.: GPO, 1958.

5. Count, Elmer E. Production of Radionuclides from 14-Mev Neutrons. M.S. Thesis. Wright-Patterson Air Force Base, Ohio: Institute of Technology, March 1961.

6. Daggett, E.H., et al. Determination of the Liquid Level in a Steel Cylinder by Gamma Absorption. Miamisburg, Ohio: Mound Laboratory, 27 September 1952.

7. Dearnaley, G. Semiconductor Nuclear Radiation Detectors. Harwell, England: Atomic Energy Research Establishment, November 1962.

8. Dearnaley, G., et al. Semiconductor Fast Neutron Detectors. Harwell, England: Atomic Energy Research Establishment, 1962.

9. Dearnaley, G. and A. B. Whitehead. The Semiconductor Surface Barrier for Nuclear Particle Detection. Harwell, England: Atomic Energy Research Establishment, February, 1961.

10. Desdeires, J. and D. Didier. Spectrometrie des Flux de Neutrons Intermediares et Rapides. (In French) Saclay, France: Comissariat al Energie Atomique, Centre de Etudes Nuclearires, 1960.

11. Evans, C. Preparation of Thick Zirconium-Tritium and and Zirconium-Deuterium Targets. Harwell, England: Atomic Energy Research Establishment, 1955.

12. Evans, R.D. The Atomic Nucleus. New York: McGraw Hill, 1955.

13. Everling, F., et al. "Consistent Set of Energies Liberated in Nuclear Reactions" in 1960 Nuclear Data Tables Parts 1 and 2. Washington 25, D.C.: GPO, February 1961.

14. Fowler, J.L. and J.B. Marion. Fast Neutron Physics, Part I in Monographs and Texts in Physics and Astronomy, Vol. IV, edited by R. E. Marshak. New York: Interscience Publishers Inc., 1960.

15. Friedland, Stephen S., et al. "Tiny Semiconductor is Fast Linear Detector." Nucleonics 18:54-59 (February 1960).

16. Friedland, Stephen S. and Frank Keywell. "Semiconductor Devices as Charged Particle Detectors and Energy Spectrometers" in Proceding of the Second Conference on Nuclear Radiation Effects on Semiconductor Devices, Materials and Circuits. New York: Cowan Publishing Corp., September, 1959.

17. Gonser, V. and K. Lücke, "The Use of Van de Graaff Accelerators for High Intensity Neutron Irradiation of Metals." Nuclear Instrumentation and Methods 11:139-143 (January 1961).

18. Kim, Chul Mo. A Theoretical Comparison of 4π Fast-Neutron Spectrometers. M.S. Thesis. Berkeley, California: University of California. Ernest O. Lawrence Radation Laboratory, November 1960.

19. Kronenberg, Stanley and H. M. Murphy, Jr. "Energy Spectrum of Protons Emitted from a Fast Neutron Irradiated Hydrogenous Material." Radiation Research 12:6 (1960).

20. Love, T.A., et al. A Silicon Surface-Barrier Fast-Neutron Spectrometer. Oak Ridge, Tennessee: Oak Ridge National Laboratory, 1961.

21. Marion, J.B. "Nuclear Reaction Graphs" in 1960 Nuclear Data Tables, Part 3. Washington 25, D.C.: GPO, August 1960.

22. McCormick, R.D. and J. D. McCormick. Hydrogen and Carbon Target Preparation for a Positive Ion Accelerator. Richland, Washington: Atomic Energy Commission, Hanford Atomic Products Operation, October 1960.

23. Moore, D. "Neutron, Electron and X-Ray Beams Used for Radiation Research from a Van de Graaff Generator." Nuclear Instruments and Methods 11:238-247 (January 1960).

24. Murphy, James F. Solid State Neutron Detectors. M.S. Thesis, U. S. Naval Postgraduate School. Washington 25, D.C.: Office of Technical Services, Department of Commerce, May 1961.

25. Nuclear Engineering Handbook. edited by Harold Etherington. New York: McGraw Hill, 1958.

26. Physical Parameters Affecting Performance of P-N Junction Detectors. Culver City, California: Hughes Aircraft Co., November 23, 1960.

27. Price, William J. Nuclear Radiation Detection. New York: McGraw Hill, 1958.

28. Research on Solid State Charged Particle Silicon Detectors. Technical Proposal. Montreal, Canada: RCA Victor Co. Ltd., 1961.

29. Rucker, Carl L. A Fast Neutron Counter Using Semiconductor Diodes and Coincidence Circuitry. M.S. Thesis. Wright-Patterson Air Force Base, Ohio: Air Force Institute of Technology, March 1961.

30. Rybakov, B.V. and V. A. Siderov. "Fast Neutron Spectroscopy" translated from Russian. in Soviet Journal of Atomic Energy, Supplement No. 6. 1958.

31. Semiconductor Nuclear Particle Detectors in Nuclear Science Series Report No. 32 edited by Dabb, J.W.T. and F. J. Walter. Washington, D.C. National Academy of Sciences, 1961.

32. Steinberg, Robert. "Semiconductor Fission Probe." Nucleonics 18:85. February 1960.

33. Whaling, Ward. "The Energy Loss of Charged Particles in Matter." in Handbuck der Physik, Vol. 34. Edited by E. Flügge. Berlin: Springer-Verlag, 1958.

Appendix A

Plot Sub-routine of IBM 1620 FORTRAN with Format

(Written by Mr. Edward Van Schaik, IBM, Dayton, Ohio)

Introduction

Since many IBM 1620 applications are in areas where a rough plot of the results can be quite useful, it was felt that a sub-routine incorporated into FORTRAN was necessary. GOTRAN provides a statement for plotting but this requires a separate program and a knowledge of GOTRAN language. This write-up presents a sub-routine which can be easily used in FORTRAN for plotting single or multiple curves without the GOTRAN problem of determining which curve has the lower magnitude. Also this method can be used to generate the curves on cards for off-line printing.

Method of Use

Since a method of plotting multiple curves with any special characters was desired, the normal method of output (PRINT or PUNCH) was utilized with the incorporation of a new type FORMAT character Z. The sub-routine is used in a different manner than normal. The basic FORTRAN statements to use this plot sub-routine are:

```
      PRINT     2, X, M, N, J
2     FORMAT    (F10.5, 3Z*+.)
```

The first variable in the list is the independent variable which can be either fixed or floated. This variable will be handled like a regular value and be printed. The Z character in the format accomplishes the following:

1. The remaining values in the list will be plotted instead of printed.
2. The Z is handled like the H except that the address compiled will be the address in the symbol table corresponding to the sub-routine so that the FORTRAN input/output package will branch to this address then to the relocated sub-routine. The number and type of plot characters are stored similarly to the H type.
3. The remaining values in the list are assumed to be fixed variables previously scaled to the range of output record--the digits in the independent variable. (Example: for the case shown, the numbers should be scaled 0 to 87-10 or 77. Normally a range of 0-70 should be the limitation for type-writer since the carriage can handle only 80 to 85 positions. Cards are 72--the digits in the independent variable.

3. (Continued)

Negative numbers, floated numbers, and numbers outside of the allowable range produce an ERROR F9 message.

4. The first plot character after the Z will be used to plot the first variable in the list to be plotted. Remaining list values will use the next character until the list is satisfied. Therefore, no limitation on the number of variables exists except the 72 character statement size. If the number of variables in list exceed the number of plot symbols, an ERROR F9 message will occur.

5. The range of plot starts at the next position after the last digit of the independent variable. Therefore, if the values of the variable to be plotted is 0, the plot symbol will be inserted in the first position after the independent variable.

The statement may be either PRINT or PUNCH dependong on whether the output is on the typewriter or cards. The sub-routine sets up the FORTRAN output area with the independent variable and all plot symbols before giving the write command. For typewriter output, a record mark is inserted in the next position after the highest plot value to conserve typing time. This produces a much faster method than GOTRAN and eliminates all problems of relative magnitude of curves.

FORTRAN Processor Modifications

To make the plot routine useable on the 20K card system, space was used where the ACCEPT TAPE and PUNCH TAPE statements were previously located. If these commands are called, an error message indicating a missing format number will occur. These changes are:

Card No. 3024

Location		New Instruction	Card Col.
2030	CM	14 17323 00069	21-32
2042	BNE	47 04022 01200	33-44
2054	B	49 02174	45-52

Card No. 3026

Location		New Instruction	Card Col.
2162	B	49 02218 00000	13-24
2174	TDM	15 08719 00001	25-36
2186	TFM	16 03493 $\bar{1}$9870	37-48
2198	TR	31 17322 17324	49-60
2210	B	49 04113	61-67

Card No. 3053

Location		New Instruction	Card Col.
4070	TFM	16 04243 0003$\bar{1}$	31-42
4082	BNE	47 02030 01200	43-54
4094	TR	31 17322 17324	55-66
4106	TFM	16 0349	67-72

Card No. 3054

Location		New Instruction	Card Col.
4112		3 $\bar{0}$4264	3-8
4118	TFM	16 03620 $\bar{0}$4174	9-20

These patches allow the processor to check for the Z format, insert the sub-routine name location, and set for sub-routine load. The instructions at 2174 and 2186 assume that the sub-routine will be the first added after the normal six from IBM. If this is not true, then the addresses of 2174 (8719 for sub-routine load) and 2186 (19870 for sub-routine address) must be changed. The normal rules for adding a sub-routine must be followed.

Plot Sub-routine

Enclosed at the end of this write-up is an SPS listing of the Plot Sub-routine for the FORTRAN sub-routine deck without automatic divide. For use with automatic divide, the address for the symbols of the input/output package must be changed. This includes CON2 which refers to the instruction in SWC.

The sub-routine requires 432 core locations. The trailer card requires a value of 00434 in Col. 1-5 as stated in the FORTRAN write-up.

General Comments

With format control, the output plot can be quite complete. The following technique which can be used in FORTRAN provides a means of printing the graph scales:

```
          PRINT 5, 0, 50, 100, 150 etc.
          PRINT 5, 1, 1, 1, 1, 1, 1, etc.
5         FORMAT (I 11, I5, I5, I5, etc.)
```

FORTRAN will print the variables in the list as the value of each quantity. The I11 can be made so that the first value prints after the independent variable. Example (using previous example)

```
          0    50    100    150    200    250    300    350    400
          1    1     1      1      1      1      1      1      1
.5000                       *             +
```

Although this write-up indicates that only the independent variable may be printed, this is not true. Assume it is desired to print x and y and also plot y. This could be done as follows:

```
          PRINT 6, X, Y, MY

6         FORMAT (F10.5, F10.5, 1Z*)
```

This will print as follows:

```
     x          y
+xxx.xxxxx+xxx.xxxxx                    *
```

Where X and Y are printed and MY (Y after scaling) is plotted. The range of MY must be reduced to keep the over record with limits.

The general rule is that any variable to the left of the first plot variable in the list will be printed under normal FORTRAN rules.

The name PLOT must not be used in the program since the compiler will assume this to be a function name.

```
05000                                          DORG   5000Z
05000  Z6 05035 07275                  PLOT    TF     *+35,BLK10+11,0Z
05012  ±1 05035 00002                          AM     *+23,2,0102
05024  26 07428 00000                          TF     T3+2Z
05036  11 05035 00002                          AM     PLOT+35,2,0102
05048  26 04998 05420                          TF     SWC+6,CON1+6,1Z
05060  11 06326 00002                          AM     BLK5+6,2,10Z
05072  12 07807 00002                          SM     P,2,10Z
05084  16 07778 08055                          TFM    PT+18,QZ+2Z
05096  49 07360 00000                          B      BRBKZ
05104                                          DORG   *-3Z
05104  12 07428 00001                  PLOT 1  SM     T3+2,1,10Z
05116  47 05378 01300                          BN     ERROR,,0Z
05128  31 00089 07994                          TR     RX-9,ZOTZ-10Z
05140  26 05163 04991                          TF     *+23,SWC-1,0Z
05152  26 00098 00000                          TF     RXZ
05164  44 05378 00095                          BNF    ERROR,RX-3,0Z
05176  24 00098 07807                          C      RX,PZ
05188  46 05378 01300                          BNL    ERROR,,0Z
05200  44 05224 00098                          BNF    *+24,RX,0Z
05212  49 05378 00000                          B      ERROR,,0Z
05224  26 05278 06326                          TF     PLOT2+6,BLK5+6,0Z
05236  21 05278 00098                          A      PLOT2+6,RX,0Z
05248  21 05278 00098                          A      PLOT2+6,RX,0Z
05260  26 05283 05035                          TF     PLOT2+11,PLOT+35,01Z
05272  26 00000 00000                  PLOT 2  TF     0,0Z
05284  24 07778 05278                          C      PT+18,PLOT2+6,1Z
05296  46 05320 01300                          BNL    *+24,,0Z
05308  26 07778 05278                          TF     PT+18,PLOT2+6,1Z
05320  43 05364 05365                          BD     PLOT3,T2,0Z
05332  16 07850 07360                          TFM    SWH+6,BRBKZ
05344  26 04998 05432                          TF     SWC+6,CON2,1Z
05356  49 04692 00000                          B      SWDZ
05364                                          DORG   *-3Z
05364  11 05035 00002                  PLOT 3  AM     PLOT+35,2,010Z
05376  42 00000 00000                          BB     Z
05378                                          DORG   *-9Z
05378  34 00000 00102                  ERROR   RCTY   Z
05390  39 07977 00100                          WATY   ERCONTZ
05402  49 05320 00000                          B      PLOT2+48,,0Z
07977                                  ERCONTDS       ,7977Z
05365                                  T2      DS     ,5365Z
```

```
08004
054p4  49 05104 00000
05432     00007
07264
07426
04992
00098
07807
06320
07760
08053
07360
04692
07844
             --     --
```

```
ZOTZ    DS      ,8004Z
CON1    B       PLOT1,,0Z
CON2    DC      7,4307876Z
BLK10   DS      ,7264Z
T3      DS      ,7426Z
SWC     DS      ,4992Z
RX      DS      ,98Z
P       DS      ,7807Z
BLK5    DS      ,6320Z
P1      DS      ,7760Z
QZ      DS      ,8053Z
BRBK    DS      ,7360Z
SWD     DS      ,4692Z
SWH     DS      ,7844Z
        DEND    Z
```

Main Program

```
08000 3     FØRMAT(/3XF8.4,5XF8.4,5XF8.4,6XF7.2,8XF7.2)
08136 4     FØRMAT(/5HAVE3=F10.6,10H     AVE4=F10.6//)
08222 6     FØRMAT(/49HENTER VALUES ØF M, N, MASS1, MASS3, MASS4, E1, Q,)
08350 7     FØRMAT(/42HINCREMENT ØF PHI, INCREMENT ØF E1 AND PHI.)
08464 8      FØRMAT(I4)
08486 14    FØRMAT(/34HREACTIØN NØT PØSSIBLE-THRESHØLD E=F8.4)
08588 13    FØRMAT(/21HREACTIØN NØT PØSSIBLE)
08660 12    FØRMAT(/6X2HE1,10X2HE3,10X2HE4,11X3HPHI,11X5HTHETA)
08876 54     FØRMAT(F8.4,F8.4,F13.8,F7.2)
08914 69     FØRMAT(///)
08946 11     FØRMAT(/36HDØUBLE VALUE ENERGIES-LARGEST LISTED)
09048        A=3.1415926/180.
09084        B=180./3.1415926
09120        DIMENSIØN E3(37),E4(37),THETA(37),PHI(38)
09120 9      PRINT6
09144        PRINT7
09168        ACCEPT,M,N,ASS1,ASS3,ASS4
09240        ACCEPT,E1,Q,VINC,ADD,PHI(1)
09312        PRINT 69
09336        PHI(1)=PHI(1)*A
09372        VINC=VINC*A
09408        DØ  40K=1,N
09420        PRINT 12
09444        SUM3=0.0
09468        SUM4=0.0
09492        DØ  301=1,M
09504        IF(Q)46,91,91
09556 46     EEF=-Q*(ASS3+ASS4)
09616        EF=EEF/(ASS3+ASS4-ASS1-(ASS1*ASS3/ASS4*((ABSF(SIN(PHI(I))))**2.)))
09832        IF(EF-E1)91,91,73
09896 73     PRINT 14.EF
```


Appendix B

Computer Output

Beginning of Main Program Listing

```
T9920          GØ TØ 25
T9928 91       V=CØS(PHI(I))*SQRT(ASS1*ASS3*E1)/(ASS3+ASS4)
T0096          W=(ASS4*Q+E1*(ASS4-ASS1))/(ASS3+ASS4)
T0240          SUM=(V*V)+W
T0288          SQRE3=V+SQRT(ABSF(SUM))
T0336          IF(SUM)43,99,99
T0388 99       IF(SQRE3)43,70,70
T0440 70       IF(W)72,71,71
T0492 72       PRINT 11
T0516 71       E3(I)=SQRE3*SQRE3
T0576          E4(I)=Q+E1-E3(I)
T0672          V1=SQRT(2.*E1/ASS1)
T0732          V3=SQRT(2.*E3(I)/ASS3)
T0816          V4=SQRT(2.*E4(I)/ASS4)
T0900          SINTH=ASS3*V3*SIN(PHI(I))/(ASS4*V4)
T1044          CØSTH=(ASS1*V1-ASS3*V3*CØS(PHI(I)))/(ASS4*V4)
T1248          IF(CØSTH)5,15,5
T1300 5        TNTH=SINTH/CØSTH
T1336          THETA(I)=ATAN(TNTH)
T1384          IF(CØSTH)61,21,21
T1436 61       THETA(I)=3.1415926+THETA(I)
T1520 21       THETA(I)=THETA(I)*B
T1604          GØ TØ 35
T1612 15       THETA(I)=90.0
T1660 35       PHI(I)=PHI(I)*B
T1744          PRINT3,E1,E3(I),E4(I),PHI(I),THETA(I)
T1912          SUM4=SUM4+E4(I)
T1972          SUM3=SUM3+E3(I)
T2032          IF(SENSE SWITCH1)20,9

T2052 20       PHI(I)=PHI(I)*A
T2136          GØ TØ 25
T2144 43       PRINT 13
T2168 25       PHI(I+1)=PHI(I)+VINC
T2252  30      CØNTINUE
T2288          VM=M
T2312          AVE3=SUM3/VM
T2348          AVE4=SUM4/VM
T2384          PRINT4,AVE3,AVE4
T2420          IF(SENSE SWITCH 2)93,41
T2440 93       DØ 92 I=1,M
T2452 92       PUNCH 54,E3(I),E4(I),PHI(I),THETA(I)
T2644          PUNCH 8,M
T2668 41       PRINT 69
T2692 40       E1=E1+ADD
T2764          IF(SENSE SWITCH3)9,31
T2784 31       STØP
T2792          END
END ØF CØMPILATIØN T6413T7520
```

Main Program Listing (Continued)

```
0008300 1      FORMAT(F8.4,F8.4,F13.8,F7.2)
0008338 8      FORMAT(I4)
0008360 17     FORMAT(I17,I15,I15,I15,I15)
0008402 19     FORMAT(F7.2,F7.2,2X2Z*+)
0008452 69     FORMAT(///)
0008484 88     FORMAT(25X24HE3=*/E4=+, ENERGY IN MEV)
0008614 98     FORMAT(13HPHI AND THETA)
0008664 2      DIMENSION E3(37),E4(37),THETA(37),PHI(37)
0008664        B=180./3.1415926
0008712 6      READ 8,M
0008736        PRINT 88
0008760        PRINT 17,0,5,10,15,20
0008832        PRINT 98
0008856        DO 90I=1,M
0008868        READ 1,E3(I),E4(I),PHI(I),THETA(I)
0009024 90     PHI(I)=PHI(I)*B
0009156        DO 80I=1,M
0009168        JP=3.*E4(I)
0009252        LP=3.*E3(I)
0009336        PRINT 19,PHI(I),THETA(I),LP,JP
0009444 80     CONTINUE
0009480        PRINT 69
0009504        IF(SENSE SWITCH 1)6,31
0009524 31     STOP
0009572        END

PROG SW 1 ONFOR SYMBOL TABLE, PUSH START
SW 1 OFF TO IGNORE SUBROUTINES, PUSH START
1620 FORTRAN SUBR.   9/30/61
PROCESSING COMPLETE
```

Plotting Program

```
ENTER VALUES OF M, N, MASS1, MASS3, MASS4, E1, Q,
INCREMENT OF PHI, INCREMENT OF E1 AND PHI.
21
2
2.
1.
3.
1.9
3.266
1.5
.1
0.0
```

Sample Input Data

$D(d,n)He^3$

E1	E3	E4	PHI	THETA
1.9000	5.1326	.0333	.00	180.00
1.9000	5.1317	.0342	1.50	169.34
1.9000	5.1288	.0371	2.99	159.21
1.9000	5.1240	.0419	4.49	149.97
1.9000	5.1172	.0487	5.99	141.79
1.9000	5.1086	.0573	7.49	134.65
1.9000	5.0981	.0678	8.99	128.47
1.9000	5.0857	.0802	10.49	123.11
1.9000	5.0715	.0944	11.99	118.42
1.9000	5.0554	.1105	13.49	114.29
1.9000	5.0375	.1284	14.99	110.62
1.9000	5.0179	.1480	16.49	107.32
1.9000	4.9965	.1694	17.99	104.33
1.9000	4.9734	.1925	19.49	101.60
1.9000	4.9487	.2172	20.99	99.08
1.9000	4.9223	.2436	22.49	96.74
1.9000	4.8943	.2716	23.99	94.55
1.9000	4.8648	.3011	25.49	92.49
1.9000	4.8338	.3321	26.99	90.55
1.9000	4.8014	.3645	28.49	88.70
1.9000	4.7675	.3984	29.99	86.93

AVE3= 5.005370 AVE4= .160628

E1	E3	E4	PHI	THETA
2.0000	5.2382	.0277	.00	180.00
2.0000	5.2372	.0287	1.50	168.23
2.0000	5.2342	.0317	2.99	157.19
2.0000	5.2291	.0368	4.49	147.32
2.0000	5.2221	.0438	5.99	138.78
2.0000	5.2132	.0527	7.49	131.50
2.0000	5.2022	.0637	8.99	125.31
2.0000	5.1893	.0766	10.49	120.02
2.0000	5.1745	.0914	11.99	115.44
2.0000	5.1578	.1081	13.49	111.45
2.0000	5.1392	.1267	14.99	107.92
2.0000	5.1188	.1471	16.49	104.76
2.0000	5.0965	.1694	17.99	101.90
2.0000	5.0725	.1934	19.49	99.29
2.0000	5.0467	.2192	20.99	96.89
2.0000	5.0193	.2466	22.49	94.65

```
     2.0000          4.9902          .2757          23.99          92.56
     2.0000          4.9595          .3064          25.49          90.60
     2.0000          4.9273          .3386          26.99          88.73
     2.0000          4.8935          .3724          28.49          86.96
     2.0000          4.8583          .4076          29.99          85.27
AVE3=  5.105743      AVE4=   .160255
```

```
ENTER VALUES OF M, N, MASS1, MASS3, MASS4, E1, Q,
INCREMENT OF PHI, INCREMENT OF E1 AND PHI.
21
3
1.
1.
3.
1.
.764
9.
9.
0.0
```

D (d,n) He^3 (Continued)

and

Input for He^3 (n,p) T

E1	E3	E4	PHI	THETA
1.0000	1.7307	.0332	.00	180.00
1.0000	1.7208	.0431	8.99	145.23
1.0000	1.6914	.0725	18.00	120.51
1.0000	1.6442	.1197	27.00	103.75
1.0000	1.5817	.1822	35.99	91.35
1.0000	1.5070	.2569	44.99	81.35
1.0000	1.4236	.3403	53.99	72.80
1.0000	1.3353	.4286	62.99	65.21
1.0000	1.2454	.5185	71.99	58.31
1.0000	1.1571	.6068	80.99	51.94
1.0000	1.072)	.6910	89.99	46.00
1.0000	.9949	.7690	98.99	40.43
1.0000	.9244	.8395	107.99	35.18
1.0000	.8622	.9017	116.99	30.19
1.0000	.8087	.9552	125.99	25.45
1.0000	.7639	1.0000	134.99	20.90
1.0000	.7278	1.0361	143.99	16.52
1.0000	.7002	1.0637	152.99	12.27
1.0000	.6806	1.0833	161.99	8.13
1.0000	.6690	1.0949	170.99	4.04
1.0000	.6652	1.0987	179.99	.00
AVE3= 1.138475	AVE4=	.625523		

E1	E3	E4	PHI	THETA
10.0000	10.7593	.0046	.00	180.00
10.0000	10.6755	.0884	8.99	97.22
10.0000	10.4292	.3347	18.00	84.79
10.0000	10.0360	.7279	27.00	76.71
10.0000	9.5197	1.2442	35.99	69.83

He^3 (n,p) T Reaction

10.0000	8.9103	1.8536	44.99	63.51
10.0000	8.2409	2.5230	53.99	57.58
10.0000	7.5446	3.2193	62.99	51.95
10.0000	6.8519	3.9120	71.99	46.61
10.0000	6.1883	4.5756	80.99	41.54
10.0000	5.5730	5.1910	89.99	36.74
10.0000	5.0188	5.7451	98.99	32.20
10.0000	4.5327	6.2312	107.99	27.92
10.0000	4.1165	6.6474	116.99	23.87
10.0000	3.7687	6.9952	125.99	20.05
10.0000	3.4856	7.2783	134.99	16.41
10.0000	3.2625	7.5014	143.99	12.93
10.0000	3.0946	7.6693	152.99	9.58
10.0000	2.9779	7.7860	161.99	6.33
10.0000	2.9093	7.8546	170.99	3.15
10.0000	2.8866	7.8773	179.99	.00

AVE3= 6.227760 AVE4= 4.536238

E1	E3	E4	PHI	THETA
19.0000	19.7615	.0024	.00	180.00
19.0000	19.6040	.1599	8.99	91.17
19.0000	19.1416	.6223	18.00	81.67
19.0000	18.4036	1.3603	27.00	74.59
19.0000	17.4354	2.3285	35.99	68.21
19.0000	16.2937	3.4702	44.99	62.20
19.0000	15.0413	4.7226	53.99	56.46
19.0000	13.7407	6.0232	62.99	50.98
19.0000	12.4493	7.3146	71.99	45.75
19.0000	11.2147	8.5492	80.99	40.77
19.0000	10.0730	9.6909	89.99	36.05
19.0000	9.0474	10.7165	98.99	31.59
19.0000	8.1502	11.6137	107.99	27.38
19.0000	7.3842	12.3797	116.99	23.40
19.0000	6.7457	13.0182	125.99	19.64
19.0000	6.2272	13.5367	134.99	16.07
19.0000	5.8194	13.9445	143.99	12.66
19.0000	5.5133	14.2506	152.99	9.38
19.0000	5.3007	14.4632	161.99	6.20
19.0000	5.1757	14.5882	170.99	3.08
19.0000	5.1344	14.6295	179.99	.00

AVE3= 11.317045 AVE4= 8.446950

He^3 (n,p) T (Continued)

E3=*/E4=+, ENERGY IN MEV

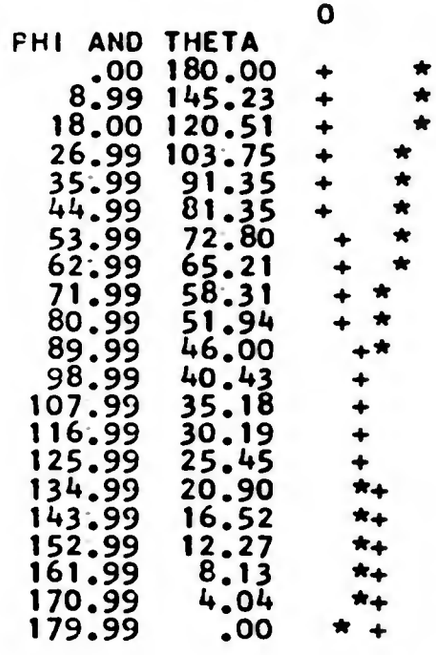

Plot He^3 (n,p) T

LOAD DATA

PHI AND	THETA
.00	180.00
8.99	97.22
18.00	84.79
26.99	76.71
35.99	69.83
44.99	63.51
53.99	57.58
62.99	51.95
71.99	46.61
80.99	41.54
89.99	36.74
98.99	32.20
107.99	27.92
116.99	23.87
125.99	20.05
134.99	16.41
143.99	12.93
152.99	9.58
161.99	6.33
170.99	3.15
179.99	.00

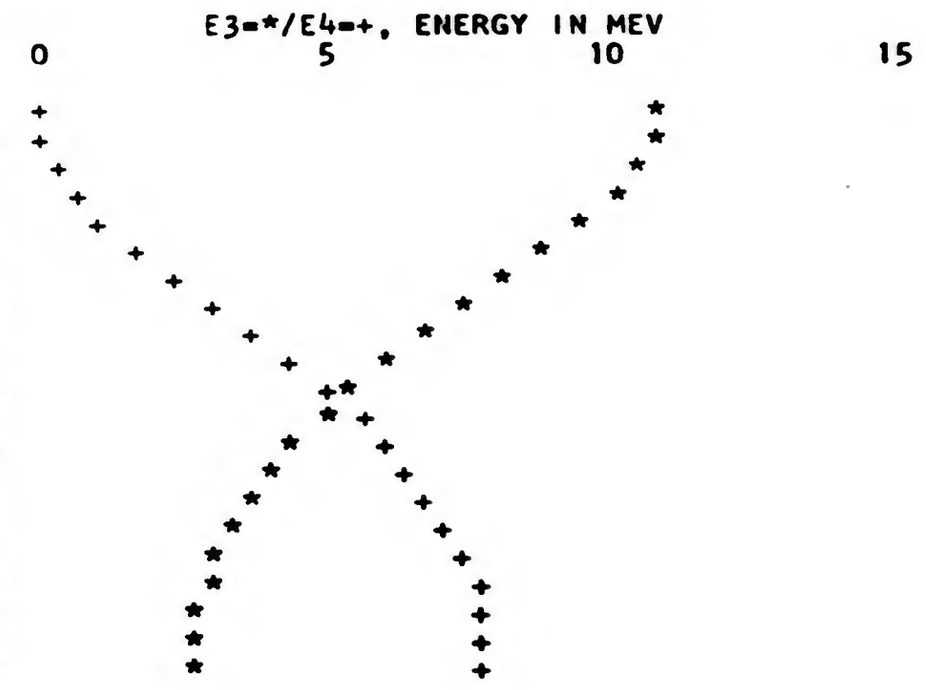

Plot He^3 (n,p) T

E1	E3	E4	PHI	THETA
2.0000	5.2382	.0277	.00	180.00
2.00	5.2382	.0277	.09	179.20
2.0000	5.2381	.0278	.20	178.41
2.0000	5.2381	.0278	.29	177.62
2.0000	5.2381	.0278	.39	176.83
2.0000	5.2381	.0278	.49	176.04
2.0000	5.2380	.0279	.59	175.25
2.0000	5.2379	.0280	.69	174.46
2.0000	5.2379	.0280	.79	173.67
2.0000	5.2378	.0281	.89	172.89
2.0000	5.2377	.0282	.99	172.11
2.0000	5.2376	.0283	1.09	171.33
2.0000	5.2375	.0284	1.19	170.55
2.0000	5.2374	.0285	1.29	169.77
2.0000	5.2373	.0286	1.39	169.00
2.0000	5.2372	.0287	1.49	168.23
2.0000	5.2370	.0289	1.59	167.47
2.0000	5.2369	.0290	1.69	166.71
2.0000	5.2367	.0292	1.79	165.95
2.0000	5.2366	.0293	1.89	165.19
2.0000	5.2364	.0295	1.99	164.44
AVE3= 5.237603	AVE4= .028395			

D (d,n) T Near 0°

```
21
1
1.
1.
3.
5.24
.764
9.
0.
0.0
```

E1	E3	E4	PHI	THETA
5.2400	5.9955	.0084	.00	180.00
5.2400	5.9506	.0533	8.99	107.49
5.2400	5.8187	.1852	18.00	90.38
5.2400	5.6080	.3959	27.00	80.54
5.2400	5.3309	.6730	35.99	72.75
5.2400	5.0032	1.0007	44.99	65.90
5.2400	4.6425	1.3614	53.99	59.60
5.2400	4.2662	1.7377	62.99	53.71
5.2400	3.8906	2.1133	71.99	48.16
5.2400	3.5293	2.4746	80.99	42.92
5.2400	3.1930	2.8109	89.99	37.97
5.2400	2.8886	3.1153	98.99	33.30
5.2400	2.6204	3.3835	107.99	28.89
5.2400	2.3897	3.6142	116.99	24.72
5.2400	2.1960	3.8079	125.99	20.77
5.2400	2.0377	3.9662	134.99	17.01
5.2400	1.9124	4.0915	143.99	13.41
5.2400	1.8179	4.1860	152.99	9.94
5.2400	1.7521	4.2518	161.99	6.57
5.2400	1.7133	4.2906	170.99	3.27
5.2400	1.7004	4.3035	179.99	.00

AVE3= 3.536094 AVE4= 2.467904

He^3 (n,p) T Reaction

E1	E3	E4	PHI	THETA
5.2400	8.2262	1.7937	.00	180.00
5.2400	8.1764	1.8435	8.99	163.42
5.2400	8.0301	1.9898	18.00	147.47
5.2400	7.7952	2.2247	27.00	132.61
5.2400	7.4843	2.5356	35.99	119.00
5.2400	7.1135	2.9064	44.99	106.65
5.2400	6.7007	3.3192	53.99	95.45
5.2400	6.2643	3.7556	62.99	85.24
5.2400	5.8217	4.1982	71.99	75.90
5.2400	5.3885	4.6314	80.99	67.31
5.2400	4.9771	5.0428	89.99	59.35
5.2400	4.5971	5.4228	98.99	51.95
5.2400	4.2550	5.7649	107.99	45.04
5.2400	3.9544	6.0655	116.99	38.53
5.2400	3.6968	6.3231	125.99	32.39
5.2400	3.4823	6.5376	134.99	26.54
5.2400	3.3098	6.7101	143.99	20.94
5.2400	3.1778	6.8421	152.99	15.54
5.2400	3.0848	6.9351	161.99	10.28
5.2400	3.0296	6.9903	170.99	5.11
5.2400	3.0113	7.0086	179.99	.00

AVE3= 5.313234 AVE4= 4.706764

E3=*/E4=+, ENERGY IN MEV

0 5 10 15

PHI AND THETA	
.00	180.00
8.99	163.42
18.00	147.47
26.99	132.61
35.99	119.00
44.99	106.65
53.99	95.45
62.99	85.24
71.99	75.90
80.99	67.31
89.99	59.35
98.99	51.95
107.99	45.04
116.99	38.53
125.99	32.39
134.99	26.54
143.99	20.94
152.99	15.54
161.99	10.28
170.99	5.11
179.99	.00

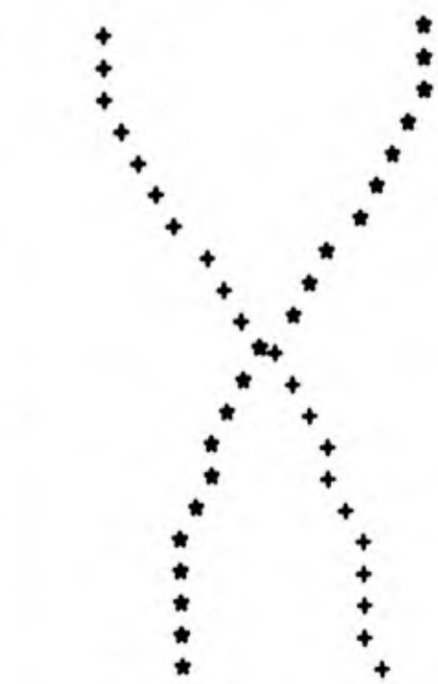

He^3 (n,p) T Reaction

(with Plot)

```
ENTER VALUES ØF M, N, MASS1, MASS3, MASS4, E1, Q,
INCREMENT ØF PHI, INCREMENT ØF E1 AND PHI.
31
5
1.
1.
7.
1.881
-1.645
1.
.001
0.0
```

E1	E3	E4	PHI	THETA
DØUBLE VALUE ENERGIES-LARGEST LISTED				
1.8810	.0396	.1963	.00	.00
DØUBLE VALUE ENERGIES-LARGEST LISTED				
1.8810	.0395	.1964	.99	.16
DØUBLE VALUE ENERGIES-LARGEST LISTED				
1.8810	.0393	.1966	2.00	.33
DØUBLE VALUE ENERGIES-LARGEST LISTED				
1.8810	.0389	.1970	2.99	.50
DØUBLE VALUE ENERGIES-LARGEST LISTED				
1.8810	.0384	.1975	3.99	.66
DØUBLE VALUE ENERGIES-LARGEST LISTED				
1.8810	.0376	.1983	4.99	.82
DØUBLE VALUE ENERGIES-LARGEST LISTED				
1.8810	.0367	.1992	5.99	.97
DØUBLE VALUE ENERGIES-LARGEST LISTED				
1.8810	.0354	.2005	6.99	1.10
DØUBLE VALUE ENERGIES-LARGEST LISTED				
1.8810	.0337	.2022	7.99	1.23
DØUBLE VALUE ENERGIES-LARGEST LISTED				
1.8810	.0310	.2049	8.99	1.31

$\underline{Li^7 (p,n) Be^7 \text{ Reaction}}$

```
REACTIØN NØT PØSSIBLE-THRESHØLD E=  1.8811
REACTIØN NØT PØSSIBLE-THRESHØLD E=  1.8813
REACTIØN NØT PØSSIBLE-THRESHØLD E=  1.8816
REACTIØN NØT PØSSIBLE-THRESHØLD E=  1.8819
REACTIØN NØT PØSSIBLE-THRESHØLD E=  1.8822
REACTIØN NØT PØSSIBLE-THRESHØLD E=  1.8825
REACTIØN NØT PØSSIBLE-THRESHØLD E=  1.8829
REACTIØN NØT PØSSIBLE-THRESHØLD E=  1.8832
REACTIØN NØT PØSSIBLE-THRESHØLD E=  1.8836
REACTIØN NØT PØSSIBLE-THRESHØLD E=  1.8840
REACTIØN NØT PØSSIBLE-THRESHØLD E=  1.8844
REACTIØN NØT PØSSIBLE-THRESHØLD E=  1.8849
REACTIØN NØT PØSSIBLE-THRESHØLD E=  1.8853
REACTIØN NØT PØSSIBLE-THRESHØLD E=  1.8858
REACTIØN NØT PØSSIBLE-THRESHØLD E=  1.8863
REACTIØN NØT PØSSIBLE-THRESHØLD E=  1.8868
REACTIØN NØT PØSSIBLE-THRESHØLD E=  1.8874
REACTIØN NØT PØSSIBLE-THRESHØLD E=  1.8879
REACTIØN NØT PØSSIBLE-THRESHØLD E=  1.8884
REACTIØN NØT PØSSIBLE-THRESHØLD E=  1.8890
REACTIØN NØT PØSSIBLE-THRESHØLD E=  1.8896
AVE3=   .011952     AVE4=   .064176
```

$Li^7(p,n)Be^7$ (Continued)

E1	E3	E4	PHI	THETA
DØUBLE VALUE ENERGIES-LARGEST LISTED				
1.8820	.0443	.1926	.00	.00
DØUBLE VALUE ENERGIES-LARGEST LISTED				
1.8820	.0442	.1927	.99	.18
DØUBLE VALUE ENERGIES-LARGEST LISTED				
1.8820	.0441	.1928	2.00	.36
DØUBLE VALUE ENERGIES-LARGEST LISTED				
1.8820	.0438	.1931	2.99	.53
DØUBLE VALUE ENERGIES-LARGEST LISTED				
1.8820	.0433	.1936	3.99	.71
DØUBLE VALUE ENERGIES-LARGEST LISTED				
1.8820	.0428	.1941	4.99	.88
DØUBLE VALUE ENERGIES-LARGEST LISTED				
1.8820	.0421	.1948	5.99	1.05
DØUBLE VALUE ENERGIES-LARGEST LISTED				
1.8820	.0413	.1956	6.99	1.21
DØUBLE VALUE ENERGIES-LARGEST LISTED				
1.8820	.0403	.1966	7.99	1.36
DØUBLE VALUE ENERGIES-LARGEST LISTED				
1.8820	.0391	.1978	8.99	1.50
DØUBLE VALUE ENERGIES-LARGEST LISTED				
1.8820	.0377	.1992	9.99	1.63
DØUBLE VALUE ENERGIES-LARGEST LISTED				
1.8820	.0360	.2009	10.99	1.74
DØUBLE VALUE ENERGIES-LARGEST LISTED				
1.8820	.0338	.2031	11.99	1.83
DØUBLE VALUE ENERGIES-LARGEST LISTED				
1.8820	.0301	.2068	12.99	1.86

REACTIØN NØT PØSSIBLE-THRESHØLD E= 1.8822
REACTIØN NØT PØSSIBLE-THRESHØLD E= 1.8825
REACTIØN NØT PØSSIBLE-THRESHØLD E= 1.8829
REACTIØN NØT PØSSIBLE-THRESHØLD E= 1.8832
REACTIØN NØT PØSSIBLE-THRESHØLD E= 1.8836
REACTIØN NØT PØSSIBLE-THRESHØLD E= 1.8840
REACTIØN NØT PØSSIBLE-THRESHØLD E= 1.8844
REACTIØN NØT PØSSIBLE-THRESHØLD E= 1.8849
REACTIØN NØT PØSSIBLE-THRESHØLD E= 1.8853
REACTIØN NØT PØSSIBLE-THRESHØLD E= 1.8858
REACTIØN NØT PØSSIBLE-THRESHØLD E= 1.8863
REACTIØN NØT PØSSIBLE-THRESHØLD E= 1.8868
REACTIØN NØT PØSSIBLE-THRESHØLD E= 1.8874
REACTIØN NØT PØSSIBLE-THRESHØLD E= 1.8879
REACTIØN NØT PØSSIBLE-THRESHØLD E= 1.8884
REACTIØN NØT PØSSIBLE-THRESHØLD E= 1.8890
REACTIØN NØT PØSSIBLE-THRESHØLD E= 1.8896
AVE3= .018178 AVE4= .088853

Li^7 (p,n) Be^7

```
      E1          E3          E4          PHI          THETA
DØUBLE VALUE ENERGIES-LARGEST LISTED
     5.0500      1.7034       .0805        .00           .00
DØUBLE VALUE ENERGIES-LARGEST LISTED
     5.0500      1.6384       .1455       8.99         31.65
DØUBLE VALUE ENERGIES-LARGEST LISTED
     5.0500      1.4480       .3359      18.00         39.91
DØUBLE VALUE ENERGIES-LARGEST LISTED
     5.0500      1.1435       .6404      27.00         37.34
DØUBLE VALUE ENERGIES-LARGEST LISTED
     5.0500       .7213      1.0626      35.99         28.96
REACTIØN NØT PØSSIBLE-THRESHØLD E=  5.2255
REACTIØN NØT PØSSIBLE-THRESHØLD E=  5.5698
REACTIØN NØT PØSSIBLE-THRESHØLD E=  5.9217
REACTIØN NØT PØSSIBLE-THRESHØLD E=  6.2343
REACTIØN NØT PØSSIBLE-THRESHØLD E=  6.4530
REACTIØN NØT PØSSIBLE-THRESHØLD E=  6.5320
REACTIØN NØT PØSSIBLE-THRESHØLD E=  6.4530
REACTIØN NØT PØSSIBLE-THRESHØLD E=  6.2343
REACTIØN NØT PØSSIBLE-THRESHØLD E=  5.9217
REACTIØN NØT PØSSIBLE-THRESHØLD E=  5.5698
REACTIØN NØT PØSSIBLE-THRESHØLD E=  5.2256
REACTIØN NØT PØSSIBLE
REACTIØN NØT PØSSIBLE
REACTIØN NØT PØSSIBLE


REACTIØN NØT PØSSIBLE
REACTIØN NØT PØSSIBLE
AVE3=    .316895     AVE4=    .107866


ENTER VALUES ØF M, N, MASS1, MASS3, MASS4, E1, Q,
INCREMENT ØF PHI, INCREMENT ØF E1 AND PHI.
```

Li^7 (p,d) Li^6

```
19
0
1.
1.
7.
2.
-1.645
10.
0.
0.0
```

E1	E3	E4	PHI	THETA
2.0000	.2302	.1247	.00	.00
2.0000	.2262	.1287	9.99	4.99
2.0000	.2144	.1405	20.00	9.19
2.0000	.1962	.1587	29.99	12.13
2.0000	.1734	.1815	39.99	13.73
2.0000	.1480	.2069	49.99	14.17
2.0000	.1224	.2325	59.99	13.74
2.0000	.0985	.2564	69.99	12.72
2.0000	.0777	.2772	79.99	11.36
2.0000	.0606	.2943	89.99	9.87
2.0000	.0472	.3077	99.99	8.38
2.0000	.0372	.3177	109.99	6.98
2.0000	.0300	.3249	119.99	5.70
2.0000	.0248	.3301	129.99	4.55
2.0000	.0211	.3338	139.99	3.50
2.0000	.0187	.3362	149.99	2.55
2.0000	.0171	.3378	159.99	1.66
2.0000	.0162	.3387	169.99	.82
2.0000	.0159	.3390	179.99	.00

AVE3= .093519 AVE4= .261480

ENTER VALUES ØF M, N, MASS1, MASS3, MASS4, E1, Q,
INCREMENT ØF PHI, INCREMENT ØF E1 AND PHI.

$\underline{Li^7(p,n)Be^7}$

```
ENTER VALUES ØF M, N, MASS1, MASS3, MASS4, E1, Q,
INCREMENT ØF PHI, INCREMENT ØF E1 AND PHI.
21
2
1.
2.
2.
5.0
-3.266
9.
.05
0.0
```

E1	E3	E4	PHI	THETA
DØUBLE VALUE ENERGIES-LARGEST LISTED				
5.0000	1.6448	.0891	.00	.00
DØUBLE VALUE ENERGIES-LARGEST LISTED				
5.0000	1.5799	.1540	8.99	30.06
DØUBLE VALUE ENERGIES-LARGEST LISTED				
5.0000	1.3897	.3442	18.00	38.37
DØUBLE VALUE ENERGIES-LARGEST LISTED				
5.0000	1.0833	.6506	27.00	35.85
DØUBLE VALUE ENERGIES-LARGEST LISTED				
5.0000	.6416	1.0923	35.99	26.77

```
REACTIØN NØT PØSSIBLE-THRESHØLD E=  5.2255
REACTIØN NØT PØSSIBLE-THRESHØLD E=  5.5698
REACTIØN NØT PØSSIBLE-THRESHØLD E=  5.9217
REACTIØN NØT PØSSIBLE-THRESHØLD E=  6.2343
REACTIØN NØT PØSSIBLE-THRESHØLD E=  6.4530
REACTIØN NØT PØSSIBLE-THRESHØLD E=  6.5320
REACTIØN NØT PØSSIBLE-THRESHØLD E=  6.4530
REACTIØN NØT PØSSIBLE-THRESHØLD E=  6.2343
REACTIØN NØT PØSSIBLE-THRESHØLD E=  5.9217
REACTIØN NØT PØSSIBLE-THRESHØLD E=  5.5698
REACTIØN NØT PØSSIBLE-THRESHØLD E=  5.2256
REACTIØN NØT PØSSIBLE
REACTIØN NØT PØSSIBLE
REACTIØN NØT PØSSIBLE
REACTIØN NØT PØSSIBLE
REACTIØN NØT PØSSIBLE
AVE3=   .301881     AVE4=   .110976
```

$\underline{He^3 (n,d) D}$

Appendix C

Calculation of Solid Angle

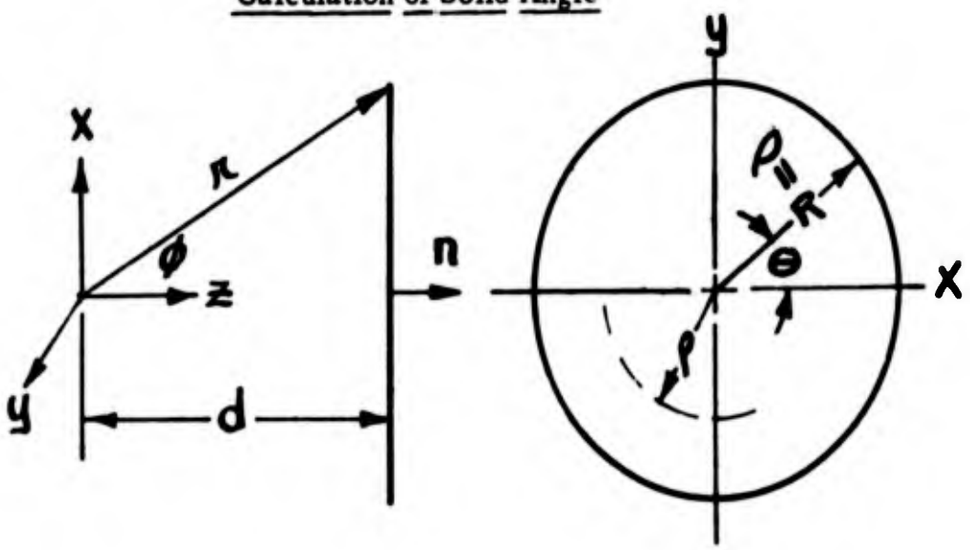

$$d\omega = \frac{dA\cos(\hat{n},\hat{r})}{r^2} \text{ by definition}$$

$$\Omega = \int \frac{\cos\phi\, dA}{r^2} \; ; \; dA = \rho\, d\rho\, d\theta$$

$$|\vec{r}| = \left[z^2 + (\rho\cos\theta)^2 + (\rho\sin\theta)^2\right]$$

$$\hat{r} = \frac{\vec{r}}{|\vec{r}|}$$

$$\vec{r} = z\hat{k} + \rho\sin\theta\,\hat{j} + \rho\cos\theta\,\hat{i}$$

$$\hat{r}\cdot\hat{n} = |\hat{r}||\hat{n}|\cos\phi \; ; \; \hat{r}\cdot\hat{n} = \hat{r}\cdot\hat{k}$$

$$\hat{r} = \frac{z\hat{k} + (\rho\cos\theta)\hat{j} + (\rho\sin\theta)\hat{i}}{\left[z^2 + (\rho\cos\theta)^2 + (\rho\sin\theta)^2\right]^{\frac{1}{2}}}$$

$$\Omega = \int_0^R \int_0^{2\pi} \frac{z\,\rho\,d\rho\,d\theta}{\left[z^2 + (\rho\cos\theta)^2 + (\rho\sin\theta)^2\right]^{\frac{3}{2}}}$$

let $z = d$

$$\Omega = 2\pi d \int_0^R \frac{\rho\,d\rho}{\left[d^2 + \rho^2\right]^{\frac{3}{2}}}$$

let $u = d^2 + \rho^2$; $du = 2\rho\,d\rho$

$$\Omega = \pi d \int_{u=d^2}^{u=R^2+d^2} \frac{du}{(u)^{\frac{3}{2}}}$$

$$\therefore \Omega = -2\pi d \left[\frac{1}{(R^2+d^2)^{\frac{1}{2}}} - \frac{1}{(d^2)^{\frac{1}{2}}} \right]$$

Appendix D

Photographs

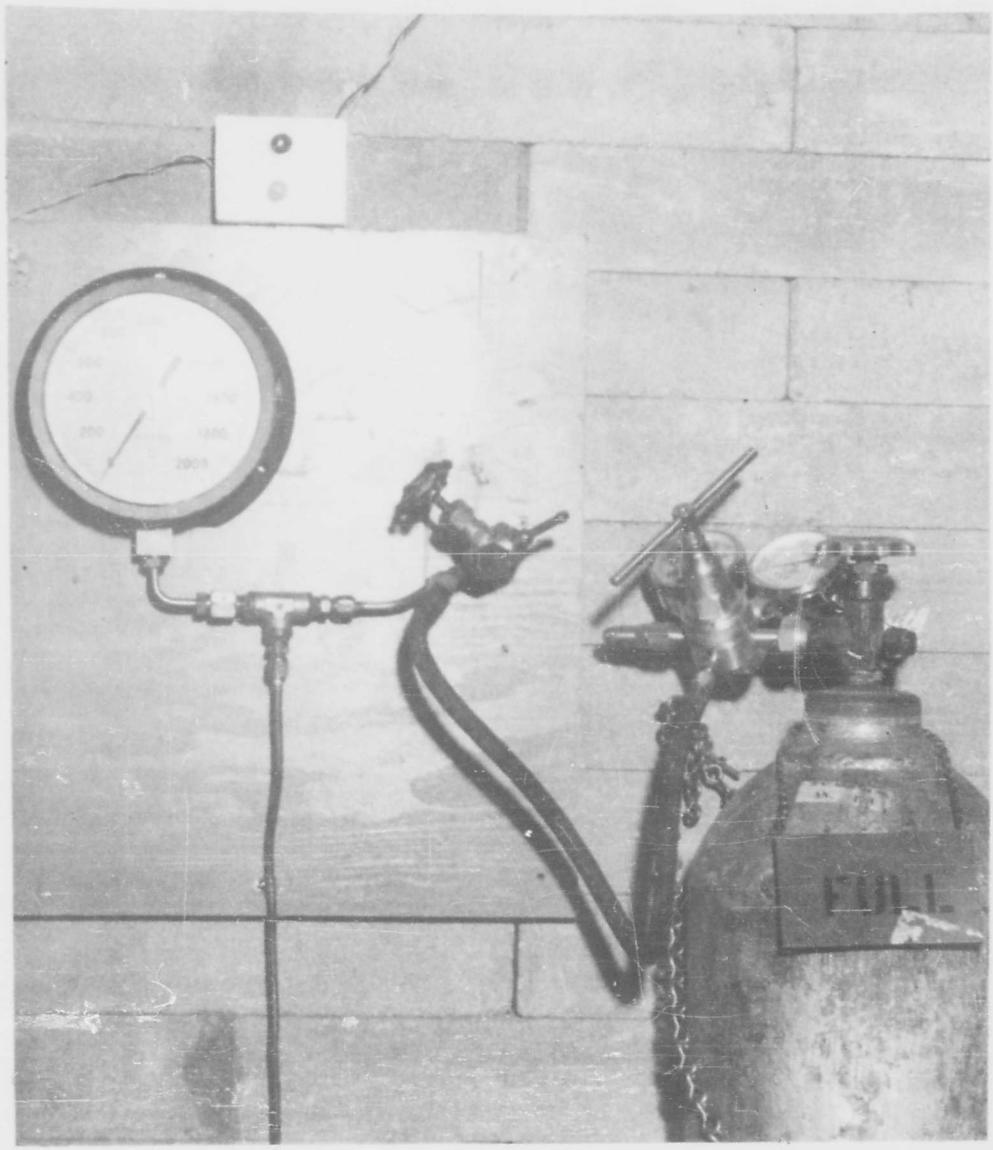

Pressure Control Panel

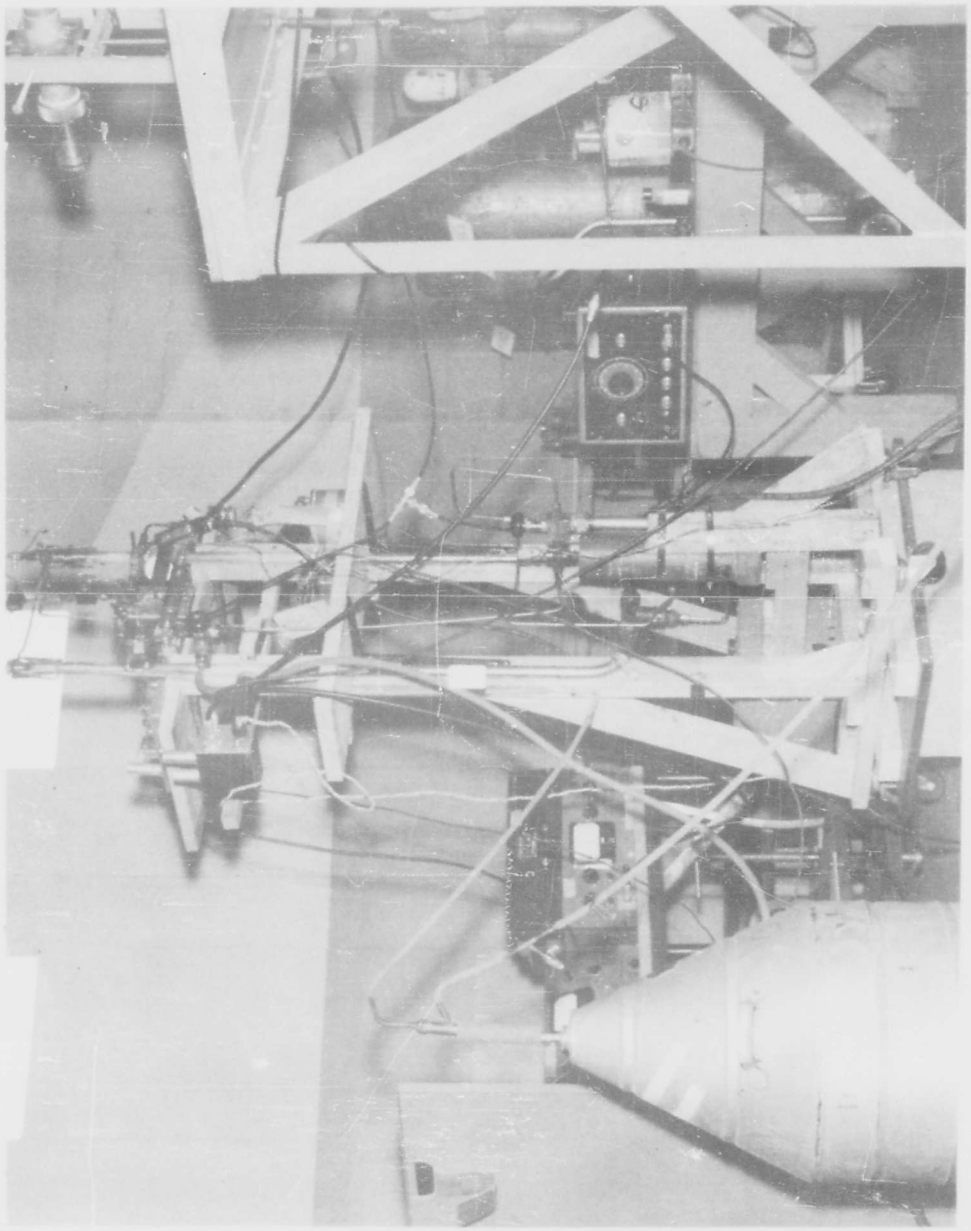

Spectrometer and Associated Equipment

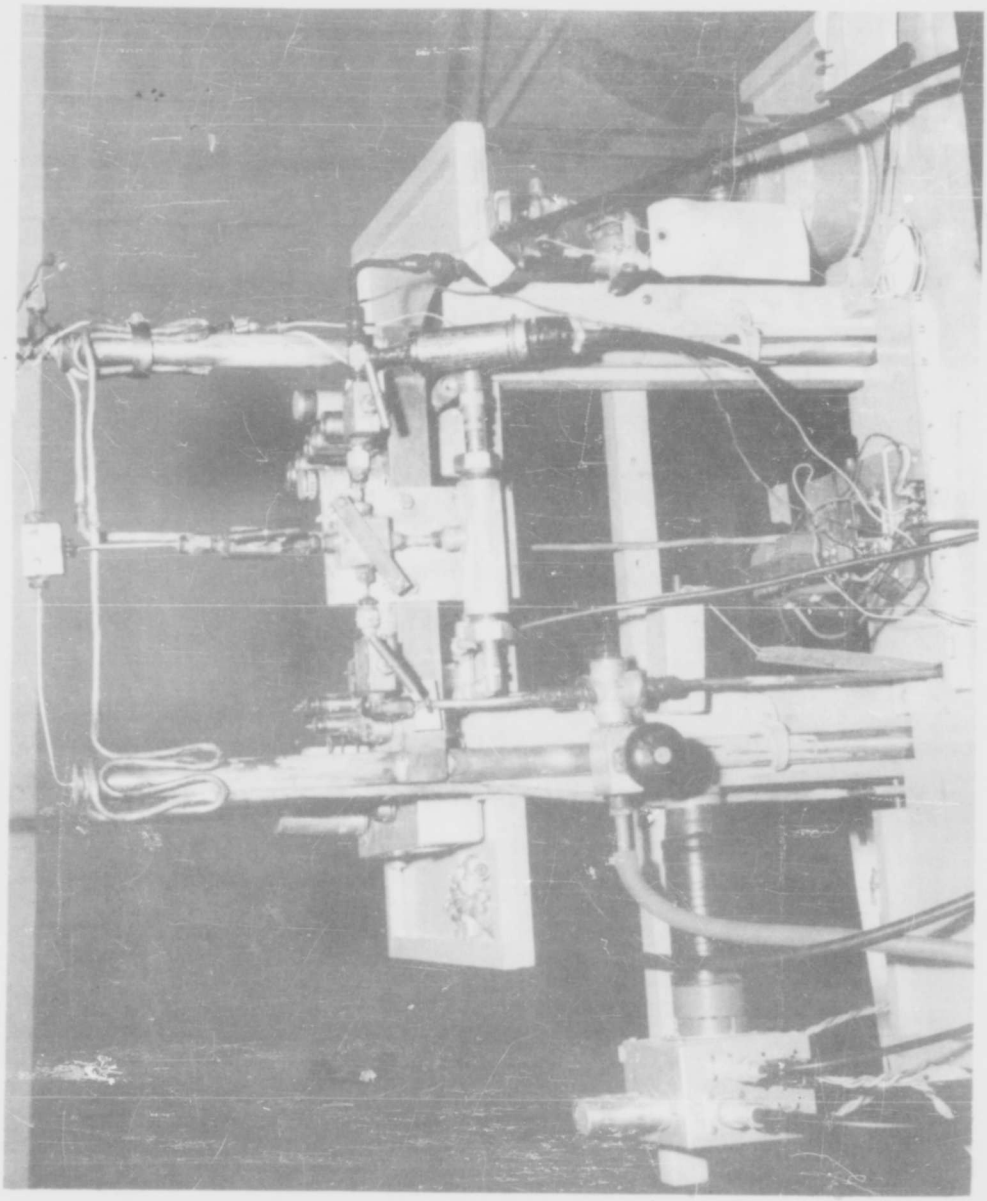

Close up of Target Chamber

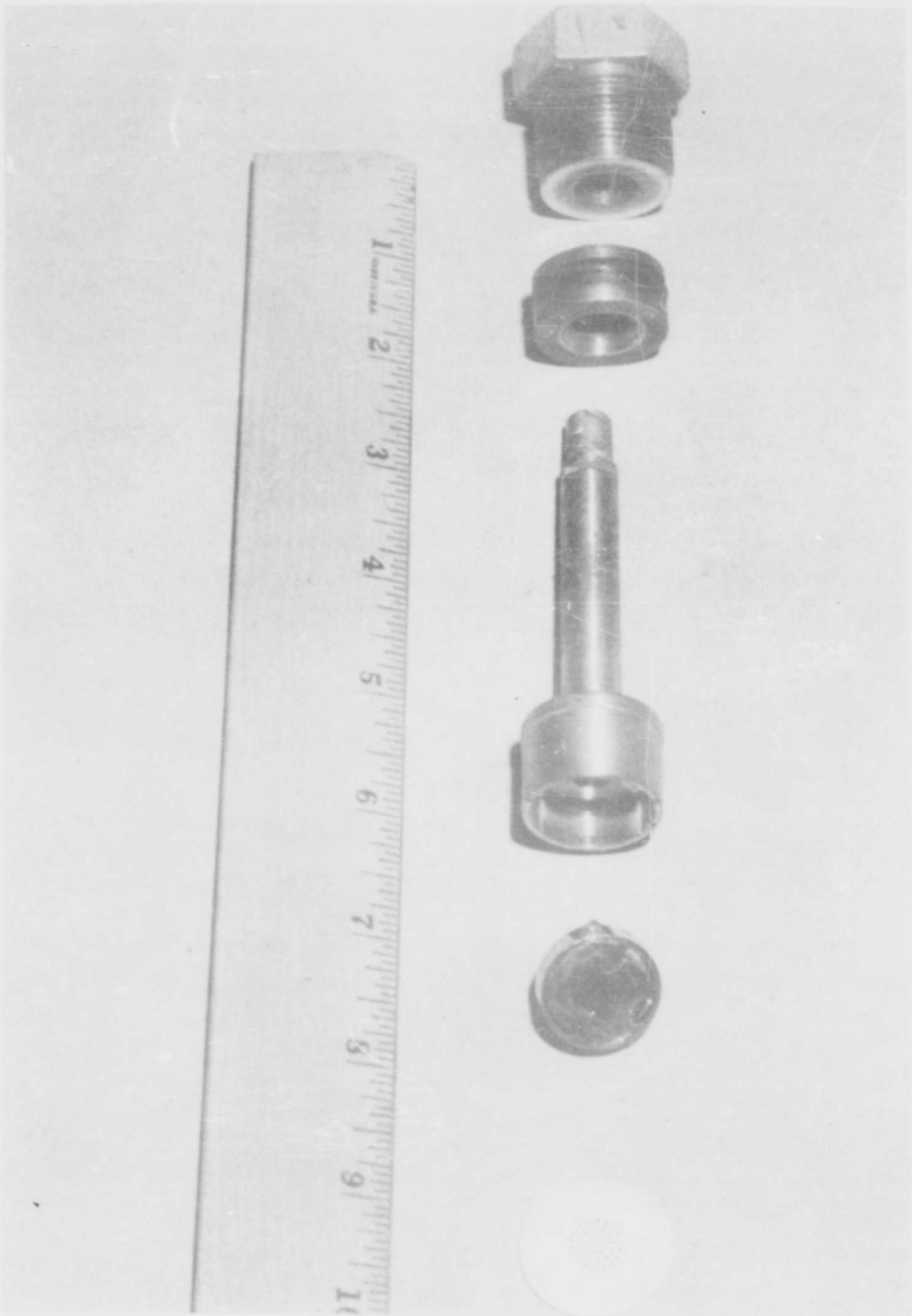

Detector Holder Assembly, Detector and Washer

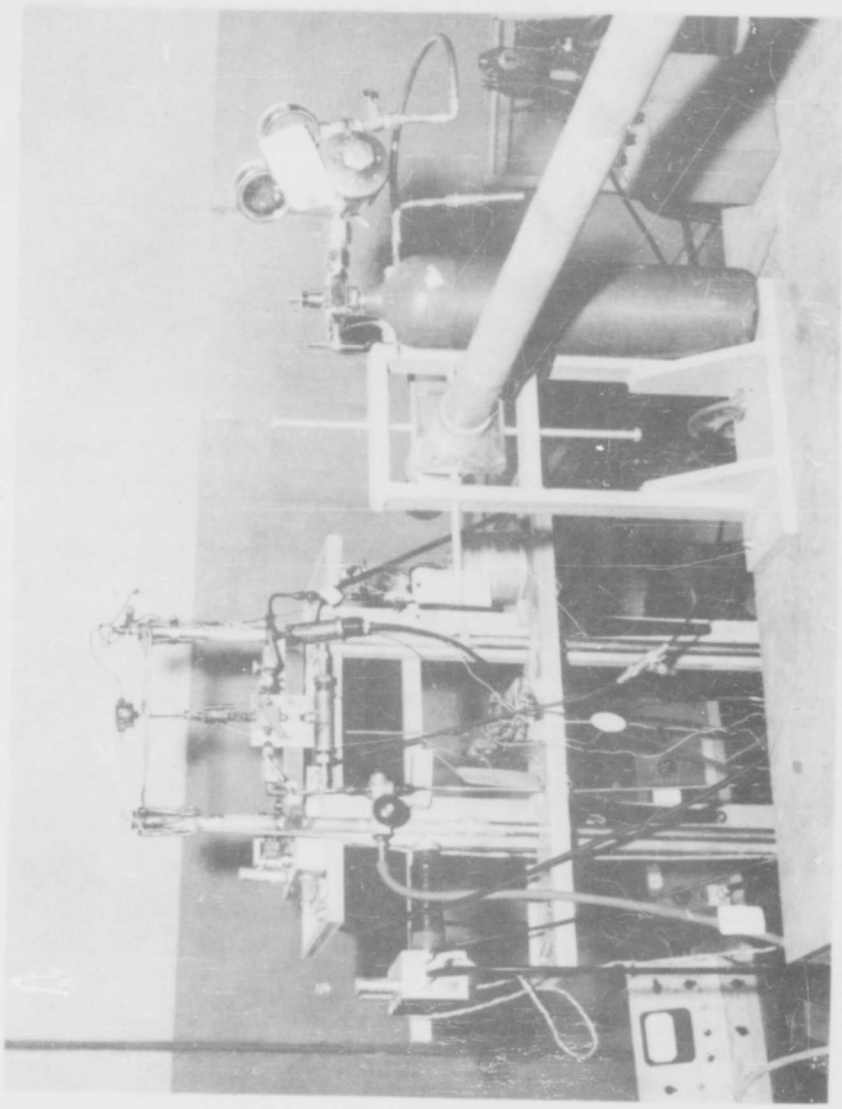

Spectrometer Looking From Beam Tube

Vita

Phillip Darden Weinert was born at Fort Sam Houston, San Antonio, Texas, the son of a career Army officer whose footsteps he is following as a regular officer in the Corps of Engineers. From his beginning in San Antonio, he traveled extensively as his father was transferred to new assignments. Six years of his life were spent in the Panama Canal Zone where he started high school, which was continued in Washington, D.C., where he graduated from Western High School in 1952. That fall he entered the A & M College of Texas as a student in civil engineering. After four years of undergraduate work, he graduated with a BS in civil engineering and a reserve commission as a second lieutenant in the Corps of Engineers. Upon completion of the Basic Officer's Course at Fort Belvoir, then Lieutenant Weinert traveled to Korea where he spent sixteen months as an assistant S-3, platoon leader and company commander in the 43rd Engineer Construction battalion. While in Korea he was tendered and accepted a regular commission in the Corps of Engineers. After return to the United States his new assignment was with the Post Engineer at Fort Ord, California, where he worked in the field of contract administration

and inspection for over two years. Completion of the tour of duty at Fort Ord was followed by his present assignment as a student at the Air Force Institute of Technology where he is working for his MS degree in nuclear engineering under the Corps of Engineers' program for advanced education of career officers. The rank of Captain was attained while at the Air Force Institute. A career in the Corps of Engineers is shared by his brother, Captain Donald Weinert, who is presently an instructor at West Point.

UNCLASSIFIED

UNCLASSIFIED